

Norwegian University of Science and Technology  
Department of Civil and Environmental Engineering

# Machine Learning Methods for Bathymetry Generation in Rivers

Master Thesis prepared by:

**Raffa Ahmed Osman Ahmed**

Supervised by:

**Prof. Knut Alfredsen**

**Eng. Elhadi Mohsen**

**Eng. Mahmoud Awadallah**

Date: 28th June 2022

## **Abstract**

Natural flood hazards resulted in more than 500,000 reported deaths during the last 20 years. This number is expected to increase in the future due to population growth, rapid urbanization and increased rainfall intensities induced by climate change. Hydrodynamic models are essential tools for simulating flooding events for proper risk management. Topographical and bathymetrical data are essential inputs for hydrodynamic models. One of the promising technology for Topographical and bathymetrical data collection is the LiDAR (Light Detection And Ranging) which has emerged in the last years. Two LiDAR technologies exist; Red LiDAR and Green LiDAR. The former cannot penetrate water surfaces while the latter can. In Norway, Green LiDAR data are collected for only few rivers while Red LiDAR data are available for most of the rivers. This study sough to investigate the suitability of two Machine learning (ML) methods, Artificial neural network (ANN) and Convolutional neural network (CNN), for extracting river bathymetry for Red Lidar data. ML models were trained in Gaula river in Norway with Green LiDAR data. Four different model training scenarios and two activation functions of ANN were tested. The accuracy of the trained ML models was tested at different reaches of Gaula from the ones used for model training and at two other rivers in Norway, Driva and Surna. Moreover, the study investigated the accuracy of the hydraulic simulations by using bathymetrical data generated by the trained ML models. The preliminarily results of the CNN were promising. However, the method was found to be computationally costly and time consuming. For ANN, the selection of input data and the choice of activation functions were found to influence the accuracy of the results. Trained ANN models were able to predict bathymetrical data with reasonable accuracy in most of the cross-sections of Gaula river. Trained ANN could also yield accurate estimation of bathymetrical data when evaluated at Driva and Surna rivers. Prediction accuracy was generally low for cross-sections that vary significantly from the ones used for model training and for cross-sections that contain islands. Regarding hydraulic simulations, terrains estimated by ANN decreased the inundation area error significantly when compared with Red LiDAR simulations. Therefore, well-trained ANN can be used to predict bathymetrical for Red LiDAR in order to improve the accuracy of hydraulic simulations.

# *Dedication*

This master thesis is dedicated

To my beloved and inspiring father may god have mercy on him, who supported me and wished to see this moment,

To my mother, who constantly encouraged me and filled me with love,

To my siblings Ruaa, Rowida, and Fyad my backbone,

To Waleed Babiker,

To Ali Ahmed who made this journey possible with his support, and always being there when I needed him,

To my friends in Sudan and Norway,

To my teachers,

Raffa Ahmed

28th June 2022

## **Acknowledement**

After two years of studying at NTNU,

I am very grateful and thankful to my supervisor Professor Knut Alfredsen, for his guidance, advice, and his support to finish this master thesis.

I would like to thank Elhadi Mohsen, Mahmoud Awadallah my co-supervisors for their endless support to guide me through this journey and for being always welcome to help.

I would like to thank all the professors at the Hydropower Development Master Program, NTNU for their dedicated and hard efforts, and the time they spent helping us gaining knowledge, I truly appreciate it.

I would like to thank Hiba Abdallah and Duaa Bushara for always being there.

Special thanks to the Sudanese community in Norway.

I would like to thank the Norwegian Agency for Development Cooperation NORAD for the full sponsorship. It wouldn't be possible without their support.

I would like to thank the Norwegian University of Science and Technology (NTNU), Department of Civil and Environmental Engineering student affairs office, and the advisors for their continuous communication throughout the COVID-19 pandemic, while we were studying from our home countries.

# Table of Contents

<b>Abstract .....</b>	<b>1</b>
<i>Dedication.....</i>	<b>2</b>
<b>Acknowledement .....</b>	<b>3</b>
<b>Table of Contents .....</b>	<b>4</b>
<b>List of Figures.....</b>	<b>6</b>
<b>List of Tables .....</b>	<b>7</b>
<b>Abbreviations.....</b>	<b>8</b>
<b>Chapter 1    Introduction.....</b>	<b>1</b>
<b>Chapter 2    Literature Review.....</b>	<b>3</b>
2.1    Topography Data .....	3
2.2    Application of LiDAR data in flood:.....	4
2.3    Neural Network .....	5
<b>Chapter 3    Method and Tools .....</b>	<b>6</b>
3.1    Image inpainting .....	6
3.1.1    Convolutional neural network CNN .....	6
3.1.2    Image inpainting and CNN .....	8
3.2    1-Dimensional training .....	9
3.2.1    Artificial Neural Network .....	9
3.2.2    Activation function.....	10
3.2.3    Loss Function .....	10
3.2.4    API Keras .....	11
3.2.5    Data .....	13
3.2.6    Artificial Neural Network Model Setup and Training Scenarios.....	15
3.2.7    Prediction and Testing.....	17
3.2.8    Hydraulic Simulation .....	17
<b>Chapter 4    Results and Discussion .....</b>	<b>18</b>
4.1    Image inpainting .....	18
4.2    1-Dimensional ANN.....	19
4.2.1    Scenario a .....	19

4.2.2	Scenario b .....	20
4.2.3	Scenario c .....	21
4.2.4	Scenario d .....	24
4.2.5	Residual Between Green LiDAR and Predicted Bathymetry (scenario c).....	25
4.2.6	Hydraulic Flood Simulation .....	26
<b>Chapter 5</b>	<b>Conclusion and Recommendation.....</b>	<b>29</b>
<b>References .....</b>	<b>31</b>	
<b>Appendices .....</b>	<b>36</b>	

## List of Figures

Fig 3.1 Convolutional Neural Network Layers { , 2018 #3} .....	6
Fig 3.2 Filter convolving over 6*6 input feature .....	7
Fig 3.3 Max and Average pooling illustration example for 6*6 input image .....	8
Fig 3.4 Random Generated Binary Mask for CNN Operation {Liu, 2018 #2} .....	8
Fig 3.5 An Example of the Input Masked Image from Gaula for CNN Training .....	9
Fig 3.6 An Example of the Randomly Generated Mask on Gaula River.....	9
Fig 3.7 General Structure of Artificial Neural Network .....	10
Fig 3.8 A, B, and C are Linear activation function, ReLU activation function, and Sigmoid activation function respectively {Sharma, 2017 #8} .....	11
Fig 3.9 Keras Sequential Model Structure and Compilation .....	12
Fig 3.10 Green LiDAR terrain for Surna river.....	13
Fig 3.11 Transects and Points Along Gaula River .....	14
Fig 3.12 A, B, and C are the clipped Green LiDAR raster, the predicted Points raster, and the mosaiced raster .....	15
Fig 3.13 Cross Section Example of Input and Output Green LiDAR Elevation Points .....	16
Fig 3.14 2D Flow Area and the Generated Mesh 5×5 m .....	17
Fig 4.1 Last Two Predictions in Image Inpainting Training .....	18
Fig 4.2 An Example of Consistency Between the Selected Number of Points and the Actual River Cross Section .....	19
Fig 4.3 An Example of Inconsistency Between the Selected Number of Points and the Actual River Cross Section.....	20
Fig 4.4 An Example of Prediction Results Using for Scenario b .....	21
Fig 4.5 A and B Comparison Between simple(A) and Complex (B) River Channel .....	22
Fig 4.6 Show the MSE model loss for training and Validation .....	23
Fig 4.7 Comparison Between ReLU and Sigmoid in Cross Sections 2420,2411, and 2412, Gaula .....	23
Fig 4.8 Comparison Between ReLU and Sigmoid in Cross Sections 133,134, and 135, Driva .....	24
Fig 4.9 Comparison Between ReLU and Sigmoid in Cross Sections 118,119, and 120, Surna .....	24
Fig 4.10 An Example of Results from Scenario d Training .....	25
Fig 4.11 Driva Green LiDAR and Prediction Residual.....	25
Fig 4.12 Flood Inundation Extent for Different Scenarios by HEC-RAS 6.0, Driva River ....	26
Fig 4.13 Flood Inundation Extent for Different Scenarios by HEC-RAS 6.0, Surna River ....	27

## List of Tables

Table 3.1 Tested Flood in m <sup>3</sup> /s Scenarios Based on NEVINA.no (Awadallah, Juárez et al. 2022) .....	13
Table 4.1 Difference Error Between the Green LiDAR Vs Red LiDAR and Green LiDAR Vs Prediction, Driva/Sigmoid.....	27
Table 4.2 Difference Error Between the Green LiDAR Vs Red LiDAR and Green LiDAR Vs Prediction, Surna/ReLU .....	27

## **Abbreviations**

AI	Artificial Intelligence
API	Application Programming Interface
DEM	Digital Elevation Model
MSE	Mean Squared Error
Qm	Mean Flood Discharge
Q10	10 years Flood Discharge
Q100	100 years Flood Discharge
Q500	500 years Flood Discharge
ReLU	Rectified Linear Activation Unit
Sigmoid	Soft Step Activation Function

# Chapter 1      Introduction

---

Rivers are crucial natural features that serve a variety of benefits, such as transportation, power production, drinking water supply, ecological system balance and irrigation (Sundt, Alfredsen et al. 2021). On the other hand, rivers can be an initiation point of natural disaster, i.e. flood. The flood damages in Europe is constantly increasing over the time, and minimizing this risk is one of the priorities of the continent. The settlements on the flood plain zones, in addition to the rapid climatic variability and environmental changes due to technology enhancement, such as land use urbanization, are significantly affecting the flood risk (Kron, Eichner et al. 2019). Moreover, the global warming and snow melt led to earlier soil saturation and increased runoff (Bloschl, Hall et al. 2017). In addition, river floods vary in spatial and temporal scale (Shrestha and Nestmann 2009). All these factors need regular studies about the floods impact and the following consequences as well as local planning.

Hydrodynamic models are extremely substantial tools that help the practitioners studying and analysing the impact of flood for risk assessment and natural hazard management. The input data for these models vary depending on the used tool and selected purpose of modelling. Each tool has a fundamental concept based on selected field of science, such as hydrology and hydraulics (Shrestha and Nestmann 2009). One of the most commonly used hydrodynamic models is perhaps the Hydrologic Engineering Center River Analysis System model (HEC-RAS) by the United States Army Corps of Engineers (Alaghmand, Abdullah et al. 2012). In 2D flood simulation using HEC-RAS, the main input data are runoff hydrograph for the selected river, upstream and downstream boundary conditions beside the topographical data and defined properties for the landuse. The topographical data is a foundational input to the model that describes the geometries of the riverbed and the flood plains.

Several topographical and bathymetrical data collection methods exist for academic and practical applications. Riverbed data collection can be manually done using shipboard and ecosounder (Gao 2009), or Acoustic Doppelr Currnet Profiler (ADCP) by maneuvering through the river. This approach generates accurate riverbed measurements. However, it is labour-intensive, costly and time-consuming. Remote sensing is another method for collecting topographical and bathymetrical data. It is becoming a major method in data collection techniques and has a wide range of applications because it provides lifelike images (i.e. Google Earth) that serve many fields (Zhang, Zhang et al. 2016). Light Detection And Ranging (LiDAR) is a remote sensing airborne technology that calculates the round distance from the light transmitter sensor to the ground object (Meng, Currit et al. 2010). LiDAR sensors provide fast and highly quality elevation measurements with three dimensional coordinate system, comparison to other surveying systems like photogrammetric system (Meng, Wang et al. 2009). Recently, LiDAR attracted attention in bathymetrical data collection of rivers (Fonstad and Marcus 2010). To measure the riverbed, LiDAR uses the green light sensor which operates in the green part of electromagnetic spectrum which can penetrates the water and recover the reflection from the riverbed (Kinzel, Legleiter et al. 2013). The above-mentioned point made the topographical data generated from LiDAR emerged as one of the most significant input for Hydraulic simulation tools and flood assessment.

As mentioned before, Green LiDAR penetrates the water unlike the Red LiDAR which consider the rivers as flat surfaces and being absorbed by the water column (Kinzel, Legleiter et al. 2013). Many studies carried out to minimize the DEMs errors, manually or by systematic editing. The former studies used explicit algorithms to correct noises across the DEM (Stevenson, Sun et al. 2010). Studies investigated the discrepancy between the bathymetry and topographical data were done, i.e.(Allouis, Bailly et al. 2010).

Recent studies investigated the application of machine learning techniques in flood assessment and natural disasters management. This is due to the fact that fast dynamic of urbanization is involving different scientific disciplines led to large number of data (Deparday, Gevaert et al. 2019). Many studies were done to improve the DEMs using ANN. For instance, (Stevenson, Sun et al. 2010) and (Wendi, Liong et al. 2016). In this research machine learning methods were used based on the characteristic of handling nonlinear data, beside the ability of processing large datasets.

In Norway, Green LiDAR was collected for only few rivers. In contrast, Red LiDAR data is covering wide space among the country and it is readily available for almost all rivers. Hence, this study aims at finding a suitable ML method to obtain the river bathymetry (wetted zone) from the Red Lidar for accurate flood modelling. The specific objectives of the study are:

- Evaluating the suitability of different ML algorithms in predicting river bathymetry for Red Lidar data.
- Evaluating the accuracy of trained ML models in different rivers
- Investigating the accuracy of hydraulic simulations using bathymetrical data generated by trained ML models

## **Chapter 2      Literature Review**

---

### **2.1 Topography Data**

There are many types of topography data generation sources that vary in their collection methods and accuracy. For instance, ground surveys, digitizing hardcopy topographic maps, photogrammetry, interferometric synthetic aperture radar (IfSAR), and light detection and ranging (LiDAR) (Hodgson, Jensen et al. 2003, Muhadi, Abdullah et al. 2020).

In Situ ground survey can have higher resolution depending on the measurement device's accuracy and the spatial distribution of the measured points. It is suitable for small-scale studies and can be very accurate (Casas, Benito et al. 2006). Traditional leveling equipment and advanced ones like total station could produce elevation maps. However, both are time-demanding and can bare a trade between spatial and temporal accuracy. Therefore, the photogrammetry tools have made it possible to acquire higher density from a small distance and even faster. Two types of photogrammetry are available: aerial (camera on the air like a plane) and terrestrial (mounted on a tripod). In the past mechanical methods were used to extract the elevation information from the photos taken by the cameras. Then with the help of computers, analytical tools were developed to create the topography maps, which allow automation of the process and creation of digital elevation models (DEMs) 100 times faster than the previous method. Lastly, data acquisition has become automatic through digitalised photogrammetry with high spatial resolution, which can reach up to 0.01 to 1 m cell size for small areas (Lane, Richards et al. 1993, Chandler 1999, Lane, James et al. 2000, Bird, Hogan et al. 2010).

Digital photogrammetry often cannot accurately represent the bathymetry of the rivers. Also, it is not possible to work in all weather conditions. In this manner, coupling the latter with total station measurement can lead to efficient results. Although these improvements can save some time, it still takes longer to create a controlled network and can have a limitation concerning visibility between the device and the point. Thus, the use Global Positioning System (GPS) can tackle these limitations and achieve accuracy of ( $2\pm3$  cm) topographic data (Brasington, Rumsby et al. 2000, Casas, Benito et al. 2006).

IfSAR working principle is based on signals emitted from microwave sensors to the earth's surface, then the scattered signal will be recorded. Two images are combined to generate the DEM using the interferometric SAR. There are two types: spaceborne IfSAR and airborne IfSAR. Airborne IfSAR can be more flexible than the other one and can have higher resolution. One famous DEM created from the spaceborne is the shuttle radar topography mission (STRM). The advantage of using IfSAR is that larger areas can be covered at any time (even at night) and in any weather conditions. The accuracy provided with airborne IfSAR is about 5 m spatial resolution and 0.5 – 3 m vertical resolution. However, in urban areas or densely vegetated areas, IfSAR has some limitations with the complexity of the structures, which scatters the signals or cannot penetrates the canopy surfaces (Dowman 2004, Mercer 2004).

Lastly, the new emerging technology, LiDAR, has the same concept as IfSAR with different sensor types. LiDAR systems are based on using a laser sensor to scan the objects and measure the distance between the platform, which usually is an airplane and the surface of reflection. Like IfSAR, GPS/INS system is installed in the aircraft to link the location information with the collected data. LiDAR data can be collected from the ground, terrestrial LiDAR, helicopter or airplane, airborne LiDAR, or space, spaceborne LiDAR. An example of the latter is Geoscience Laser Altimeter System (GLAS). LiDAR has some advantages compared to the other methods. Such as, data can be collected anytime during the day, even in cloudy conditions, very efficiently. Also, it can have better penetration for the vegetation covers and better representation of urban areas. Kraus and Pfeifer (1998) stated that LiDAR can produce DEM in forest areas, similar to the accuracy of photogrammetry in open areas. The accuracy of the DEM generated by airborne LiDAR is 0.5 – 2 m spatially and 10 cm vertically (Hodgson, Jensen et al. 2003, Dowman 2004, Mercer 2004).

## **2.2 Application of LiDAR data in flood:**

Mapping flood areas is an important task when dealing with risk assessment. A crucial factor for producing inundation maps is DEM. Webster, Forbes et al. (2004) used airborne LiDAR to create high-resolution DEM to assess the sea-level rise and climate change risk in a coastal area. The flood model from the generated DEM accurately mapped the flood zones. Bales, Wagner et al. (2007) prepared 1.5 by 1.5 m DEM from airborne LiDAR with vertical accuracy of 20 cm to make flood inundation area maps for study sites in North Carolina. HEC-RAS model was developed for the study area to simulate water levels. The difference between observed and simulated water levels was beneath 25cm.

Sampson, Fewtrell et al. (2012) used terrestrial LiDAR to develop DEM with a resolution of 10 cm to simulate an urban flood in the UK. Two models were implemented, LISFLOOD-FP and ISIS-FAST. The result showed how small details in the topography, like road pumps, can influence the flood simulation. The LiDAR well-represented these features, and as a finding when finer details are required like in the case of urban flood modeling, terrestrial LiDAR can be used.

Chen, Krajewski et al. (2017) investigated the applicability of using LiDAR data in flood modelling. LiDAR data was collected during a flood and classified as flooded and non-flooded points. The resulted flood DEM has been subtracted from earth DEM. The root mean squared error was 30 cm compared to high water marks. This study demonstrated the potential of using LiDAR data in flood inundation maps and calibrating and validating flood models.

Santillan, Makinano-Santillan et al. (2016) illustrated the application of LiDAR when combined with flood models in determining the vulnerability of buildings. Abdalla, Pons et al. (2021) introduced a method for collecting finer resolution LiDAR data to be used in flood. The method was tested in small mountain area and large urban area to see the time needed for collecting the data. It took 5 h and 2 days respectively. In the end, the model results showed how the additional gained information from developing very high resolution DEM improved the simulation and can be more reliable.

## 2.3 Neural Network

Neural networks are resembling for human neural cells, it was inspiration from the brain system complexity, it started with one layer of neurons (Montesinos-López, Montesinos et al. 2022), then the shallow neural network SNN consisting from 1 or 2 hidden layer (Feng, Zhou et al. 2018). The artificial neural networks ANNs kept developing to multiple hidden layers resulting in deep learning systems.

Data-driven models are widely used in hydrological applications where sufficient data sets are available. These models build a mathematical relationship between observed and simulated data. Machine Learning is an advanced type of these models.

Neural network (NN) was adopted in many applications in hydrology. To begin with, rainfall-running models where NN models were preferable compared to physical models. Especially when model parameters are difficult to measure and can have uncertainties when calibrated based on assumptions. Furthermore, complex systems can not be fully understood to be represented by physical equations (Machado, Mine et al. 2011, Bloschl, Hall et al. 2017). Also, ANN model has been used as a surrogate for a process-based model to reduce the computational time needed to calibrate or run many scenarios (Semiromi, Omidvar et al. 2018).

In the field of groundwater, ANN has been used for parameter estimation for the groundwater flow model (Shigidi and Garcia 2003), groundwater level prediction (Sreekanth, Geethanjali et al. 2009, Semiromi, Omidvar et al. 2018, Roshni, Jha et al. 2020), groundwater quality (Jinlong and JinTao 2009, Kulisz, Kujawska et al. 2021, Stylianoudaki, Trichakis et al. 2022), and Karst discharges (Cheng, Qiao et al. 2021).

Moreover, NN models were used in processes related to the hydrological cycle. For instance, rainfall forecasting (Khaniani, Motieyan et al. 2021), predicting evaporation (Algretawee and Alshama 2021, Sivastava, Naidu et al. 2022), downscaling temperature and precipitation data (Wang, Huang et al. 2020), and global climate models (Weber, Corotan et al. 2020). Other applications include water level and inflow in reservoir prediction (Qi, Zhou et al. 2019), and land cover maps (Abdi, Samadzadegan et al. 2018).

# Chapter 3      Method and Tools

---

This section presents the two main methods used for predicting the river cross-sections, image inpainting, and 1-D machine learning training. All the data were prepared with the help of ArcGIS Pro. Different scenarios were also examined for the 1-D trained model. The results from the prediction were tested in a flood simulation model.

Machine learning concept was applied for both model trainings. Machine learning means computer algorithms for data analysis to derive intelligent predictions on an iterative process without explicit programming (Das and Behera 2017).

## 3.1 Image inpainting

Image inpainting is a method to fill the missing data in image pixels by taking advantage of an existing relatively large data set with similar pixel values (Bertalmio, Sapiro et al. 2000). Several methods for image inpainting can fill the missing data. The technique used here is based on a deep learning convolution neural network for image processing CNN. The method has different applications, for example, revert deterioration, add or remove an element, remove scratches from images, etc.

### 3.1.1 Convolutional neural network CNN

CNN is a deep learning neural network that uses multiple hidden layers for image analysis or classification problems (O'Shea and Nash 2015). The multi-hidden layers are: convolutional layers, non-linearity or ReLU layers, pooling layers, and fully connected layers. Each one will be explained in further detail.

#### 3.1.1.1 Convolutional Layers

If we have image pixels as input data for the CNN model and this image has features to be detected through the deep learning procedure, the filter will work as a feature patterns detector convolving over the entire image with a specific stride. In each convolutional layer, we should specify the number of filters for pattern detections, such as edges detector, face detector, or other different features, as shown in Fig 3.1.

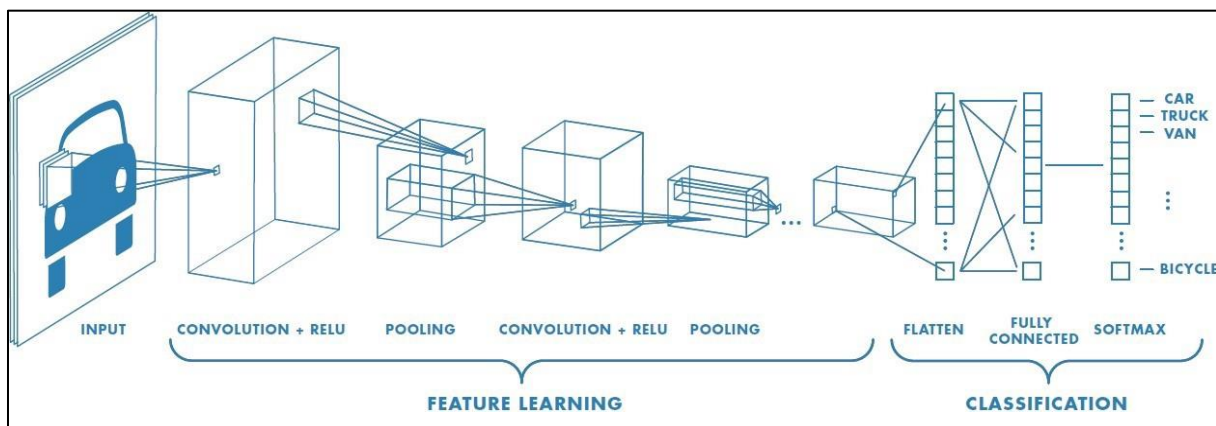


Fig 3.1 Convolutional Neural Network Layers (2018)

### 3.1.1.2 Filters

A filter can be a relatively small matrix where we decide the number of rows and columns defined also by kernel size (Albawi, Mohammed et al. 2017) . Values within the matrix are initialized with random numbers; for example, if we have a filter 5\*5, the filter will convolve over every 5\*5 pixels.

We need a filter with a selected dimension on a specific convolutional layer. When this convolutional layer receives input, the filter will slide over each image patch with a size similar to the filter. As shown in Fig 3.2, the filter slides over each 3\*3 pixel from the input itself until it moves over each 3\*3 pixel of the entire image. The sliding process is referred to as convolving, which multiplies the input by the filter element-wise multiplication and then calculates the summation.

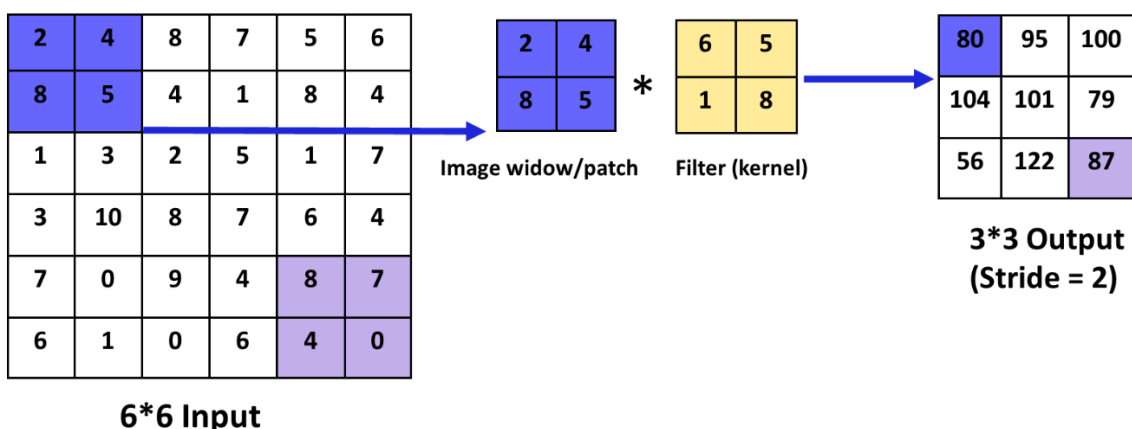


Fig 3.2 Filter convolving over 6\*6 input feature

### 3.1.1.3 Non-Linearity Layer

The convolutional layers are typically linear networks when applying the filter for weight and bias calculation. Nevertheless, to apply image processing such as classification, non-linearity is required. This is achieved by using the activation function in most cases. ReLU has recently been the most popular activation function due to the fast convergence and fast processing.

### 3.1.1.4 Pooling Layers

Pooling is a method used for dimensionality reduction to minimize the computation expensiveness in model training and fasten the major features detection. Pooling has the same mechanism concept as filters, but statistical operations are addressed instead of the element-wise multiplication. It has different types: max pooling, average pooling, global max pooling, and global average pooling. These types apply statistical operations like maximum and average for the pool of values.

For example, in Fig 3.3 we have 4 windows and filter 2\*2 with stride 2. The output values are the maximum value in each window; therefore, the dimension will be reduced from 4\*4 to 2\*2, giving a new image representation.

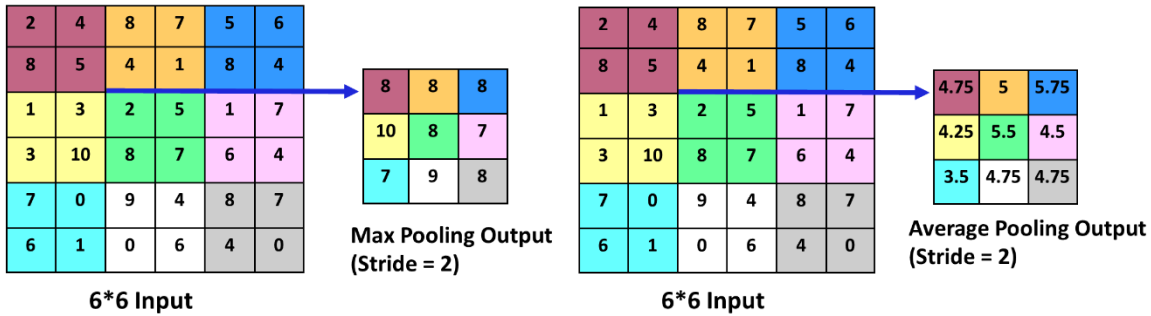


Fig 3.3 Max and Average pooling illustration example for 6\*6 input image

### 3.1.1.5 RGB Colour Model

RGB is a red-green-blue colour scheme that defines the image colour. The three colours are added together to reproduce diverse different colours. In CNN image processing, each colour is encoded by numbers from 0 to 255, where 255 is black, and 0 is white (brightest). Colours other than red, green, and blue can be represented by 3 different values “R G B”. For example, “210 0 210” is an RGB representation of the magenta colour. Also dark blue is R = 0, G = 0, and B = 100 or “0 0 100”

## 3.1.2 Image inpainting and CNN

Compared to other methods, this method exploits the avoided post-processing for the images since it uses partial CNN, which robustly works on predicting missed pixel values. The predicted image will no further need blending operations. (Liu, Reda et al. 2018)

Partial CNN means no modification will take place on non-hole regions on the image where the pixels have missing data; instead, the filters will only operate on the unmasked pixels. The process will look into local regions rather than the whole image, efficiently decreasing the number of parameters. In addition, the code has an automated updating mask in each step where the CNN kernel was successfully predicted, resulting in filled pixels. Hence, decrement of the operations in each successive time step, and the filled valid pixels will be part of predicting the missing values in the next time steps (Liu, Reda et al. 2018).

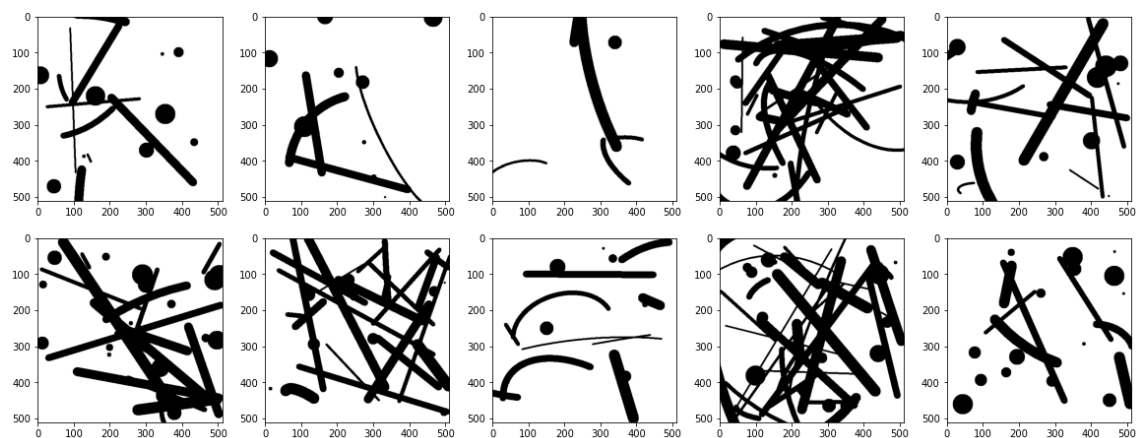
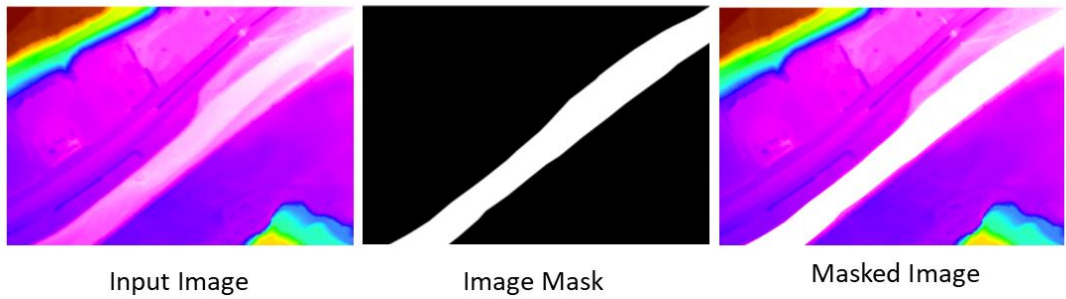


Fig 3.4 Random Generated Binary Mask for CNN Operation (Liu, Reda et al. 2018)

This study sought to examine the potential of image inpainting using CNN for predicting river subsurface bathymetry of Red Lidar data. The general idea of this method was to train the CNN model to predict the missing pixel value based on the neighboring RGB pixel values. Green and Red Lidar have the same topographical values and differ only on subsurface bathymetry.

Therefore, the concept was clipping large number of Green LiDAR images with the masked river as input and a sufficient number of targeted outputs to have a fully trained model with the capability of predicting the missing pixel values on areas with Green Lidar data to evaluate the model performance. Fig 3.5 presents an example of masked image data From Gaula river for CNN training. A trained CNN model can be used for predicting river bathymetry for rivers where only Red LiDAR are available. The predicted bathymetry can be used as an input for hydraulic models to determine inundated areas for vaying flood discharge scenarios



*Fig 3.5 An Example of the Input Masked Image from Gaula for CNN Training*

### 3.1.2.1 Preliminary Test for the Method

Data used on a preliminary test for the method was a bathymetry image clipped from a Green LiDAR image with multi RGB values representing the elevations. The image was clipped from Gaula DEM. The tested image was one fixed image as shown on the left image in Fig 3.6, while the mask (middle image) was rotating over large masks database. This implies, the training was done on different shapes of masks. The test used the image inpainting algorithm by (MathiasGruber 2019) as machine learning operator for the CNN model. At the same time, the full clipped image is used as the targeted output for the model.

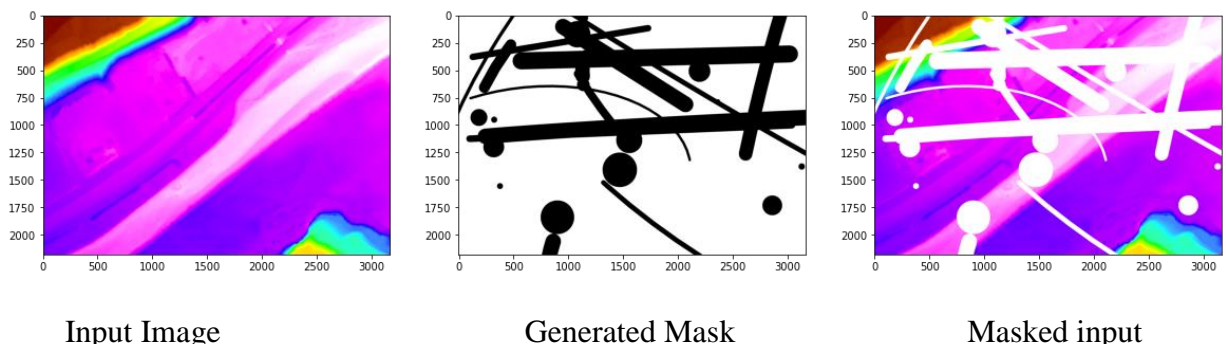


*Fig 3.6 An Example of the Randomly Generated Mask on Gaula River*

## 3.2 1-Dimensional training

### 3.2.1 Artificial Neural Network

Artificial neural networks are computation systems consisting of fully or partially connected neurons or nodes (Yegnanarayana 2009). ANN structure consists of an input, hidden, and output layer. Each layer has a specified number of neurons that transmit the information to other neurons through mathematical equations. The receiver node processes the equation and transfers it to the next layer until the output layer (Fig 3.7).

The mathematical signal applied to the network training is based on weight (w) and bias (b). They are the learnable/trainable parameters that transform the data to find the best fitting model between the input and the output, as represented in  $O = f(W_1X_1 + W_2X_2 + \dots + W_nX_n + b)$  Eq 3.1, where O is a neuron output, X is changeable variables. Each neuron will receive a weighted sum of input from the previous layer plus the bias.

Bias values are the threshold to determine whether the neuron is activated and be passed forward to the rest of the network, considering more model flexibility. Flexibility means more neurons will be activated for forward propagation.

$$O = f(W_1X_1 + W_2X_2 + \dots + W_nX_n + b) \quad \text{Eq 3.1}$$

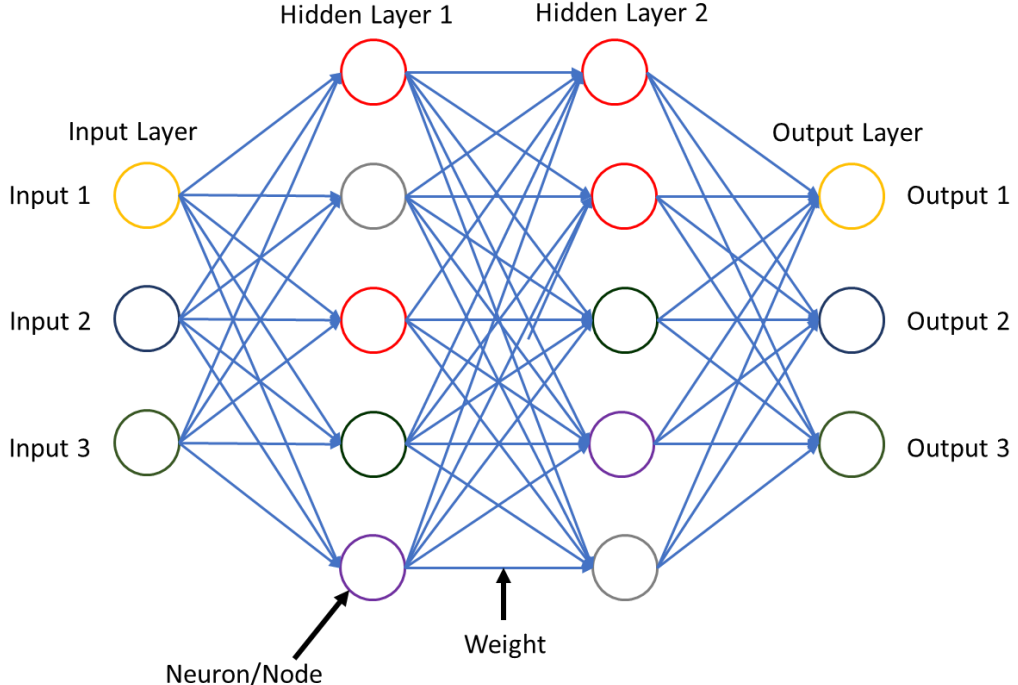


Fig 3.7 General Structure of Artificial Neural Network

### 3.2.2 Activation function

Machine learning algorithms will learn linear regression fitting straight lines to the training set as a first step. In this case, not all the data will reasonably be represented and capture the true relationship between the input and output data. Therefore, the activation functions are essential tools for adding nonlinear properties to the model output since the model will have considerable bias. In other words, the bias will help the activation function in increasing the model flexibility to fit the data. The weighted sum added to the bias received from a neuron will be passed to the activation function.

The activation function has many types, 3 of them have been tested here (Linear, ReLU, and Sigmoid) as shown in Fig 3.8. The selection of the adequate activation function has many factors, such as the data type and the targeted task.

### 3.2.3 Loss Function

The loss function or cost function is one of the structured parameters in building a training model in machine learning. It is a method of quantifying the error between the fed or targeted output and the algorithm output. Several loss functions are used in measuring the error. Each of these types has a different algorithm for loss evaluation. In this model, the MSE is used to

find the squared difference between what the model predicted and the targeted output ( $e$ ), then finding the average as shown below in Eq 3.2.

$$MSE = \frac{e1^2 + e2^2 + \dots + en^2}{n} \quad Eq\ 3.2$$

The loss calculation is executed at the end of each training step or epoch. It will be updated constantly since the model weight and bias are changing in forward and backward propagation. The loss is calculated for both training and validation.

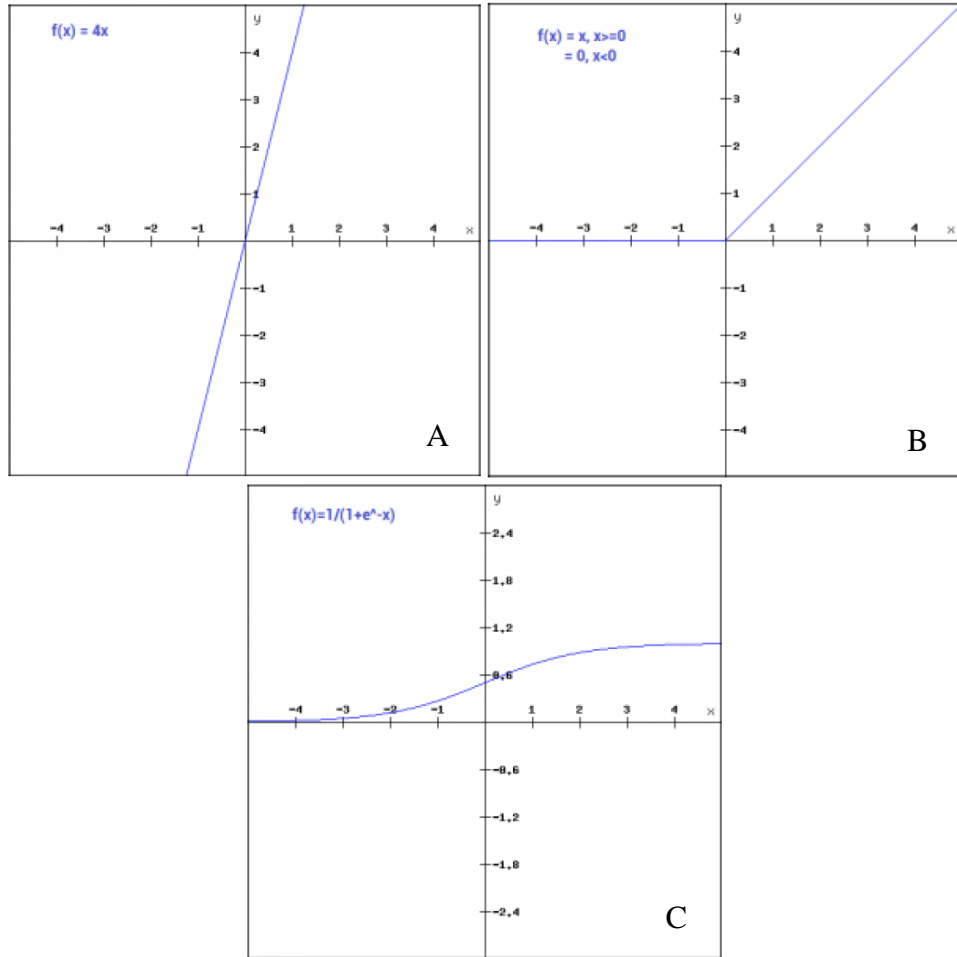


Fig 3.8 A, B, and C are Linear activation function, ReLU activation function, and Sigmoid activation function respectively (Sharma, Sharma et al. 2017)

### 3.2.4 API Keras

In this method, neural network high-level API code Keras was used for easy implementation of neural networks. It is written in Python and runs on a machine learning platform. Keras is one of the robust machine learning problem solvers. It has a high iteration velocity; it uses deep learning frameworks such as TensorFlow as a backend for faster computation.

In Keras, we can build a sequential model for machine learning problems. The sequential model can simply be built in Python as shown in Fig 3.9. Keras sequential is defined as a “model is appropriate for a plain stack of layers where each layer has exactly one input tensor and one output tensor” (TensorFlow 2022).

The full sequential model architecture includes the number of hidden dense layers, input shape, and the suitable activation function connected to each layer.

```
# model creation & adding Layers
model = Sequential([
    Dense(164, activation= "relu", input_shape=(400,)),
    Dense(164, activation= "relu"),
    Dense(400, activation= "linear"),
])

model.summary()

Model: "sequential"
-----  

Layer (type)          Output Shape         Param #
-----  

dense (Dense)         (None, 164)          65764  

dense_1 (Dense)       (None, 164)          27060  

dense_2 (Dense)       (None, 400)           66000  

-----  

Total params: 158,824  

Trainable params: 158,824  

Non-trainable params: 0  

-----  

# compile model
model.compile(optimizer = "rmsprop",
              loss= "mse")
model.summary()

Model: "sequential"
-----  

Layer (type)          Output Shape         Param #
-----  

dense (Dense)         (None, 164)          65764  

dense_1 (Dense)       (None, 164)          27060  

dense_2 (Dense)       (None, 400)           66000  

-----  

Total params: 158,824  

Trainable params: 158,824  

Non-trainable params: 0
```

*Fig 3.9 Keras Sequential Model Structure and Compilation*

To summarize the neural network training workflow, input data is passed into a structured model, the weights are multiplied by each neuron variable and added to bias, and the output is passed to an activation function for non-linearities. This will be a definition for the neurons in

the next layer. This operation is called forward propagation as we propagate the information from the first input layer to the final output. When the output value is calculated, the difference error between the output and the calculated output is found. This loss is used to compute the partial derivative with respect to the weights in each layer propagating backward, and then the weights will be updated. The process is repeated for each epoch until the error is the smallest.

### 3.2.5 Data

#### Terrain

The data used in this study has been prepared with the help of ArcGis Pro, using the river terrain for both topography and bathymetry raster images. The Green LiDAR is a representation of the true river bathymetry. The Red LiDAR is considered in this study to have identical topographical data with Green LiDAR, and minor discrepancies are ignored, except for river wetted zones. Gaula, Surna, and Driva are selected for the model training and testing. The LiDAR terrain was generated by the Norwegian Mapping Authority on [Høydedata.no](https://www.hoydedata.no). The DEMs has resolution of 0.25 m for Driva and Gaula and 0.5 m for Surna (Awadallah, Juárez et al. 2022).

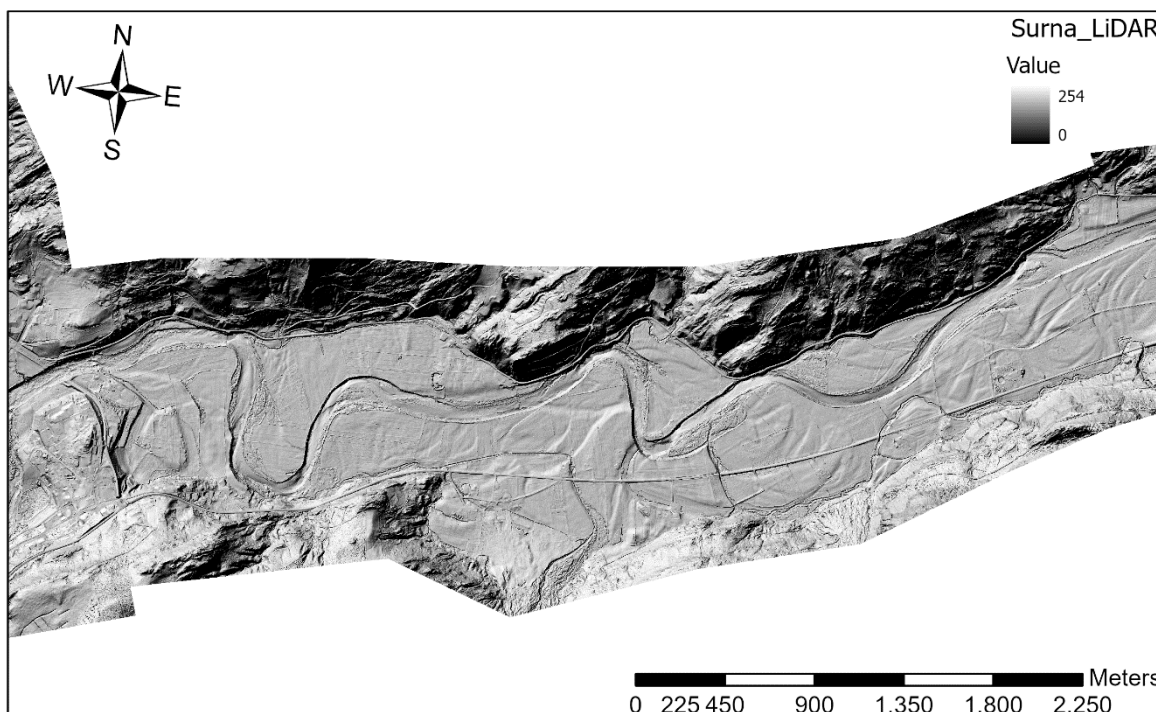


*Fig 3.10 Green LiDAR terrain for Surna river*

#### Flood Data

The flood values have been selected from a previous study based on the Norwegian Water Resources Directorate NVE [NEVINA.no](https://www.nve.no). The flood scenarios are calculated with regional flood frequency analysis.

*Table 3.1 Tested Flood in m<sup>3</sup>/s Scenarios Based on [NEVINA.no](https://www.nve.no) (Awadallah, Juárez et al. 2022)*

River	Qm	Q10	Q100	Q500
Driva	545	725	960	1115
Surna	171	230	306	355

### *Data Preparation Using ArcGIS Pro*

ArcGIS Pro supported by ESRI, is the tool used for data preparation. It was used to prepare the input training data for the ANN algorithm model and the hydraulic simulation.

For the input training data, the DEMs for Green and Red LiDAR for Gaula were used for cross sections extraction. The mainstream polygons for Gaula, Driva, and Surna were taken from this study (Awadallah, Juárez et al. 2022). The polygons were edited to fit the mainstream boundaries. A centreline was created for the existing polygon. Considering the observed average river width, 200 m length transects were created each 10 m distance along the river centreline. After that, points were generated along the transects every 0.5 m for elevations values extraction, then the average pixel value from neighboring pixels was extracted into the points for both Green and Red LiDARs. The attribute table now contains the Green and Red LiDAR elevation points value for each transect along Gaula.

The attribute table was extracted as a CSV file to provide input data for the ANN model and easier implementation.

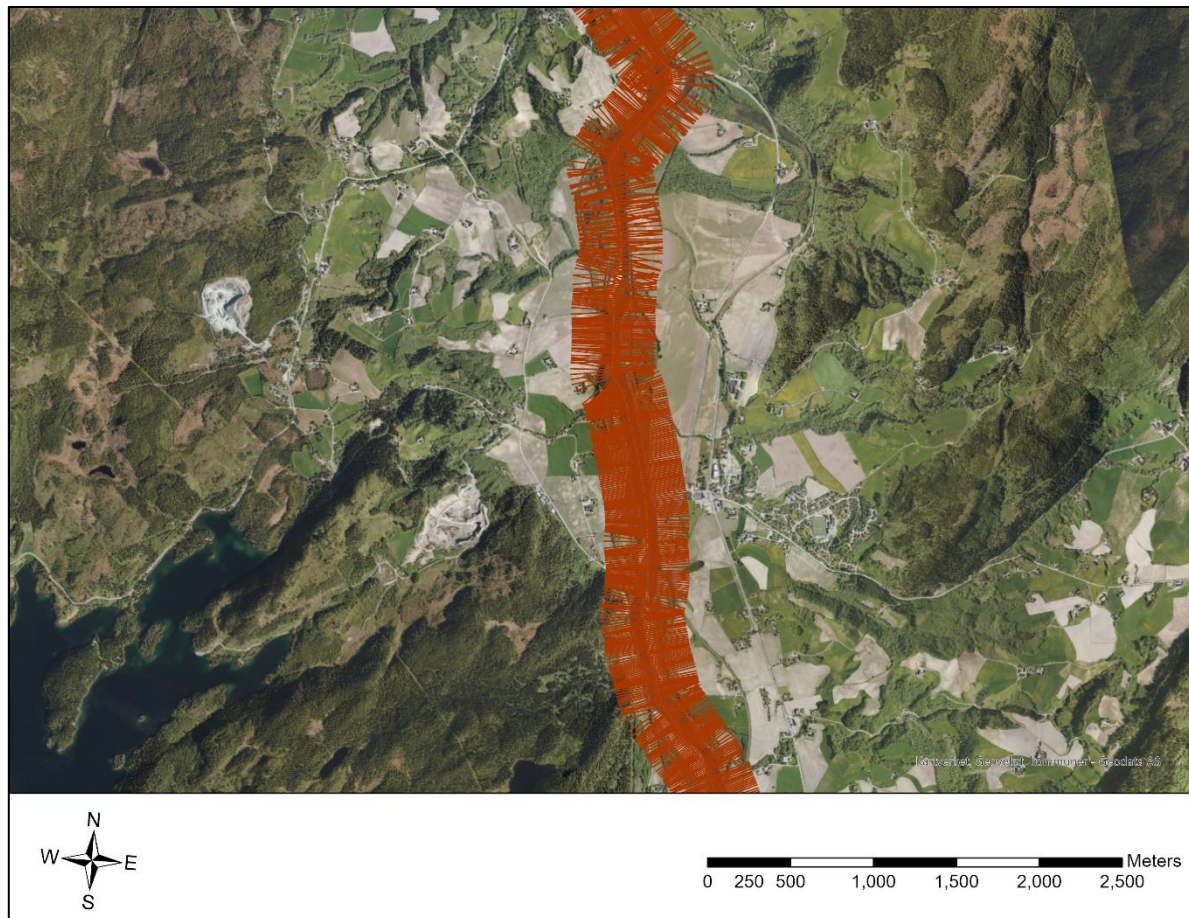


*Fig 3.11 Transects and Points Along Gaula River*

The predicted bathymetry points were extracted from Python as a CSV file with X, Y coordinates system ETRS1989\_UTM\_Zone\_32N and imported into the ArcGIS program. The predicted cross-sections contained a prediction for the topography elevation values (riverbanks) that were covered by Red LiDAR and not targeted in this study. Therefore, the predicted points were clipped to keep only the wetted zone using the geoprocessing clipping tool. The clipped points transformed into raster as shown in Fig 3.12 B, the raster's cell size is 0.25 m for Driva and 0.5 m for Surna. To test the flood inundation coverage, the Green LiDAR terrain was

clipped using a generated polygon domain, then the mainstream was erased, this will give the geometry for the banks as illustrated in Fig 3.12 A. The predicted bathymetry raster and the Green LiDAR topography domain raster merged into one terrain and processed to fill missing pixel values (Fig 3.12 C) to achieve a DEM with identical banks for the accurate bathymetry and prediction. In addition, the residual between the Green LiDAR and predicted bathymetry was found. This procedure has been done for Driva and Surna.

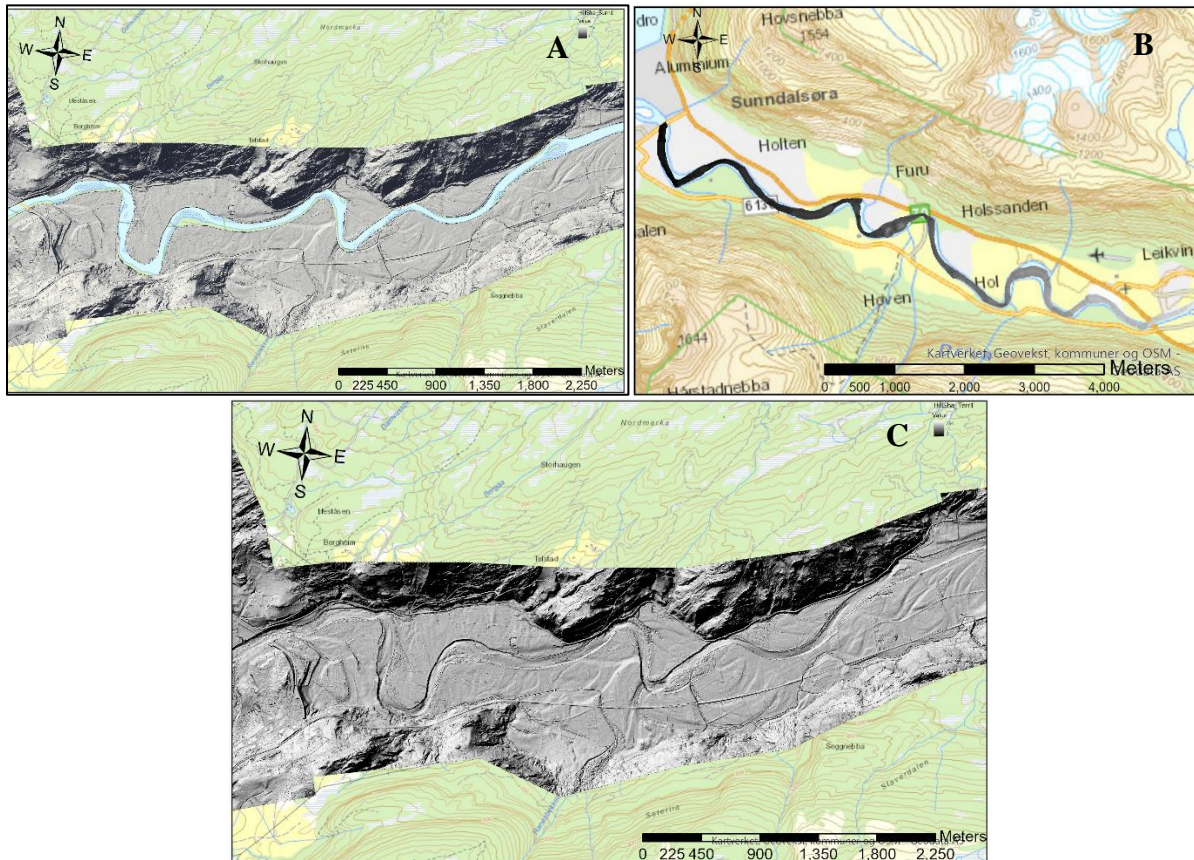


Fig 3.12 A, B, and C are the clipped Green LiDAR raster, the predicted Points raster, and the mosaiced raster

### 3.2.6 Artificial Neural Network Model Setup and Training Scenarios

For ANN application, API Keras code was applied for different scenarios. All the training trials were applied to the exported data from Gaula river. The data structures were Pandas dataframe and NumPy arrays for easier analysis. Jupyter Notebook platform through ANACONDA distributor was chosen for Python script writing. The three rivers later for testing were selected based on approximate sizes.

The deep learning model structure with Keras Sequential model linked with TensorFlow is created from one input dense or fully connected layer, two hidden dense layer with 164 neurons, and one output dense layer. The input and output neurons shape had a length similar to the number of points on relevant transects. For model compilation, parameters passed into the model structure are: root mean square error optimizer (rmsprop) to optimize and update the weights and learning rate to minimize the loss score through back propagation. The other parameter is the loss function selection, in this case, MSE was selected. For training arguments were passed to Keras *model.fit* which is the operator for applying the optimizer connected to the loss function to train machine learning algorithm. The data for all training trials were split

into 80% for training and 20% for validation. The shuffling argument was selected for random training.

Three different scenarios for data training have been tested to investigate the most reasonable output predicted results:

- From Gaua 200 m transects with 400 points covering the mainstream and parts of the floodplains were considered. 100 Green LiDAR elevation points on right and left banks were fixed, forming the model input from 1200 cross-sections. The input dataframe dimension = [number of trained cross-sections × 200].

The mainstream Green LiDAR elevation points were the targeted output, represented by 200 points in the middle. The output dataframe = [number of trained cross-sections × 200]. The number of trained cross-sections was changed according to different trials.

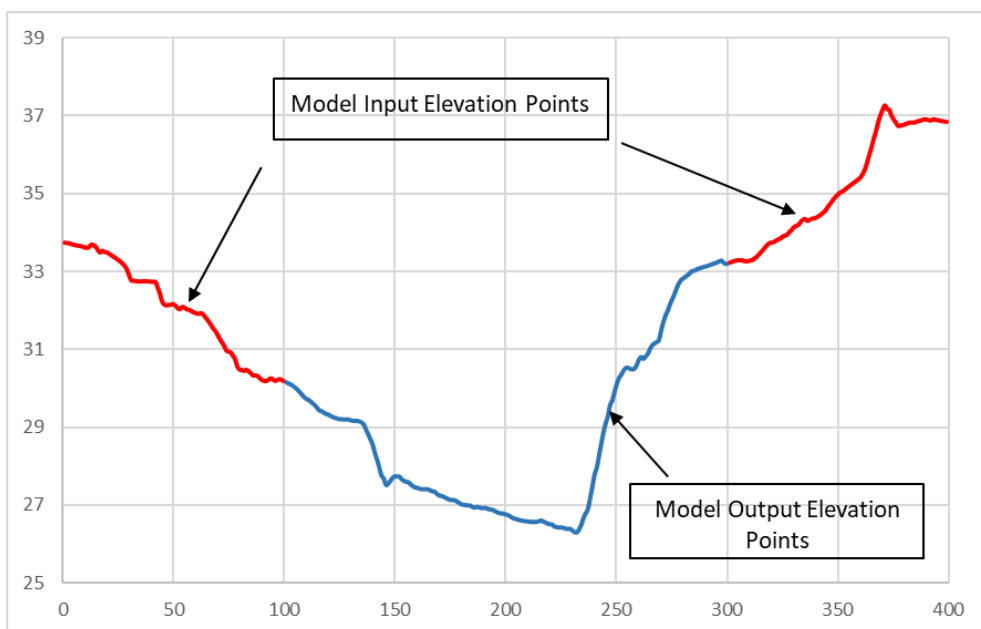


*Fig 3.13 Cross Section Example of Input and Output Green LiDAR Elevation Points*

- Since the river width was varying along the stream and fixed number of points in banks and mainstream will not be representative in different parts, the second trial was trying to make the input dataframe flexible with each river cross-section width. Meanwhile, the dataframe is fully controlled by a rectangle shape. Therefore, the input and output dataframe size considered the widest cross-section along the river. To maintain the network shape for the input and the output, the empty zones in shorter cross sections filled with Zeros as Keras does not support the NaN or Na values.
- The fourth trial was lengthening the transect for more data consideration. 400, 500, 600, and 700 m transect lengths were tested. The input shape was similar to trial c with more input points.
- The third trial considered the full Red LiDAR elevation points as input data for the model, and the full Green LiDAR elevation points are the targeted output. Dataframe size was controlled because the transects had the same length along the whole river. The number of points varied by one point, some transects has 399 points and others has 400 points. To fit the dataframe size, one last row was added to the 399 points, the row elevation values were equal to row number 399.

### 3.2.7 Prediction and Testing

After the last epoch step, the model algorithm was ready for testing on different rivers. For each mentioned trial, testing was carried out on parts of Gaula where the cross-sections were not included in the deep learning training to investigate the model performance out of the training set zone. Then to generalize the algorithm application, it was also tested on the other two rivers, Driva and Surna.

### 3.2.8 Hydraulic Simulation

The predicted elevation points from Surna and Driva were tested in a flood model using Hydrological Engineering Center's River Analysis System HEC-RAS (version 6.0.0). The model setup was taken from a previous study for Red and Green LiDAR (Awadallah, Juárez et al. 2022). The generated raster terrain for Surna and Driva was used to run the flood simulation.

2D simulation with a  $5 \times 5$  m mesh cell size was used, applying a diffusive wave equation for speed iterations and steady flow simulation. Different scenarios for flood flow hydrograph was considered for upstream boundary conditions and normal depth for downstream boundary condition considering unsteady flow simulation. A Manning's coefficient value of 0.06 was used for river banks and 0.03 for the wetted zone (Awadallah, Juárez et al. 2022). The hydraulic simulation compared the flood inundation area from the predicted bathymetry with both Green and Red LiDAR inundations using the error formula.

$$\text{Percentage Error} = \frac{\text{Green LiDAR inundation area} - \text{Prediction inundation area}}{\text{Green LiDAR inundation area}} \times 100\% \quad Eq\ 3.3$$

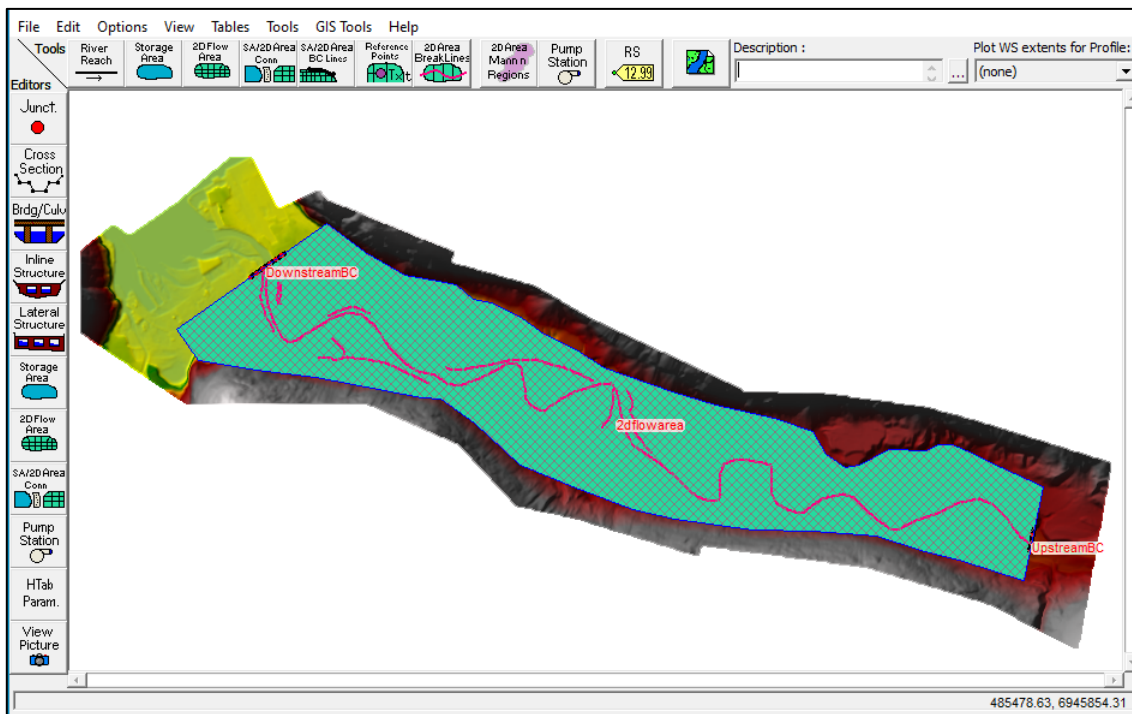


Fig 3.14 2D Flow Area and the Generated Mesh  $5 \times 5$  m

# Chapter 4 Results and Discussion

---

This section presents the results from the two machine learning methods. The first method is image inpainting, precursory test output will be illustrated and discussed. Secondly, ANN training results for trials a, b, c, and d will be shown. In addition, the flood hydraulic simulation inundation maps for mean, 10, 100, and 500 years flood discharge will be presented. More detailed graphs and maps for CNN output, ANN cross-sections training for each scenario, and Python scripts for both methods are appended to the Appendices section.

## 4.1 Image inpainting

The image inpainting is based on the RBG colouring index for image processing. The masked white areas were predicted with partial CNN, where the kernels filled the masked pixels depending on surrounding pixels values. Fig 4.1 shows the predicted image progress in the last two epochs. The missing pixel values were reasonably predicted compared to the targeted output image. Meanwhile, the mainstream at non-holed areas were deepened even though the pixels have existing values before the training. Higher altitudes impact is not significant, but it worth to mention the change of colours in the top left colour.

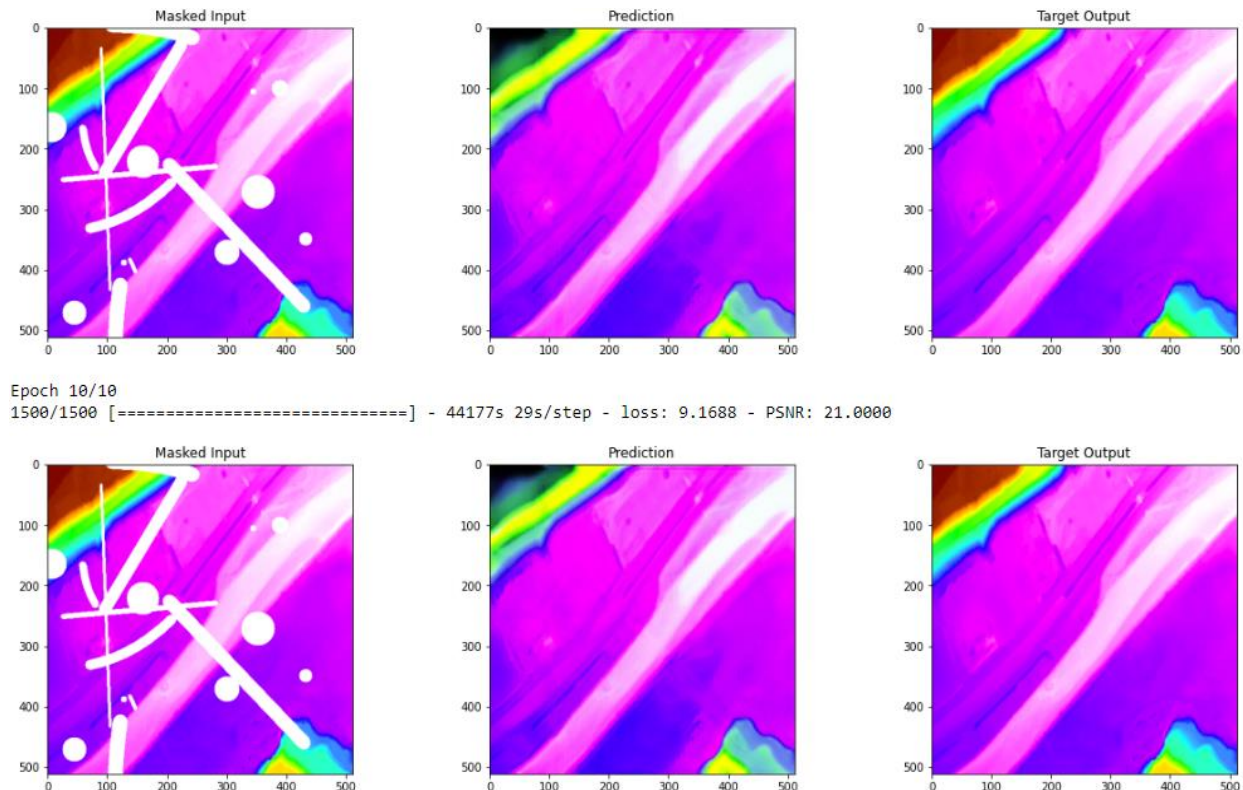


Fig 4.1 Last Two Predictions in Image Inpainting Training

Image inpainting is expected to be more successful with further testing and modifications on the targeted output and the masking type. However, training CNN on images was found to be computationally expensive and time consuming process. For instance, running the preliminary test took 8 days for completion. Moreover, data pre-processing for training was complicated and demanding task; more than 55000 masks were prepared for the training dataset, and 12000 masks for testing datasets. In return, preparing the river masks, the corresponding masked images, and the full targeted output images will be time-consuming. As the masked zones will be along the mainstream, unlike the preliminary test, more missing values exist. Thus, the algorithm requires huge amount of Green LiDAR images and masks to predict the missing data with acceptable accuracy. The method application was stopped, and we decided to move to another faster machine learning method with one-dimensional training using ANN.

## 4.2 1-Dimensional ANN

The training datasets were taken from Gaula in all scenarios. The remaining cross-sections, which were not included in the training, were used in testing the model performance. In addition, the models were tested in two other rivers. All the figures below illustrate results tested on sections out of the training zone in Gaula. Besides, selected results from Driva and Surna.

### 4.2.1 Scenario a

In this scenario, a fixed number of Green LiDAR elevation points was chosen in the banks (input data) and mainstream (targeted output) to train the model. The fixed lengths of inputs and outputs points of the cross-section was representative to some of the parts of Gaula river. The trained model in this scenario performed well for some cross-sections in which river and banks widths was similar to those used for model training. Fig 4.2 presents examples of these results which shows a slight discrepancy between the prediction and the Green LiDAR.

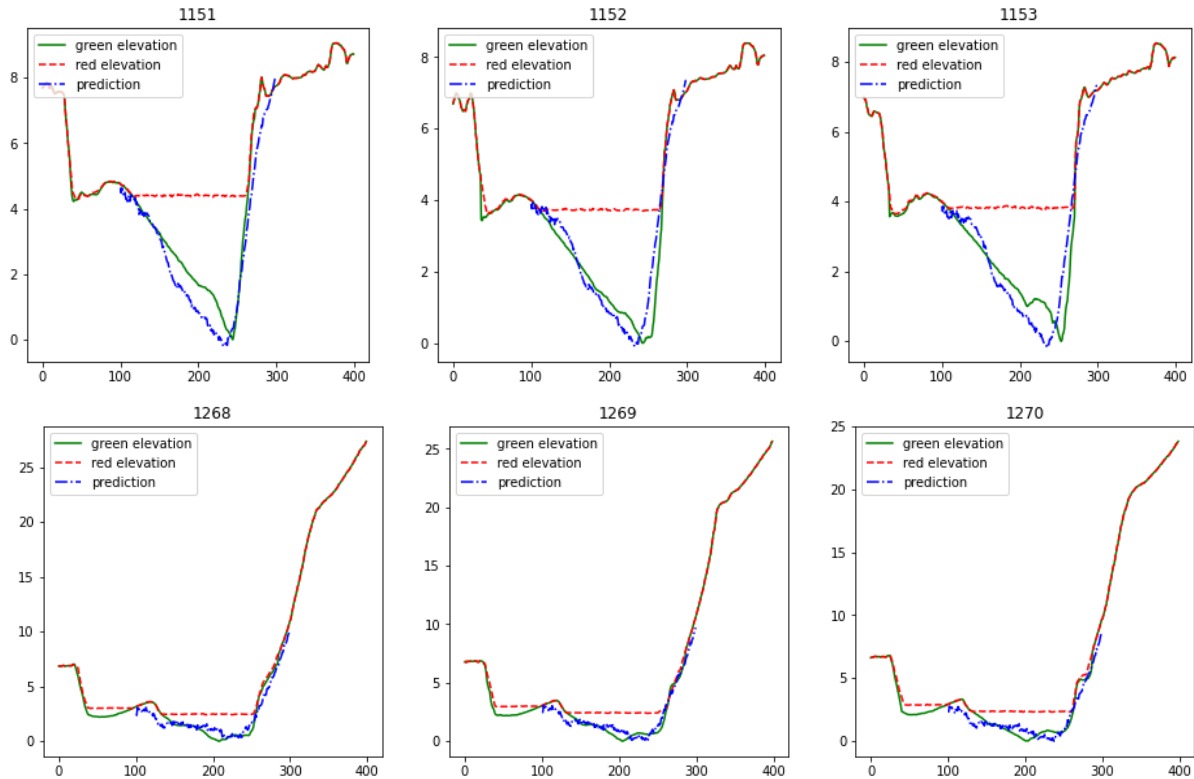


*Fig 4.2 An Example of Consistency Between the Selected Number of Points and the Actual River Cross Section*

In contrast, the majority of the predicted results have a large discrepancy between the prediction and the actual riverbed as illustrated in Fig 4.3. This happens for cross-sections in which the river and bank widths differ significantly from those used in model training. Therefore, selecting fixed number of points will increase the model sensitivity to the river width and banks steepness. Moreover, decreasing the model flexibility.

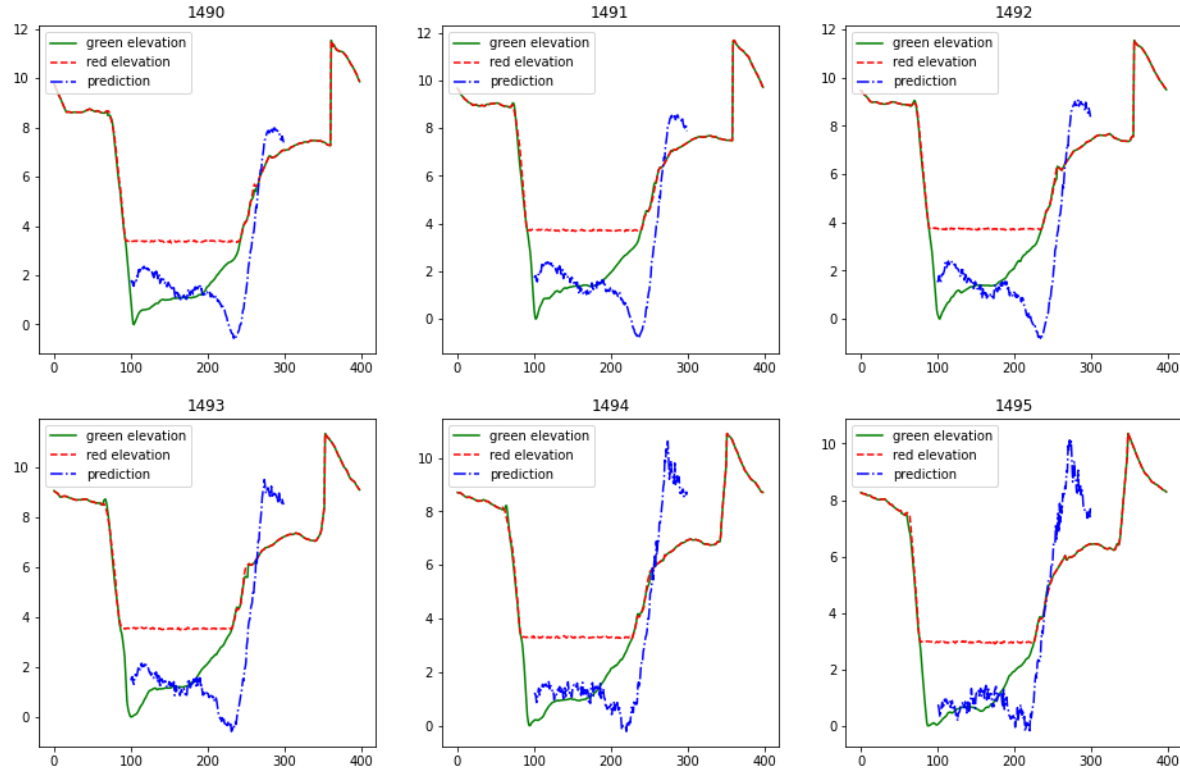


*Fig 4.3 An Example of Inconsistency Between the Selected Number of Points and the Actual River Cross Section*

#### 4.2.2 Scenario b

As mentioned before inflexible model will not perform well in different river widths. Therefore, the idea of inserting changeable input and output in each river transect according to the mainstream polygon was adopted in this scenario. Where outside the polygon domain is considered input, and the points inside the polygon domain are considered as targeted output. The river width varied between 300 to 1000 points. The dataframe missing values filled with zeros to maintain the input/output structure. Keras was considering the Zeros as integer values during training, which severely affected the algorithm results as shown in Fig 4.4. The zeros were arbitrary values for maintaining the input and output dataframe shape. The method has predicted a riverbed below the Red LiDAR but with large deviation. The dataframe width is equal to the longest cross section. Hence, when predicting the narrow cross sections, the algorithm will fill the banks with zero values.

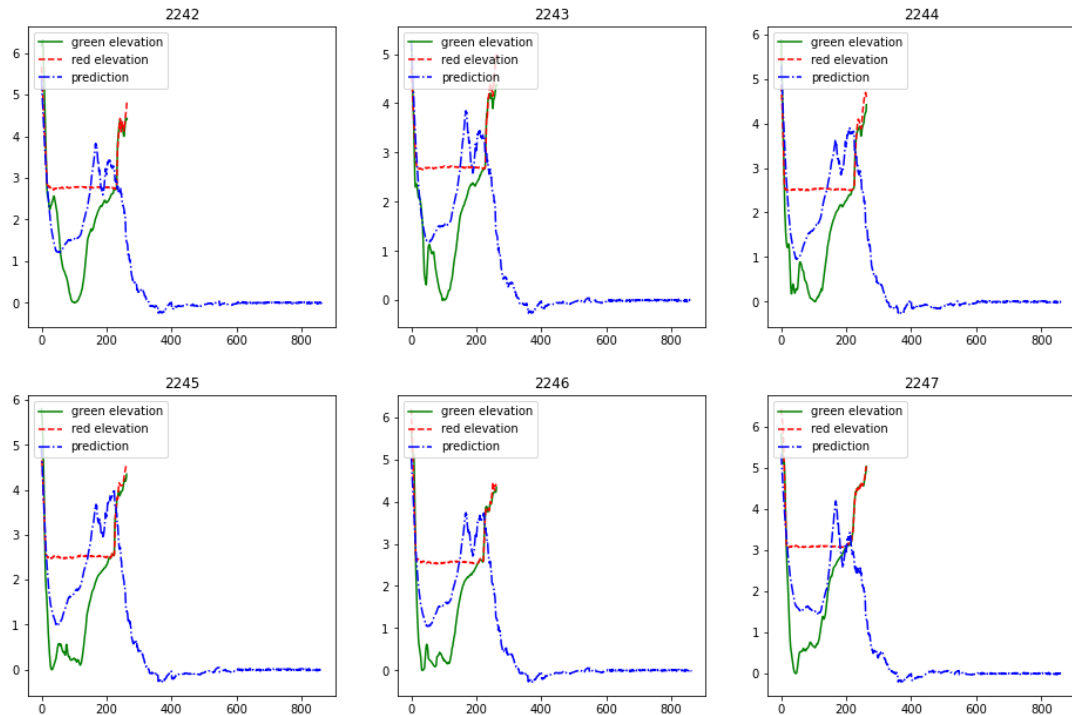


*Fig 4.4 An Example of Prediction Results Using for Scenario b*

#### 4.2.3 Scenario c

Entire section training was used to overcome the gap filling issue on a dataframe. In comparison with the previous two scenarios, and complete neglection to the predicted banks, the algorithm adequately derived the predicted bathymetry on simple cross sections formations as shown in Fig 4.5 A. Nevertheless, some parts have detected deviations from the actual riverbed. On the other hand, complex formation with two or more channels or islands had a relatively large discrepancy (Fig 4.5 B). In view of the fact that the majority of training datasets was simply shaped cross sections. The model was tested in other two different rivers, Driva and Surna. The model performance was acceptable and introduced good results, despite the fact that the model was trained only in Gaula.

In this scenario, further investigation was done, Sigmoid and ReLU activation functions were tested. Two different convergence states were achieved for the same tested rivers. For example, in the Driva river (cross-section 135), the algorithm using ReLU was, to some extent, able to predict the river bathymetry on complex shape, even though the same dataset was used for the training using Sigmoid and ReLU. This highlights the importance of hyperparameter tuning for machine learning models. Hyperparameter tuning refers to the process of finding the most suitable machine learning structural parameters for the modelling task. These include activation functions, number of hidden layers, number of neurons and optimization parameters (i.e. algorithm, learning rate, momentum). Hyperparameter tuning is done by trial-and-error, or by optimization algorithms, such as genetic algorithm or Bayesian optimization. A proper hyperparameter tuning is expected to improve the accuracy of machine learning prediction. Therefore, it is recommended for future studies.

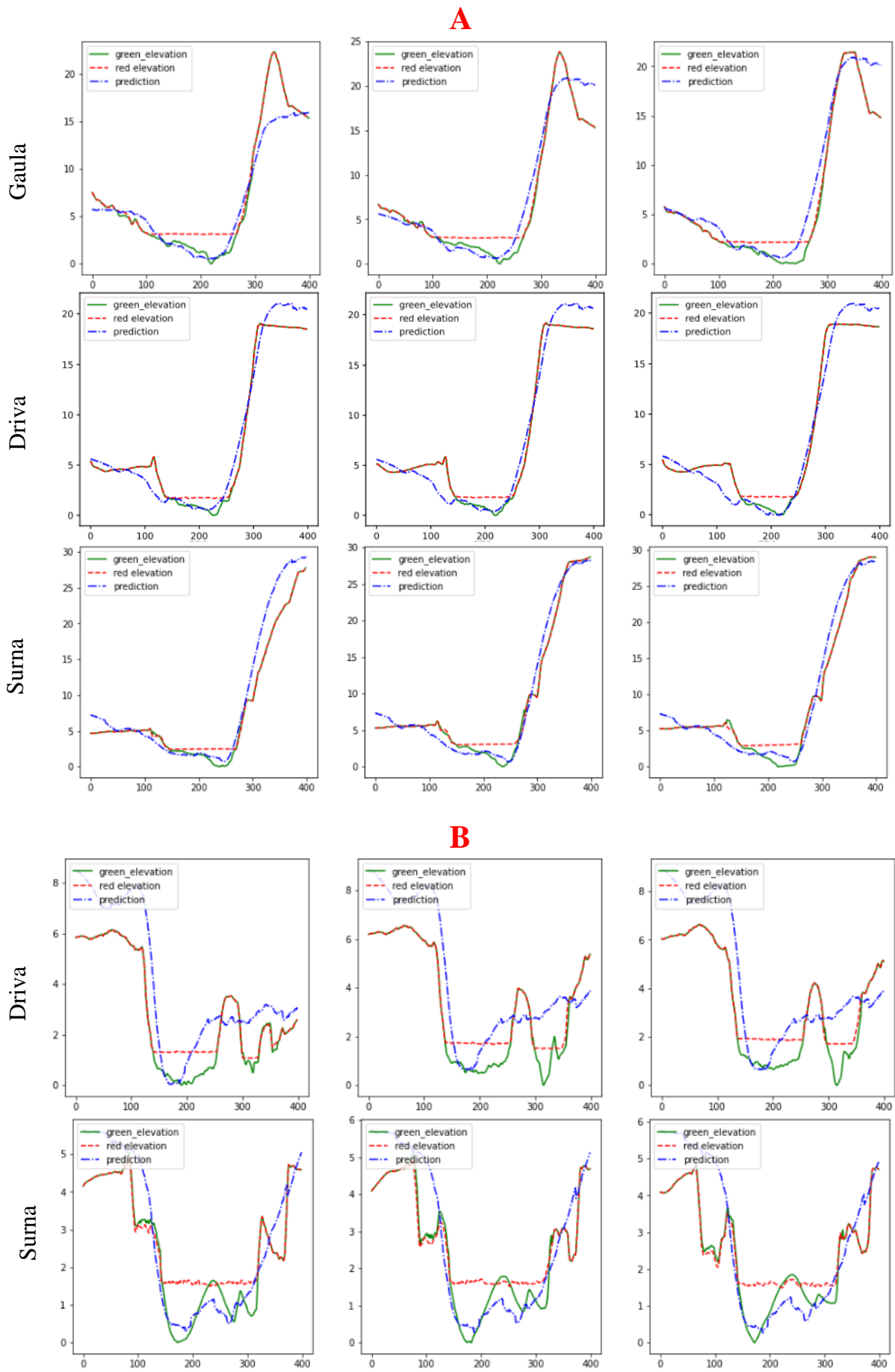


Fig 4.5 A and B Comparison Between simple(A) and Complex (B) River Channel

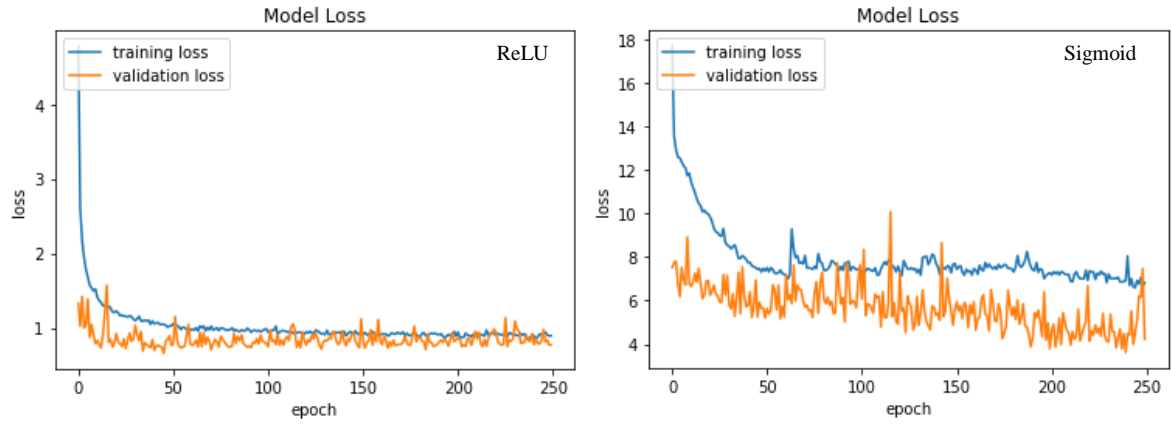


Fig 4.6 Show the MSE model loss for training and Validation

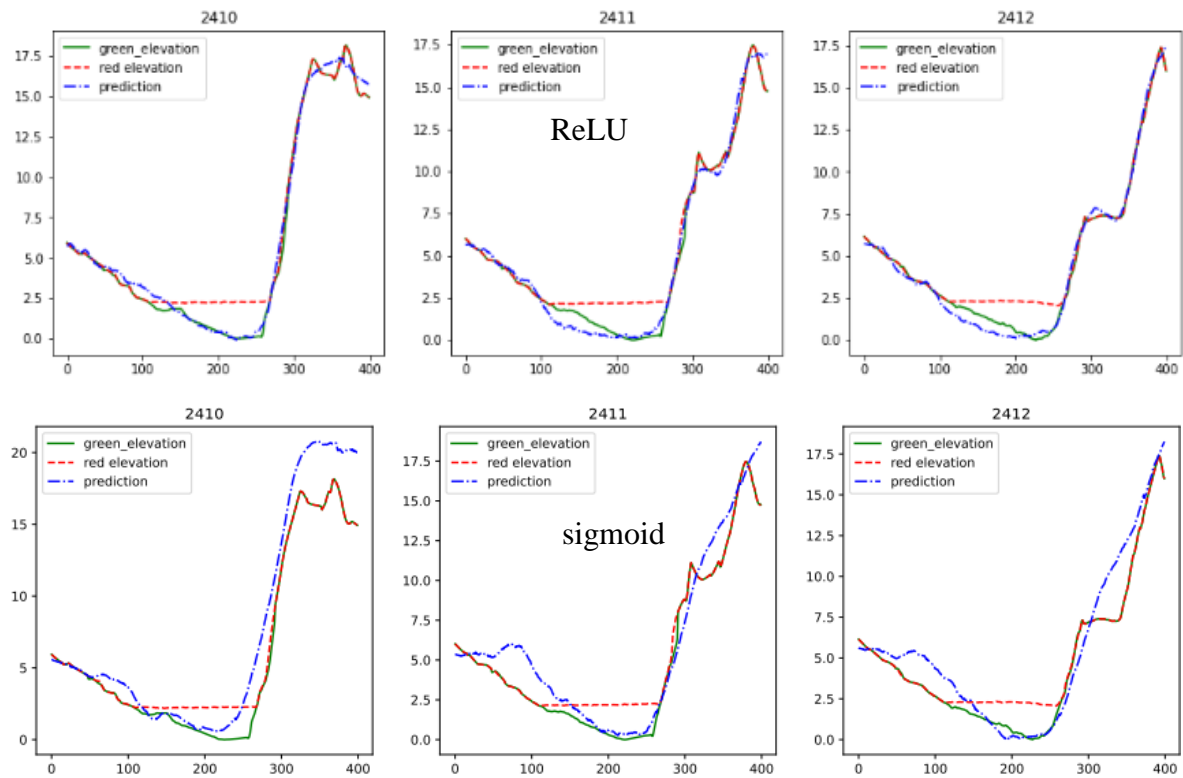


Fig 4.7 Comparison Between ReLU and Sigmoid in Cross Sections 2420,2411, and 2412, Gaula

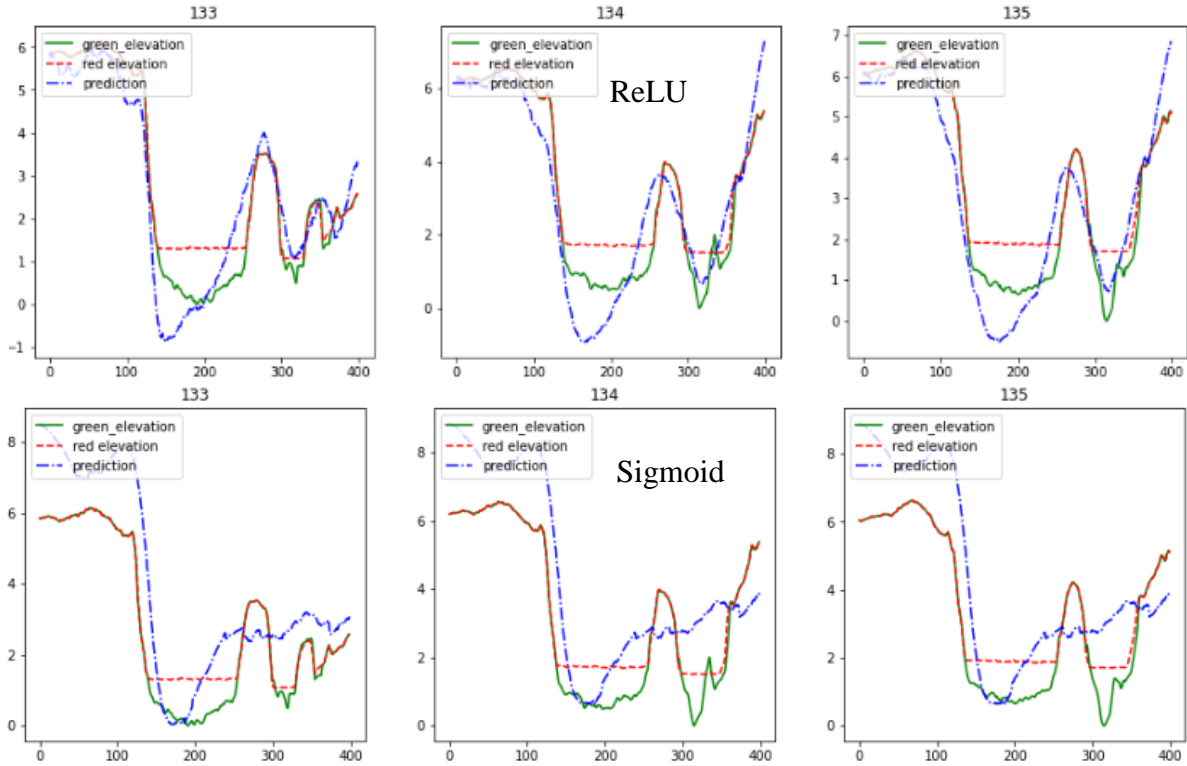


Fig 4.8 Comparison Between ReLU and Sigmoid in Cross Sections 133,134, and 135, Driva

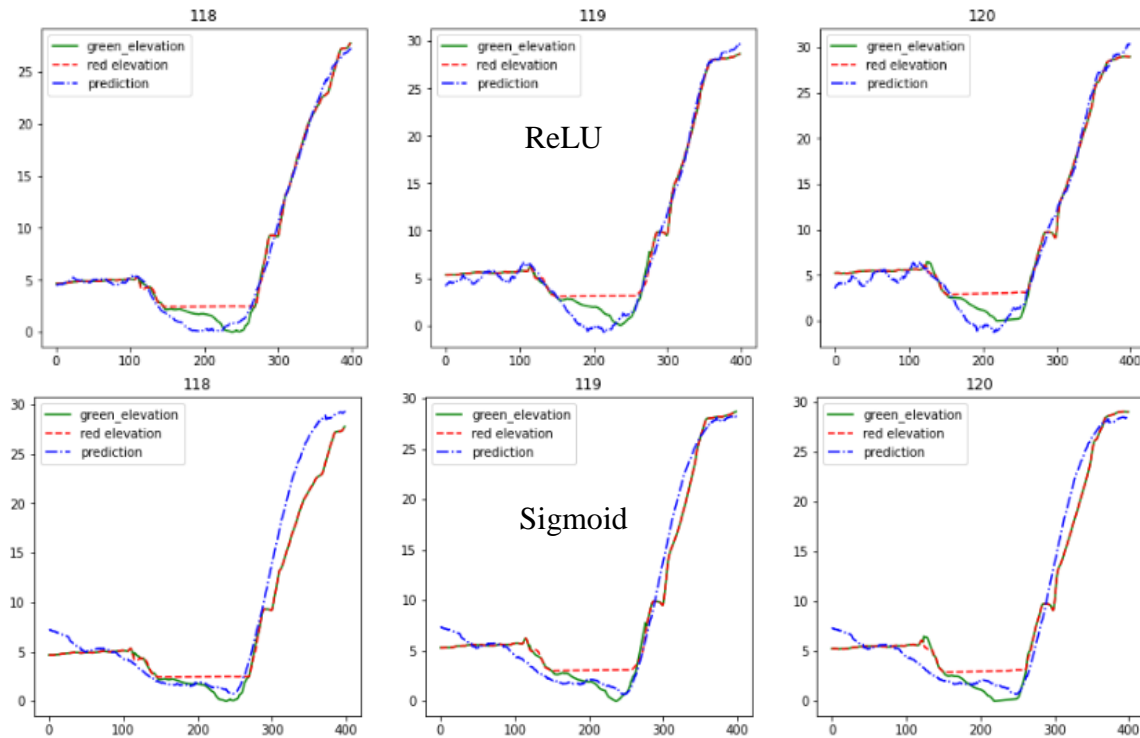


Fig 4.9 Comparison Between ReLU and Sigmoid in Cross Sections 118,119, and 120, Surna

#### 4.2.4 Scenario d

The training output from this scenario was affected by the banks' topography. Longer transects with more elevation points were extracted to test the model demand for data. Gaula river has

quite steep banks. Consequently, the algorithm considered higher values and could not predict the river bathymetry. The banks' training was under predicting the river bottom as shown in Fig 4.10. As a result, the transect length in correspondence to the river width is a significant factor in cross-sections extraction.

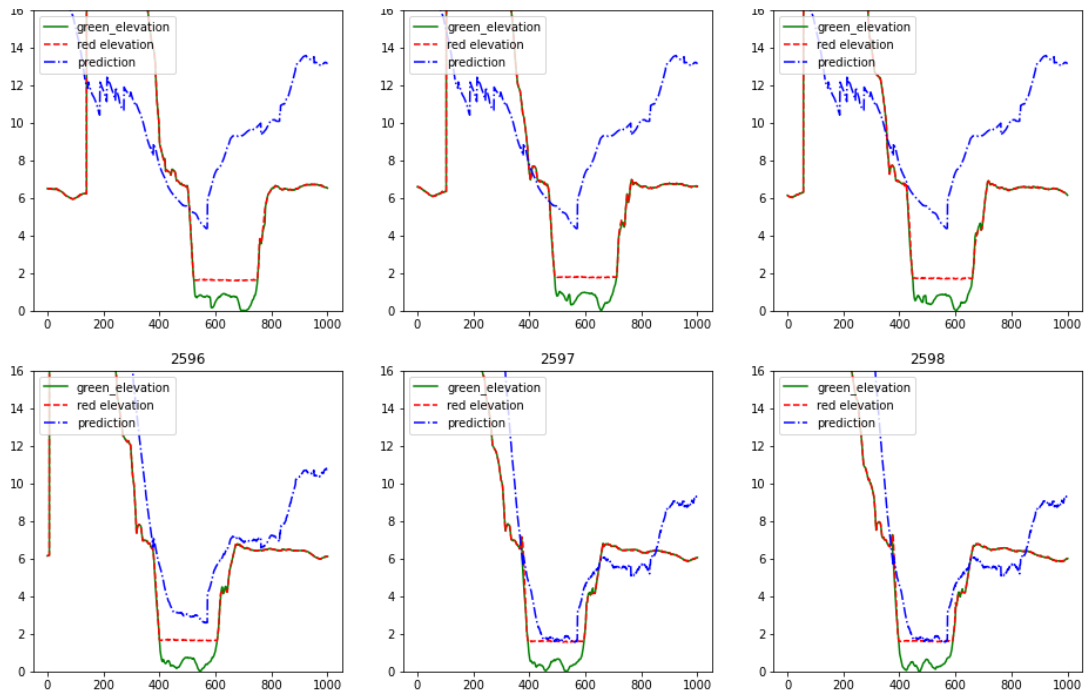


Fig 4.10 An Example of Results from Scenario d Training

#### 4.2.5 Residual Between Green LiDAR and Predicted Bathymetry (scenario c)

The vertical difference between Green LiDAR and Prediction rasters was found using the Minus tool in ArcGis Pro. The residual magnitude was higher in positive values, which means the algorithm overpredicted the bathymetry. On the other hand, the underprediction is more distributed among the residual map, as shown in Fig 4.11. In addition, the outer river bends are underpredicted where the riverbed has sediments accumulation. Residual = Green LiDAR raster – Prediction raster



Fig 4.11 Driva Green LiDAR and Prediction Residual

#### 4.2.6 Hydraulic Flood Simulation

Fig 4.12 illustrates the inundation areas obtained from the hydraulic flood simulation using 2D HEC-RAS in Driva. The prepared prediction DEM was used along with the Green and Red LiDAR DEM for comparison. For Driva river, flood inundation was overestimated in reaches with multiple streams (i.e. island), as shown in figure 4.11. This due to fact that ANN model failed to predict river bathymetries for section with islands, (see figure 4.5 and 4.6). On the other hand, flood inundation from the predicted terrain data matched well with those predicted by the Green lidar in reaches with single streams (i.e. without islands).

Table 4.1 compares the inundation areas generated by Green Lidar, Red lidar and the predicted terrains by the ANN. The latter yielded inundation areas with lower prediction errors than the Red LiDAR, when compared with the Green LiDAR. The error was reduced to approximately half in the mean flood scenario. While on the large flood scenarios, the improvement was 5%. In this simulation, the algorithm used to predict the geometry was built on the Sigmoid activation function. Due to time limitations, the geometry from the algorithm using ReLU was not used for flood investigation in Driva.

Table 4.2 shows the difference error in Surna. The algorithm used for the geometry prediction is based on ReLU activation function. From the presented values for all flood scenarios, the inundation area error was decreased. For example, in mean flood discharge the error decreased from 44.4% to -0.6%. However, the model overpredicted the riverbed in most cases and underestimated the flood with 8% in high flood scenarios. The model performed well in the reach where the bed formation is simple and missed the prediction in complex formations.

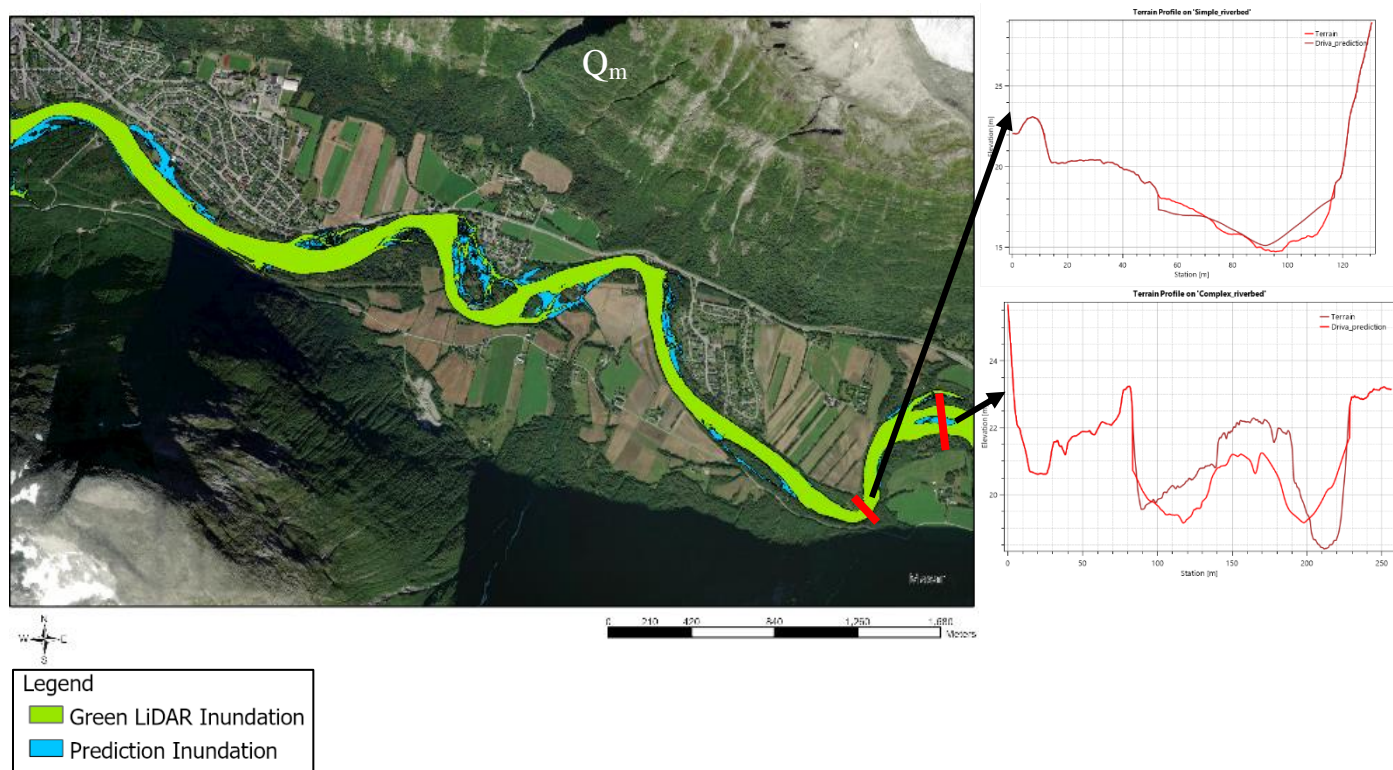
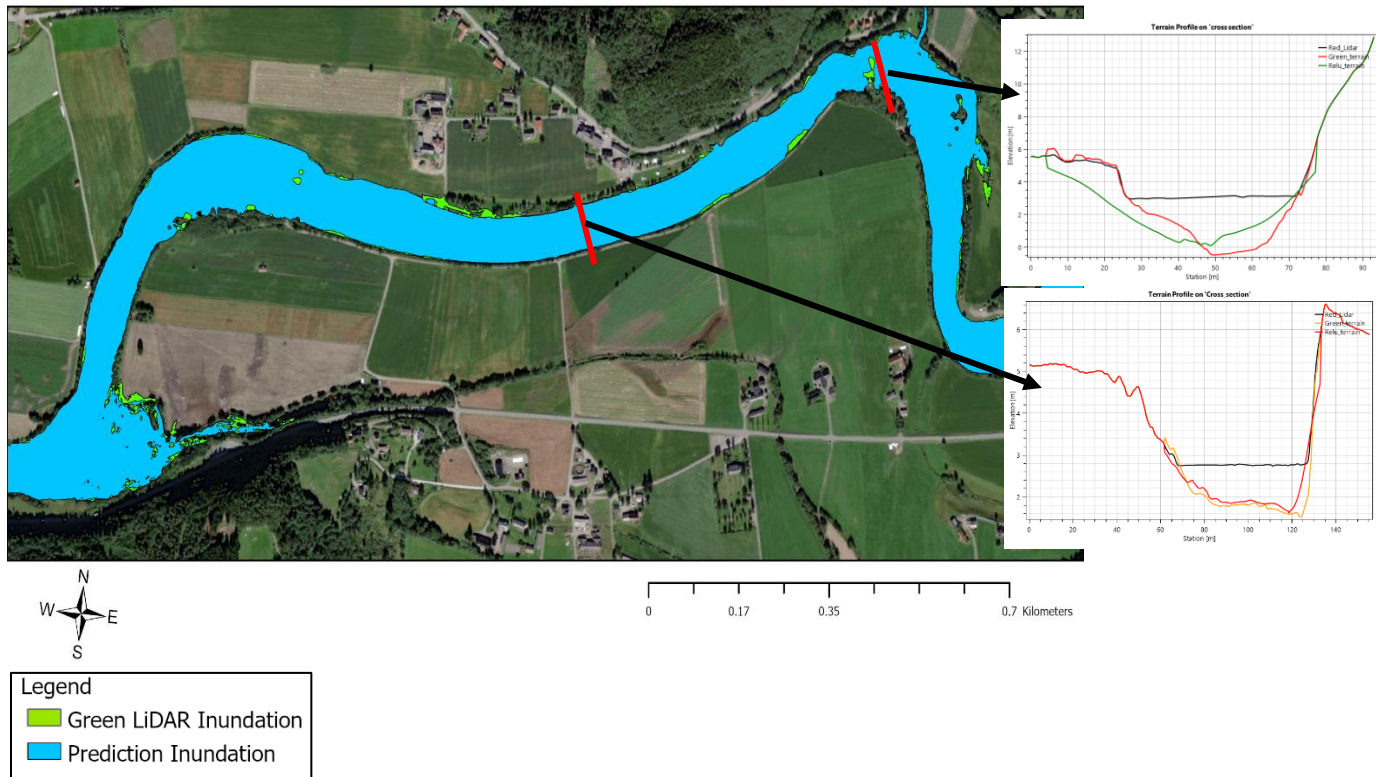


Fig 4.12 Flood Inundation Extent for Different Scenarios by HEC-RAS 6.0, Driva River

*Table 4.1 Difference Error Between the Green LiDAR Vs Red LiDAR and Green LiDAR Vs Prediction, Driva/Sigmoid*

Driva Flood Discharge	Green Lidar	Red Lidar	Prediction	Red Lidar Error	Prediction Error
QM	1,220,677.40	1750052.557	1,507,336.70	43.37%	23.48%
Q10	1459846.578	2059523.198	1818428.647	41.08%	24.56%
Q100	2340286.781	2909453.02	2747041.226	24.32%	17.38%
Q500	2630167.4	3190311.572	3024614.245	21.30%	15.00%



*Fig 4.13 Flood Inundation Extent for Different Scenarios by HEC-RAS 6.0, Surna River*

*Table 4.2 Difference Error Between the Green LiDAR Vs Red LiDAR and Green LiDAR Vs Prediction, Surna/ReLU*

Surna Flood Discharge	Green Lidar	Red Lidar	Prediction	Red Lidar Error	Prediction Error
QM	1,686,383.11	2434351.484	1,676,015.81	44.35%	-0.61%
Q10	2122146.106	3240414.104	2032909.973	52.70%	-4.20%
Q100	2983980.914	4452881.525	2742850.585	49.23%	-8.08%
Q500	3747158.765	5275807.478	3418006.752	40.79%	-8.78%

A study was done to obtain the river bathymetry using aerial images by (Sundt, Alfredsen et al. 2021). The study found a linear regression model using aerial images and training polygons for riverbed retrieval. The model well performed in high resolution images with and rivers with lower turbidity, and shallow river sections lower than 2 m depth.

The study limitation concluded in underestimating deeper depths in river basins, beside lower performance in low quality images and dependency on weather conditions when the images were taken and riverbanks land use status. The applied ANN machine learning method in this study is not influenced by the river depth or riverbanks vegetation and shadow. On the other hand, the regression model wasn't influenced by the existence of the island, unlike this study.

In Norway, 80% of the topography is covered by Red LiDAR survey and most of the rivers are covered, while Green LiDAR is a new and expensive technology, with limited number of covered rivers. Nevertheless, the significance of morphology and geomorphological data is increasing in river management and studying hydropeaking, sediment transport, and the ecological footprint, in addition to flood risk assessment and flood defense. This study showed promising results using ANN scenario c, reflected by the accuracy in the flood inundation area (table 4.1, 4.2). The speed of implementation and testing is fast in powerful computers such as workstation PC. The model can be transferred to other catchment areas or regions for predicting the river bathymetry. Therefore, this method is a valuable tool for river management and specifically for flood control. Another global application could be decreasing the cost by implementing the Green LiDAR survey in selected parts of the targeted river basin instead of the whole river, then using the covered areas to train a model that able to predict the remaining sections from the stream based on the Red LiDAR data.

## Chapter 5 Conclusion and Recommendation

---

The objective of this study is to find an applicable method for obtaining river bathymetry from red lidar data. These images or DEMs are used for improving the hydraulic simulation compared to the results from Red LiDAR DEM. Two machine learning methods were applied, Image inpainting using CNN and ANN method applying Keras API code using Python. Many scenarios have been tested and evaluated for ANN. Eventually, full training for the cross-sections using the elevation points from Red LiDAR as input and Green LiDAR as targeted output from extracted points gave the best performance. The main findings from the study gave promising results on using Deep AI machine learning methods and can be summarized as follows:

- Image inpainting CNN method implied a potential in testing the method and might give high spatial resolution as it considers DEM colouring index. The need for data and the computation time was challenging with time limitations for further investigation.
- Improving the model through hyperparameter tuning, more factors consideration, and training datasets would increase the algorithm prediction accuracy with specified uncertainties. Therefore, reasonable predictions in complex cross-sections and different river sizes.
- Two activation functions were tested on the model training. The model architecture is input layer, 2 hidden layers and output layer. ReLU and Sigmoid were applied in the two hidden layers, the output prediction from ReLU activation function model was more accurate than Sigmoid.
- The resulted algorithm from the ReLU model was tested in Surna geometry. Hydraulic simulation was done to find the inundation areas with Green LiDAR, it varied between 0.6 % to 9% less inundation area (overpredicted riverbed).

To conclude, machine learning (ML) is a very robust and flexible tool for data-driven models. It can be modified and investigated by adjusting the datasets. The drawback is that ML is a black box model, which will need trial and error to achieve the best performance. To parametrize and weight the input factors significance, it will require time-intense mathematical computations

Future recommendations for the two machine learning methods:

- Firstly, image inpainting method: the colouring scheme for the mainstream in the targeted output has a light colour gradient, this might disturb the kernel between masked and unmasked zones, as the masked zones have a white colour index. Therefore, it affects the partial CNN functionality. Changing the colouring scheme to avoid the kernel confusion might decrease the effect of filters targeting the non-holed area, and maintaining the original mainstream pixel values.
- Transforming the mask from randomly generated mask over the entire image, to masks covering the mainstream to train the model. The targeted output should be enough number of RGB images along the trained river, toward an algorithm that is able to predict the missing values on other testing streams.

- Secondly, the ANN model: hyperparameter tuning and model selection to avoid overfitting while testing on other rivers by examining different hyperparameters settings such as; the number of epochs, batch size, optimizer, activation function, etc. it is recommended to apply the hyperparameter tuning in scenario c.
- A new scenario could be, training the model based on the wetted zone only excluding the banks and fully depend on the bathymetry. Considering the Red LiDAR elevation points on the wetted zone as input, beside the Green LiDAR elevation points as targeted output. This will help to avoid the model confusion by diverse banks steepness. Again, maintain the dataframe shape will be an issue; this could be solved by masking the inserted values to keep the dataframe structure.
- In this study only Gaula was considered for the model training. Other different rivers in Norway have high-quality bathymetry information could be added to the trained model. This will include varied cross sections formations and sizes, to investigate the model capability of predicting different sizes. For example, if the model is able to predict islands existence, this will significantly improve the flood simulation
- Another different factors impact can be studied, such as including the river discharge, banks slope in case of full sections training, and do some uncertainty analysis.
- Although the flood inundation areas are more reasonable in comparison to Red LiDAR, but the water velocity was not investigated in this study.

## References

- Abdalla, E. M. H., et al. (2021). "Evaluating different machine learning methods to simulate runoff from extensive green roofs." *Hydrol. Earth Syst. Sci.* **25**(11): 5917-5935.
- Abdi, G., et al. (2018). "Deep learning decision fusion for the classification of urban remote sensing data." *Journal of Applied Remote Sensing* **12**(1): 016038.
- Alaghmand, S., et al. (2012). "Comparison between capabilities of HEC-RAS and MIKE11 hydraulic models in river flood risk modeling (a case study of Sungai Kayu Ara River basin, Malaysia)." *International Journal of Hydrology Science and Technology* **2**: 270-291.
- Albawi, S., et al. (2017). Understanding of a convolutional neural network. 2017 international conference on engineering and technology (ICET), Ieee.
- Algretawee, H. and G. Alshama (2021). "Modeling of Evapotranspiration (ETo) in a Medium Urban Park within a Megacity by Using Artificial Neural Network (ANN) Model." *Periodica Polytechnica Civil Engineering* **65**(4): 1260-1268.
- Allouis, T., et al. (2010). "Comparison of LiDAR waveform processing methods for very shallow water bathymetry using Raman, near-infrared and green signals." *Earth Surface Processes and Landforms: The Journal of the British Geomorphological Research Group* **35**(6): 640-650.
- Awadallah, M. O. M., et al. (2022). "Comparison between Topographic and Bathymetric LiDAR Terrain Models in Flood Inundation Estimations." *Remote Sensing* **14**(1): 227.
- Bales, J. D., et al. (2007). LiDAR-derived flood-inundation maps for real-time flood-mapping applications, Tar River Basin, North Carolina, Geological Survey (US).
- Bertalmio, M., et al. (2000). Image inpainting. Proceedings of the 27th annual conference on Computer graphics and interactive techniques.
- Bird, S., et al. (2010). "Photogrammetric monitoring of small streams under a riparian forest canopy." *Earth surface processes and landforms* **35**(8): 952-970.
- Bloschl, G., et al. (2017). "Changing climate shifts timing of European floods." *Science* **357**(6351): 588-590.
- Brasington, J., et al. (2000). "Monitoring and modelling morphological change in a braided gravel-bed river using high resolution GPS-based survey." *Earth Surface Processes and Landforms: The Journal of the British Geomorphological Research Group* **25**(9): 973-990.
- Casas, A., et al. (2006). "The topographic data source of digital terrain models as a key element in the accuracy of hydraulic flood modelling." *Earth Surface Processes and Landforms: The Journal of the British Geomorphological Research Group* **31**(4): 444-456.
- Chandler, J. (1999). "Effective application of automated digital photogrammetry for geomorphological research." *Earth surface processes and landforms* **24**(1): 51-63.

Chen, B., et al. (2017). "Using LiDAR surveys to document floods: A case study of the 2008 Iowa flood." Journal of Hydrology **553**: 338-349.

Cheng, S., et al. (2021). "Machine learning for predicting discharge fluctuation of a karst spring in North China." Acta Geophysica **69**(1): 257-270.

Das, K. and R. N. Behera (2017). "A survey on machine learning: concept, algorithms and applications." International Journal of Innovative Research in Computer and Communication Engineering **5**(2): 1301-1309.

Deparday, V., et al. (2019). "Machine learning for disaster risk management."

Dowman, I. (2004). "Integration of LIDAR and IFSAR for mapping." International Archives of Photogrammetry and Remote Sensing **35**(B2): 90-100.

Feng, S., et al. (2018). "Using deep neural network with small dataset to predict material defects." Materials & Design **162**.

Fonstad, M. A. and W. A. Marcus (2010). "High resolution, basin extent observations and implications for understanding river form and process." Earth Surface Processes and Landforms: The Journal of the British Geomorphological Research Group **35**(6): 680-698.

Gao, J. (2009). "Bathymetric mapping by means of remote sensing: methods, accuracy and limitations." Progress in Physical Geography **33**(1): 103-116.

Hodgson, M. E., et al. (2003). "An evaluation of LIDAR-and IFSAR-derived digital elevation models in leaf-on conditions with USGS Level 1 and Level 2 DEMs." Remote sensing of environment **84**(2): 295-308.

Jinlong, Z. and Y. JinTao (2009). Application of neural network in groundwater denitrification process. 2009 Asia-Pacific Conference on Information Processing, IEEE.

Khaniani, A. S., et al. (2021). "Rainfall forecast based on GPS PWV together with meteorological parameters using neural network models." Journal of Atmospheric and Solar-Terrestrial Physics **214**: 105533.

Kinzel, P. J., et al. (2013). "Mapping river bathymetry with a small footprint green LiDAR: applications and challenges 1." JAWRA Journal of the American Water Resources Association **49**(1): 183-204.

Kraus, K. and N. Pfeifer (1998). "Determination of terrain models in wooded areas with airborne laser scanner data." ISPRS Journal of Photogrammetry and Remote Sensing **53**(4): 193-203.

Kron, W., et al. (2019). "Reduction of flood risk in Europe - Reflections from a reinsurance perspective." Journal of Hydrology **576**: 197-209.

Kulisz, M., et al. (2021). "Forecasting water quality index in groundwater using artificial neural network." Energies **14**(18): 5875.

Lane, S., et al. (2000). "Application of digital photogrammetry to complex topography for geomorphological research." The Photogrammetric Record **16**(95): 793-821.

Lane, S., et al. (1993). "Developments in photogrammetry; the geomorphological potential." Progress in Physical Geography **17**(3): 306-328.

Liu, G., et al. (2018). Image inpainting for irregular holes using partial convolutions. Proceedings of the European conference on computer vision (ECCV).

Machado, F., et al. (2011). "Monthly rainfall-runoff modelling using artificial neural networks." Hydrological Sciences Journal–Journal des Sciences Hydrologiques **56**(3): 349-361.

MathiasGruber (2019). "Image Inpainting Code." from <https://github.com/MathiasGruber/PConv-Keras.git>.

Meng, X., et al. (2010). "Ground filtering algorithms for airborne LiDAR data: A review of critical issues." Remote Sensing **2**(3): 833-860.

Meng, X., et al. (2009). "A multi-directional ground filtering algorithm for airborne LIDAR." ISPRS Journal of Photogrammetry and Remote Sensing **64**(1): 117-124.

Mercer, B. (2004). DEM}s created from airborne IFSAR—an update. Proceedings of the ISPRS XXth Congress.

Montesinos-López, O., et al. (2022). Fundamentals of Artificial Neural Networks and Deep Learning: 379-425.

Muhadi, N. A., et al. (2020). "The use of LiDAR-derived DEM in flood applications: A review." Remote Sensing **12**(14): 2308.

O'Shea, K. and R. Nash (2015). "An introduction to convolutional neural networks." arXiv preprint arXiv:1511.08458.

Qi, Y., et al. (2019). "A decomposition-ensemble learning model based on LSTM neural network for daily reservoir inflow forecasting." Water Resources Management **33**(12): 4123-4139.

Roshni, T., et al. (2020). "Neural network modeling for groundwater-level forecasting in coastal aquifers." Neural Computing and Applications **32**(16): 12737-12754.

Saha, S. (2018). "A Comprehensive Guide to Convolutional Neural Networks — the ELI5 way." from <https://towardsdatascience.com/a-comprehensive-guide-to-convolutional-neural-networks-the-eli5-way-3bd2b1164a53>.

Sampson, C. C., et al. (2012). "Use of terrestrial laser scanning data to drive decimetric resolution urban inundation models." Advances in water resources **41**: 1-17.

Santillan, J. R., et al. (2016). Integrating LiDAR and flood simulation models in determining exposure and vulnerability of buildings to extreme rainfall-induced flood hazards. 2016 IEEE international geoscience and remote sensing symposium (IGARSS), IEEE.

Semiromi, M. T., et al. (2018). "Reducing computational costs of automatic calibration of rainfall-runoff models: meta-models or high-performance computers?" Water **10**(10): 1440.

Sharma, S., et al. (2017). "Activation functions in neural networks." towards data science **6**(12): 310-316.

Shigidi, A. and L. A. Garcia (2003). "Parameter estimation in groundwater hydrology using artificial neural networks." Journal of computing in civil engineering **17**(4): 281-289.

Shrestha, R. and F. Nestmann (2009). "Physically Based and Data-Driven Models and Propagation of Input Uncertainties in River Flood Prediction." Journal of Hydrologic Engineering **14**: 1309-1319.

Sivastava, A. K., et al. (2022). "Neural Network based Predictors for Evaporation Estimation at Jabalpur in Central India." Journal of Scientific and Industrial Research (JSIR) **81**(03): 319-328.

Sreekanth, P., et al. (2009). "Forecasting groundwater level using artificial neural networks." Current science: 933-939.

Stevenson, J. A., et al. (2010). "Despeckling SRTM and other topographic data with a denoising algorithm." Geomorphology **114**(3): 238-252.

Stylianoudaki, C., et al. (2022). "Modeling groundwater nitrate contamination using artificial neural networks." Water **14**(7): 1173.

Sundt, H., et al. (2021). "Regionalized Linear Models for River Depth Retrieval Using 3-Band Multispectral Imagery and Green LIDAR Data." Remote Sensing **13**(19): 3897.

TensorFlow (2022). "Keras Sequential ". from  
[https://www.tensorflow.org/guide/keras/sequential\\_model](https://www.tensorflow.org/guide/keras/sequential_model).

Wang, Q., et al. (2020). "Sequence-based statistical downscaling and its application to hydrologic simulations based on machine learning and big data." Journal of Hydrology **586**: 124875.

Weber, T., et al. (2020). "Deep learning for creating surrogate models of precipitation in Earth system models." Atmospheric Chemistry and Physics **20**(4): 2303-2317.

Webster, T. L., et al. (2004). "Using topographic lidar to map flood risk from storm-surge events for Charlottetown, Prince Edward Island, Canada." Canadian Journal of Remote Sensing **30**(1): 64-76.

Wendi, D., et al. (2016). "An innovative approach to improve SRTM DEM using multispectral imagery and artificial neural network." Journal of Advances in Modeling Earth Systems **8**(2): 691-702.

Yegnanarayana, B. (2009). Artificial neural networks, PHI Learning Pvt. Ltd.

Zhang, L., et al. (2016). "Deep learning for remote sensing data: A technical tutorial on the state of the art." IEEE Geoscience and remote sensing magazine **4**(2): 22-40.

# Appendices

This code for image inpainting is developed by (MathiasGruber 2019)

```
In [45]: # Load image
img = cv2.imread('C:/Users/raffa/Desktop/River_mask/Sokna.jpg')
img = cv2.cvtColor(img, cv2.COLOR_BGR2RGB)
shape = img.shape
print(f"Shape of image is: {shape}")

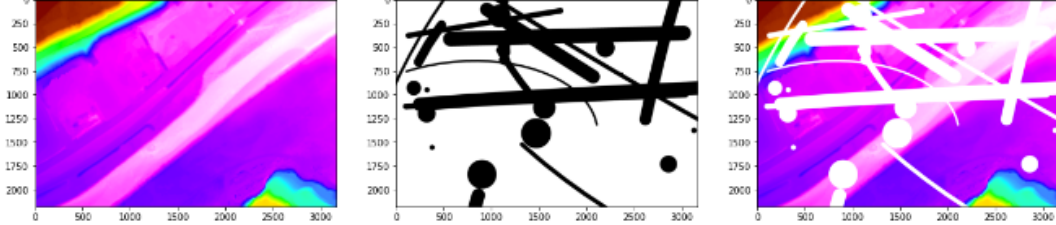
# Instantiate mask generator
mask_generator = MaskGenerator(shape[0], shape[1], 3, rand_seed=42)

# Load mask
mask = mask_generator.sample()

# Image + mask
masked_img = deepcopy(img)
masked_img[mask==0] = 255

# Show side by side
_, axes = plt.subplots(1, 3, figsize=(20, 5))
axes[0].imshow(img)
axes[1].imshow(mask*255)
axes[2].imshow(masked_img)
plt.show()
```

Shape of image is: (2180, 3164, 3)



```
In [46]: from Lidpack.pconv_layer import PConv2D

# Input images and masks
input_img = Input(shape=(shape[0], shape[1], shape[2]))
input_mask = Input(shape=(shape[0], shape[1], shape[2]))
output_img, output_mask1 = PConv2D(8, kernel_size=(7,7), strides=(2,2))([input_img, input_mask])
output_img, output_mask2 = PConv2D(16, kernel_size=(5,5), strides=(2,2))([output_img, output_mask1])
output_img, output_mask3 = PConv2D(32, kernel_size=(5,5), strides=(2,2))([output_img, output_mask2])
output_img, output_mask4 = PConv2D(64, kernel_size=(3,3), strides=(2,2))([output_img, output_mask3])
output_img, output_mask5 = PConv2D(64, kernel_size=(3,3), strides=(2,2))([output_img, output_mask4])
output_img, output_mask6 = PConv2D(64, kernel_size=(3,3), strides=(2,2))([output_img, output_mask5])
output_img, output_mask7 = PConv2D(64, kernel_size=(3,3), strides=(2,2))([output_img, output_mask6])
output_img, output_mask8 = PConv2D(64, kernel_size=(3,3), strides=(2,2))([output_img, output_mask7])

# Create model
model = Model(
    inputs=[input_img, input_mask],
    outputs=[
        output_img, output_mask1, output_mask2,
        output_mask3, output_mask4, output_mask5,
        output_mask6, output_mask7, output_mask8
    ]
)
model.compile(optimizer='rmsprop', loss='categorical_crossentropy', metrics=['accuracy'])

# Show summary of the model
model.summary()
```

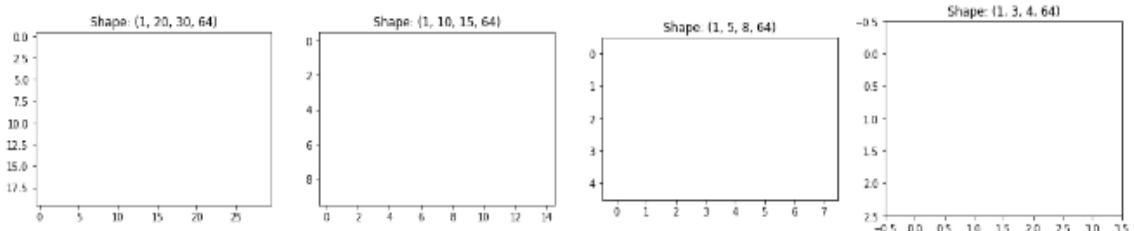
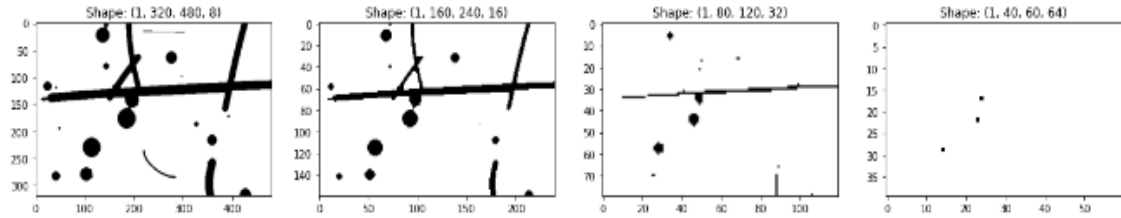
Layer (type)	Output Shape	Param #	Connected to
input_17 (InputLayer)	(None, 2180, 3164, 3 0		
input_18 (InputLayer)	(None, 2180, 3164, 3 0		
p_conv2d_97 (PConv2D)	[(None, 1090, 1582, 1184	input_17[0][0]	
		input_18[0][0]	
p_conv2d_98 (PConv2D)	[(None, 545, 791, 16 3216	p_conv2d_97[0][0]	
		p_conv2d_97[0][1]	
p_conv2d_99 (PConv2D)	[(None, 273, 396, 32 12832	p_conv2d_98[0][0]	
		p_conv2d_98[0][1]	

```
In [47]: formatted_img = np.expand_dims(masked_img, 0) / 255
formatted_mask = np.expand_dims(mask, 0)
print(f"Original Mask Shape: {formatted_mask.shape} - Max value in mask: {np.max(formatted_mask)}")

output_img, o1, o2, o3, o4, o5, o6, o7, o8 = model.predict([formatted_img, formatted_mask])

Original Mask Shape: (1, 2180, 3164, 3) - Max value in mask: 1
```

```
In [37]: _, axes = plt.subplots(2, 4, figsize=(20, 10))
axes[0][0].imshow(o1[0, :, :, 0], cmap = 'gray', vmin=0, vmax=1)
axes[0][1].imshow(o2[0, :, :, 0], cmap = 'gray', vmin=0, vmax=1)
axes[0][2].imshow(o3[0, :, :, 0], cmap = 'gray', vmin=0, vmax=1)
axes[0][3].imshow(o4[0, :, :, 0], cmap = 'gray', vmin=0, vmax=1)
axes[1][0].imshow(o5[0, :, :, 0], cmap = 'gray', vmin=0, vmax=1)
axes[1][1].imshow(o6[0, :, :, 0], cmap = 'gray', vmin=0, vmax=1)
axes[1][2].imshow(o7[0, :, :, 0], cmap = 'gray', vmin=0, vmax=1)
axes[1][3].imshow(o8[0, :, :, 0], cmap = 'gray', vmin=0, vmax=1)
axes[0][0].set_title(f"Shape: {o1.shape}")
axes[0][1].set_title(f"Shape: {o2.shape}")
axes[0][2].set_title(f"Shape: {o3.shape}")
axes[0][3].set_title(f"Shape: {o4.shape}")
axes[1][0].set_title(f"Shape: {o5.shape}")
axes[1][1].set_title(f"Shape: {o6.shape}")
axes[1][2].set_title(f"Shape: {o7.shape}")
axes[1][3].set_title(f"Shape: {o8.shape}")
plt.show()
```



```
In [48]: import os
import gc
import copy

import numpy as np
from PIL import Image

from keras.preprocessing.image import ImageDataGenerator
from keras.callbacks import TensorBoard, ModelCheckpoint, LambdaCallback

import matplotlib
import matplotlib.pyplot as plt

# Change to root path
if os.path.basename(os.getcwd()) != 'PConv-Keras':
    os.chdir('..')

from Lidpack.util import MaskGenerator
from Lidpack.pconv_model import PConvUnet

# Settings
BATCH_SIZE = 4

# Imagenet Rescaling
MEAN = np.array([0.485, 0.456, 0.406])
STD = np.array([0.229, 0.224, 0.225])

%matplotlib inline
%load_ext autoreload
%autoreload 2
```

The autoreload extension is already loaded. To reload it, use:  
 %reload\_ext autoreload

```
In [49]: PConvUnet().summary()
```

Layer (type)	Output Shape	Param #	Connected to
<hr/>			
inputs_img (InputLayer)	(None, 512, 512, 3)	0	
inputs_mask (InputLayer)	(None, 512, 512, 3)	0	
p_conv2d_105 (PConv2D)	[(None, 256, 256, 64)	9472	inputs_img[0][0] inputs_mask[0][0]
activation_33 (Activation)	(None, 256, 256, 64)	0	p_conv2d_105[0][0]
p_conv2d_106 (PConv2D)	[(None, 128, 128, 12)	204928	activation_33[0][0] p_conv2d_105[0][1]
EncBN1 (BatchNormalization)	(None, 128, 128, 128)	512	p_conv2d_106[0][0]
activation_34 (Activation)	(None, 128, 128, 128)	0	EncBN1[0][0]

### Testing out on single image

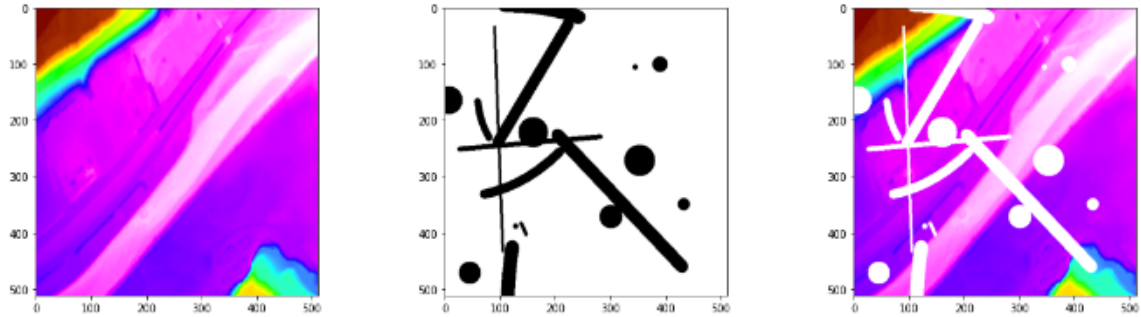
```
In [50]: # Instantiate mask generator
mask_generator = MaskGenerator(512, 512, 3, rand_seed=42)

# Load image
img = np.array(Image.open('C:/Users/raffaa/Desktop/River_mask/Sokna.jpg').resize((512, 512))) / 255

# Load mask
mask = mask_generator.sample()

# Image + mask
masked_img = copy.deepcopy(img)
masked_img[mask==0] = 1

# Show side by side
_, axes = plt.subplots(1, 3, figsize=(20, 5))
axes[0].imshow(img)
axes[1].imshow(mask*255)
axes[2].imshow(masked_img)
plt.show()
```



### Creating data generator

```
In [51]: def plot_sample_data(masked, mask, ori, middle_title='Raw Mask'):
    _, axes = plt.subplots(1, 3, figsize=(20, 5))
    axes[0].imshow(masked[:, :, :])
    axes[0].set_title('Masked Input')
    axes[1].imshow(mask[:, :, :])
    axes[1].set_title(middle_title)
    axes[2].imshow(ori[:, :, :])
    axes[2].set_title('Target Output')
    plt.show()

class DataGenerator(ImageDataGenerator):
    def flow(self, x, *args, **kwargs):
        while True:

            # Get augmented image samples
            ori = next(super().flow(x, *args, **kwargs))

            # Get masks for each image sample
            mask = np.stack([mask_generator.sample() for _ in range(ori.shape[0])], axis=0)

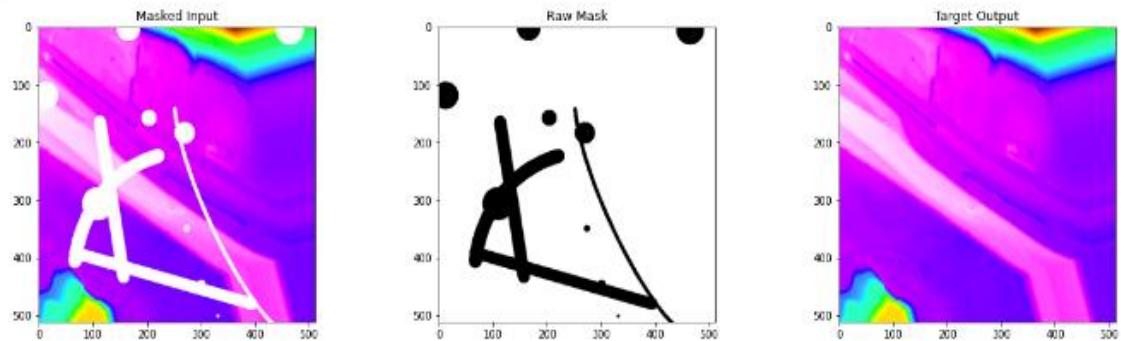
            # Apply masks to all image sample
            masked = copy.deepcopy(ori)
            masked[mask==0] = 1

            # Yield ([ori, masl], ori) training batches
            # print(masked.shape, ori.shape)
            gc.collect()
            yield [masked, mask], ori

    # Create datagen
datagen = DataGenerator(
    rotation_range=20,
    width_shift_range=0.2,
    height_shift_range=0.2,
    horizontal_flip=True
)

# Create generator from numpy array
batch = np.stack([img for _ in range(BATCH_SIZE)], axis=0)
generator = datagen.flow(x=batch, batch_size=BATCH_SIZE)
```

```
In [52]: [m1, m2], o1 = next(generator)
plot_sample_data(m1[0], m2[0]*255, o1[0])
```

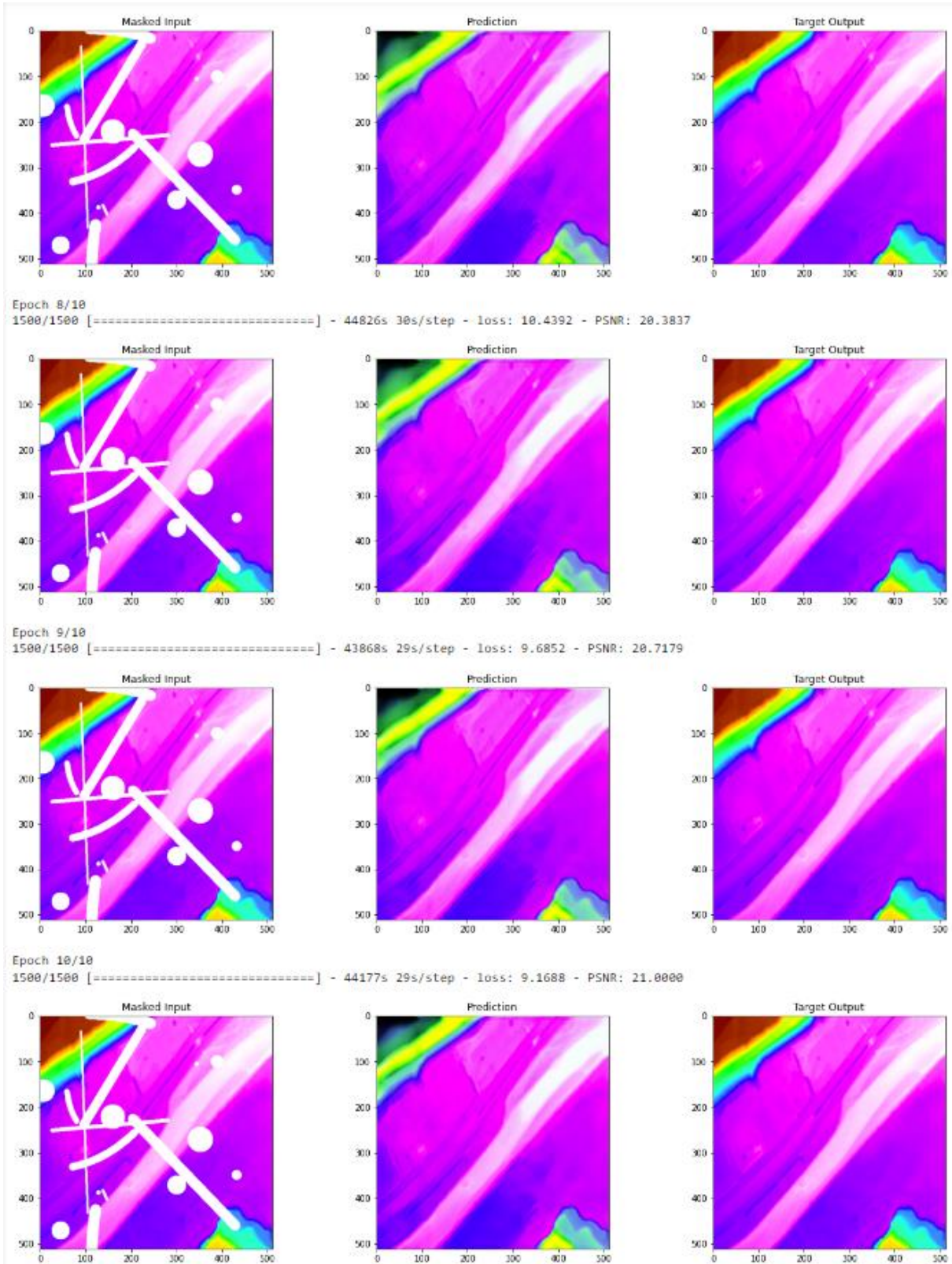


### Training the inpainting UNet on single image

```
In [53]: model = PConvUnet(vgg_weights="imagenet")
```

```
In [54]: model.fit_generator(
    generator,
    steps_per_epoch=1500,
    epochs=10,
    callbacks=[
        TensorBoard(
            log_dir='C:/Users/raffaa/Desktop/River_masks/River_train',
            write_graph=False
        ),
        ModelCheckpoint(
            'C:/Users/raffaa/Desktop/River_masks/River_train/weights.{epoch:02d}-{loss:.2f}.h5',
            monitor='loss',
            save_best_only=True,
            save_weights_only=True
        ),
        LambdaCallback(
            on_epoch_end=lambda epoch, logs: plot_sample_data(
                masked_img,
                model.predict(
                    [
                        np.expand_dims(masked_img, 0),
                        np.expand_dims(mask, 0)
                    ]
                )[0]
            ),
            img,
            middle_title='Prediction'
        )
    ],
)
```

## Last four epoch in CNN training



For ANN method, all the codes developed specifically for this study. All the results are testing results (out of the training zone)

Scenario a

```
In [1]: import os  
cwd=os.getcwd()  
  
In [2]: import pandas as pd  
Gaula_data = pd.read_csv(r'C:\Users\raffaa\Desktop\ID_model\Gaula_points.csv')  
#print (Gaula_data)  
  
In [3]: from matplotlib import pyplot as plt  
print(plt.style.available)  
  
['Solarize_Light2', '_classic_test_patch', '_mpl-gallery', '_mpl-gallery-nogrid', 'bmh', 'classic', 'dark_background', 'fast',  
'fivethirtyeight', 'ggplot', 'grayscale', 'seaborn', 'seaborn-bright', 'seaborn-colorblind', 'seaborn-dark', 'seaborn-dark-pale'  
'tte', 'seaborn-darkgrid', 'seaborn-deep', 'seaborn-muted', 'seaborn-notebook', 'seaborn-paper', 'seaborn-pastel', 'seaborn-post'  
'er', 'seaborn-talk', 'seaborn-ticks', 'seaborn-white', 'seaborn-whitegrid', 'tableau-colorblind10']  
  
In [4]: a = 101  
b = 300  
z = 400  
#sample = random.sample()
```

```
In [6]: from matplotlib import pyplot as plt
from matplotlib.backends.backend_pdf import PdfPages
import numpy as np
import pandas as pd

list = []
sample = np.arange(1,1000,5)
count = 1
fig = plt.figure(figsize = [16,16])
pdfFile = PdfPages("plotting.pdf")
# plt.style.use('fivethirtyeight')

for j in sample:
    data_cross = Gaua_data.loc[Gaua_data["ORIG_FID"] == j]
    data_cross = data_cross.reset_index(drop=True)
    Green = data_cross["green_elevation"]
    #Green[(a-1):b] = None
    Min = data_cross["green_elevation"].min()
    data_cross["green_elevation"] = data_cross["green_elevation"] - Min
    data_cross["red_elevation"] = data_cross["red_elevation"] - Min

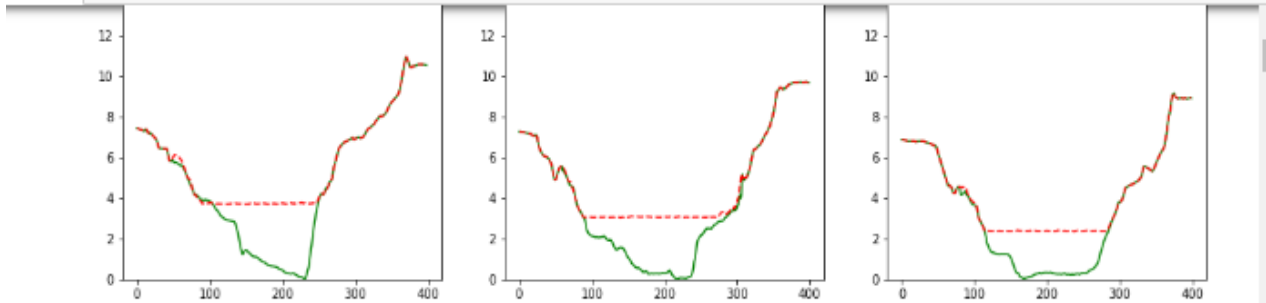
    #Making sure the min Length is 399
    Length = len(data_cross)
    list.append(Length)

    #plotting

    plt.subplot(3,3,count)
    plt.plot(data_cross["green_elevation"],label = "green elevation",color = "g",linestyle= "-")
    plt.plot(data_cross["red_elevation"],"--r",label = "red elevation")
    plt.legend(loc = "upper left", fontsize = 10)
    plt.title(j)
    plt.ylim([0,16])

    if count < 9:
        count += 1
    else:
        count = 1
        pdfFile.savefig(fig)
        fig = plt.figure(figsize = [16,16])

pdfFile.close()
```



## Trainning

```
[11]: import tensorflow as tf
from keras.models import Sequential
from tensorflow.keras.layers import Activation, Dense
from tensorflow.keras.optimizers import Adam
from tensorflow.keras.metrics import categorical_crossentropy

[12]: # model creation & adding layers
model = Sequential([
    Dense(164, activation= "relu", input_shape=(200,)),
    Dense(164, activation= "relu"),
    Dense(200, activation= "linear"),
])
model.summary()

Model: "sequential"
-----  

Layer (type)          Output Shape         Param #  

-----  

dense (Dense)         (None, 164)          32964  

dense_1 (Dense)       (None, 164)          27060  

dense_2 (Dense)       (None, 200)          33000  

-----  

Total params: 93,024  

Trainable params: 93,024  

Non-trainable params: 0  

-----  

[13]: # compile model
model.compile(optimizer = "rmsprop",
              loss= "mse")
model.summary()

Model: "sequential"
-----  

Layer (type)          Output Shape         Param #  

-----  

dense (Dense)         (None, 164)          32964  

dense_1 (Dense)       (None, 164)          27060  

dense_2 (Dense)       (None, 200)          33000  

-----  

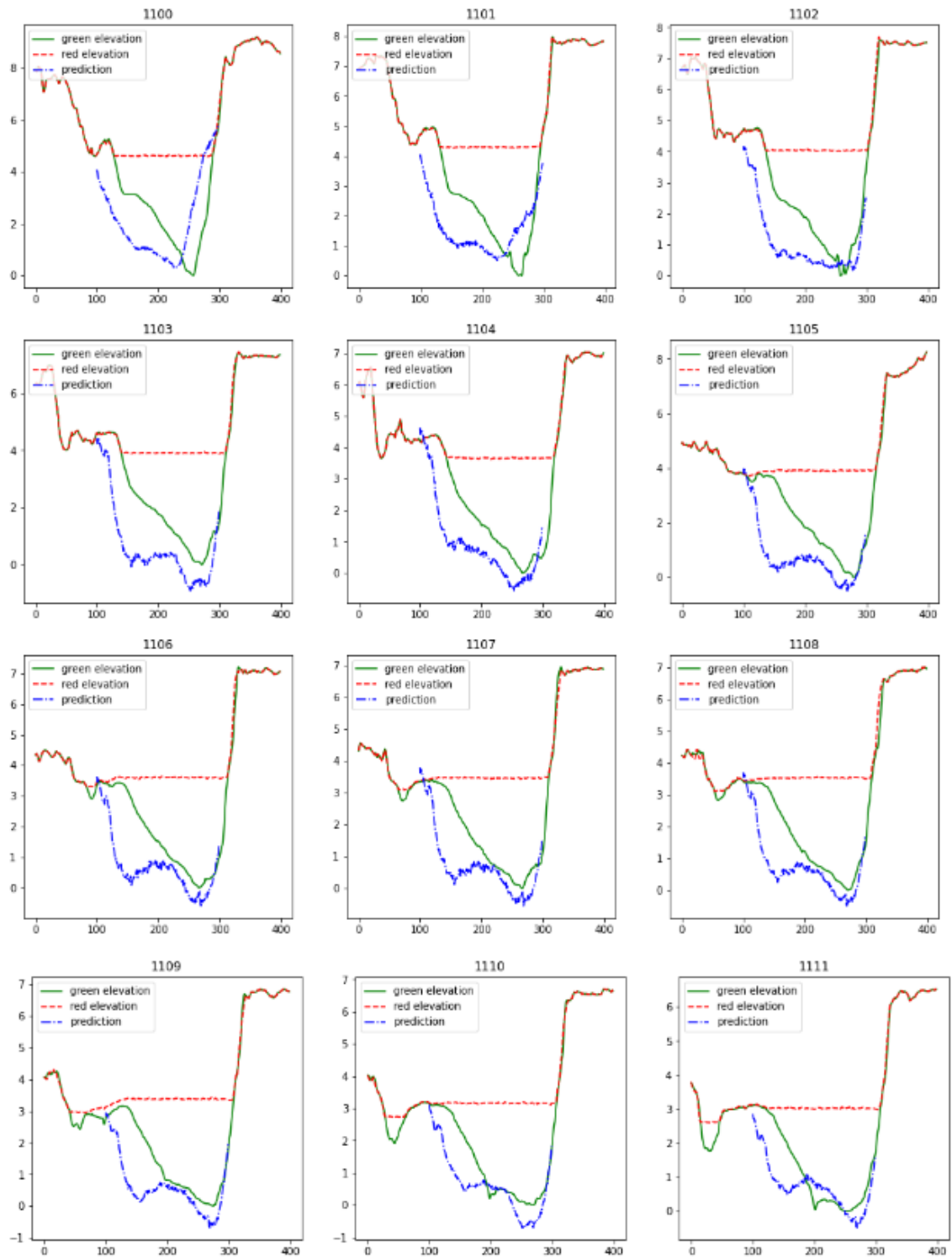
Total params: 93,024  

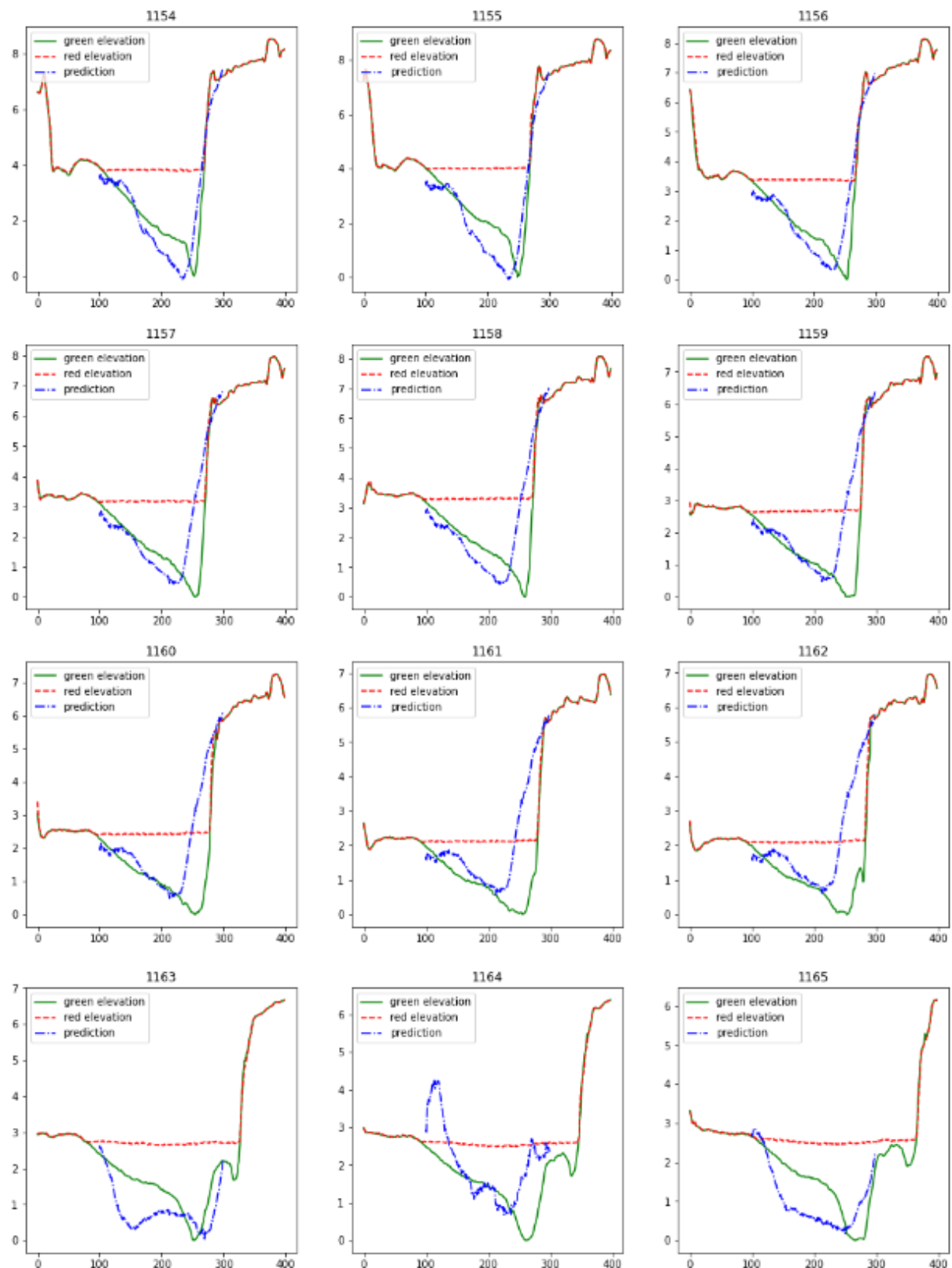
Trainable params: 93,024  

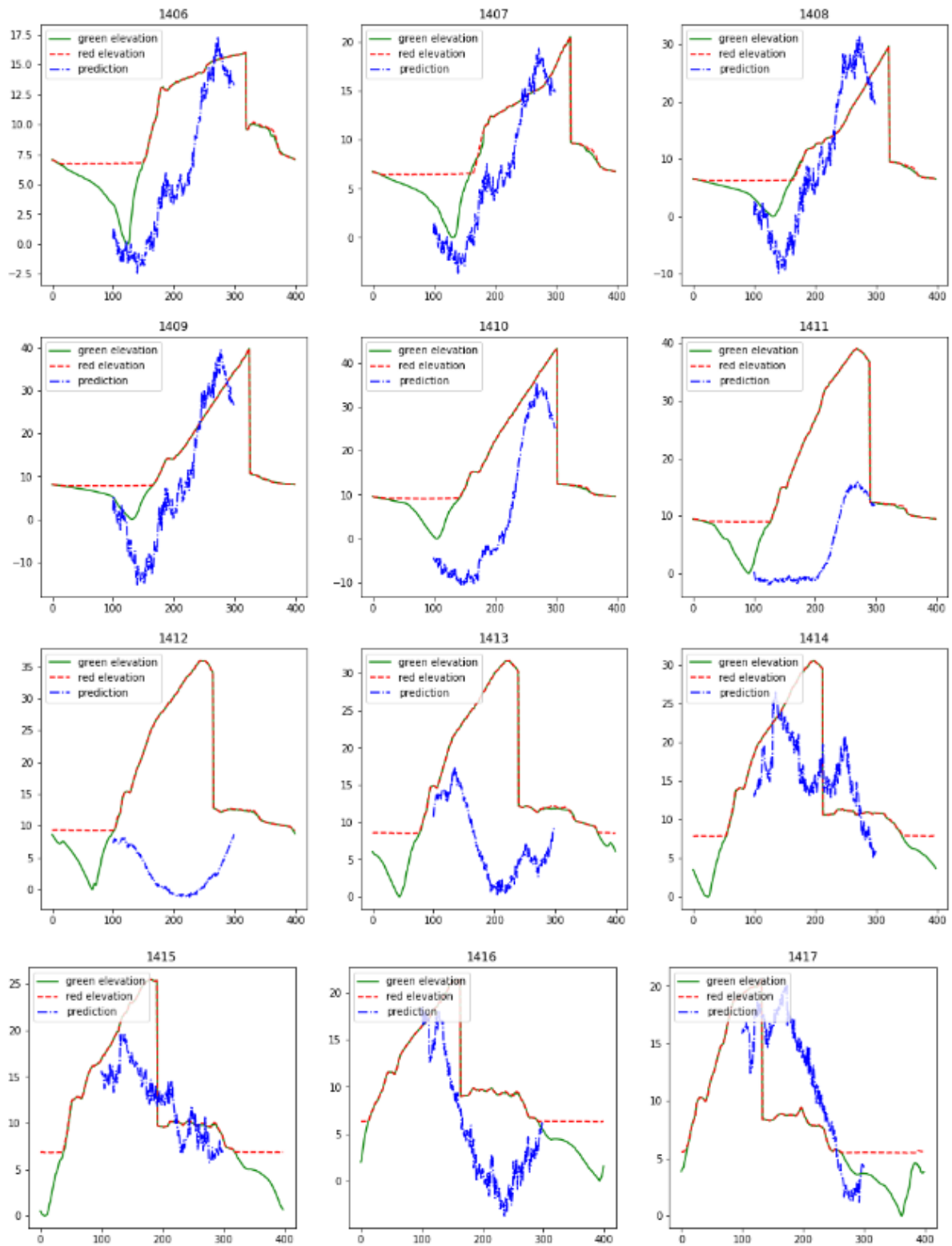
Non-trainable params: 0  

-----  

[14]: # Trainning
model.fit(
input1,
Middle,
batch_size=1,
epochs=250, verbose=2,
callbacks=None,
validation_split=0.2,
validation_data=None,
shuffle=True,
class_weight=None,
sample_weight=None,
initial_epoch=0)
```







## Scenario b

```
: import os
cwd=os.getcwd()

: import numpy as np
import pandas as pd
Gaula_data = pd.read_csv(r'C:\Users\raffaa\Desktop\ID_model\Gaula_points.csv')
#print (Gaula_data)

#  

: middle_points = pd.read_csv(r'C:\Users\raffaa\Desktop\ID_model\Points_clip.csv')

: middle_points= middle_points.sort_values(by=["copy_id"],ascending=True)

: middle_points

: Middle1.iat[0,0] = 5

: Middle1

: import pandas as pd

Middle1 = pd.DataFrame(0, index= np.arange(0,2000,1), columns = [np.arange(0,863,1)])

sample = np.arange(0,2000,1)
list = []
count = 0
for j in sample:
    data_cross = middle_points.loc[middle_points["transectID"] == j]
    data_cross = data_cross.reset_index(drop=True)
    Min = data_cross['Green_Lida'].min()
    data_cross["Green_Lida"] = data_cross["Green_Lida"] - Min
    data_cross["Red_Lidar"] = data_cross["Red_Lidar"] - Min
    Green = data_cross["Green_Lida"]

    list.append(len(Green))

    Middle1.iloc[count,0:len(Green)] = Green.values
    #print(Len(Green))
    count= count +1
#max(List)

: Middle1

: np.shape(Middle1)

##  

: Banks_points = pd.read_csv(r'C:\Users\raffaa\Desktop\ID_model\main_points.csv')

: Banks_points= Banks_points.sort_values(by=["copy_id"],ascending=True)

: Banks_points
```

```

: import pandas as pd

left_right = pd.DataFrame(0, index= np.arange(0,2000,1), columns = [np.arange(0,863,1)])

sample = np.arange(1,2000,1)
list = []
count = 0
for j in sample:
    data_cross = Banks_points.loc[Banks_points["transectID"] == j]
    data_cross = data_cross.reset_index(drop=True)
    Min = data_cross['Green_Lida'].min()
    data_cross["Green_Lida"] = data_cross["Green_Lida"] - Min
    data_cross["Red_Lidar"] = data_cross["Red_Lidar"] - Min
    Green = data_cross["Green_Lida"]

    list.append(len(Green))

    left_right.iloc[count,0:len(Green)] = Green.values
    #print(len(Green))
    count+= count +1
#max(list)
min(list)

: left_right

: np.shape(left_right)

```

##

```
: !pip install keras==2.6
```

## Training

```

: import tensorflow as tf
from keras.models import Sequential
from tensorflow.keras.layers import Activation, Dense
from tensorflow.keras.optimizers import Adam
from tensorflow.keras.metrics import categorical_crossentropy

: # model creation & adding Layers
model = Sequential([
    Dense(164, activation= "sigmoid", input_shape=(863,)),
    Dense(164, activation= "sigmoid"),
    Dense(863, activation= "linear"),
])
model.summary()

: # compile model
model.compile(optimizer = "rmsprop",
              loss= "mse")
model.summary()

: # Training
model.fit(
left_right,
Middle1,
batch_size=1,
epochs=200, verbose=2,
callbacks=None,
validation_split=0.2,
validation_data=None,
shuffle=True,
class_weight=None,
sample_weight=None,
initial_epoch=0)

```

```

]: import numpy as np
import pandas as pd
from matplotlib.backends.backend_pdf import PdfPages
from matplotlib import pyplot as plt

count = 1

fig = plt.figure(figsize = [16,16])
pdfFile = PdfPages("Zeros_predictions.pdf")

for j in range(2100,2400):
    data_cross = middle_points.loc[middle_points["transectID"] == j]
    data_cross = data_cross.reset_index(drop=True)

    Min = data_cross['Green_Lida'].min()
    data_cross["Green_Lida"] = data_cross["Green_Lida"] - Min
    data_cross["Red_Lidar"] = data_cross["Red_Lidar"] - Min
    Green = data_cross["Green_Lida"]

    #filling the df with the prediction input for j cross section

    df = pd.DataFrame(0, index= np.arange(0,1,1), columns = [np.arange(0,863,1)])

    data_predict = Banks_points.loc[Banks_points["transectID"] == j]
    data_predict = data_predict.reset_index(drop=True)
    Min = data_predict['Green_Lida'].min()
    data_predict["Green_Lida"] = data_predict["Green_Lida"] - Min
    data_predict["Red_Lidar"] = data_predict["Red_Lidar"] - Min
    Green_predict = data_predict["Green_Lida"]

    df.iloc[0:0:len(Green_predict)] = Green_predict.values

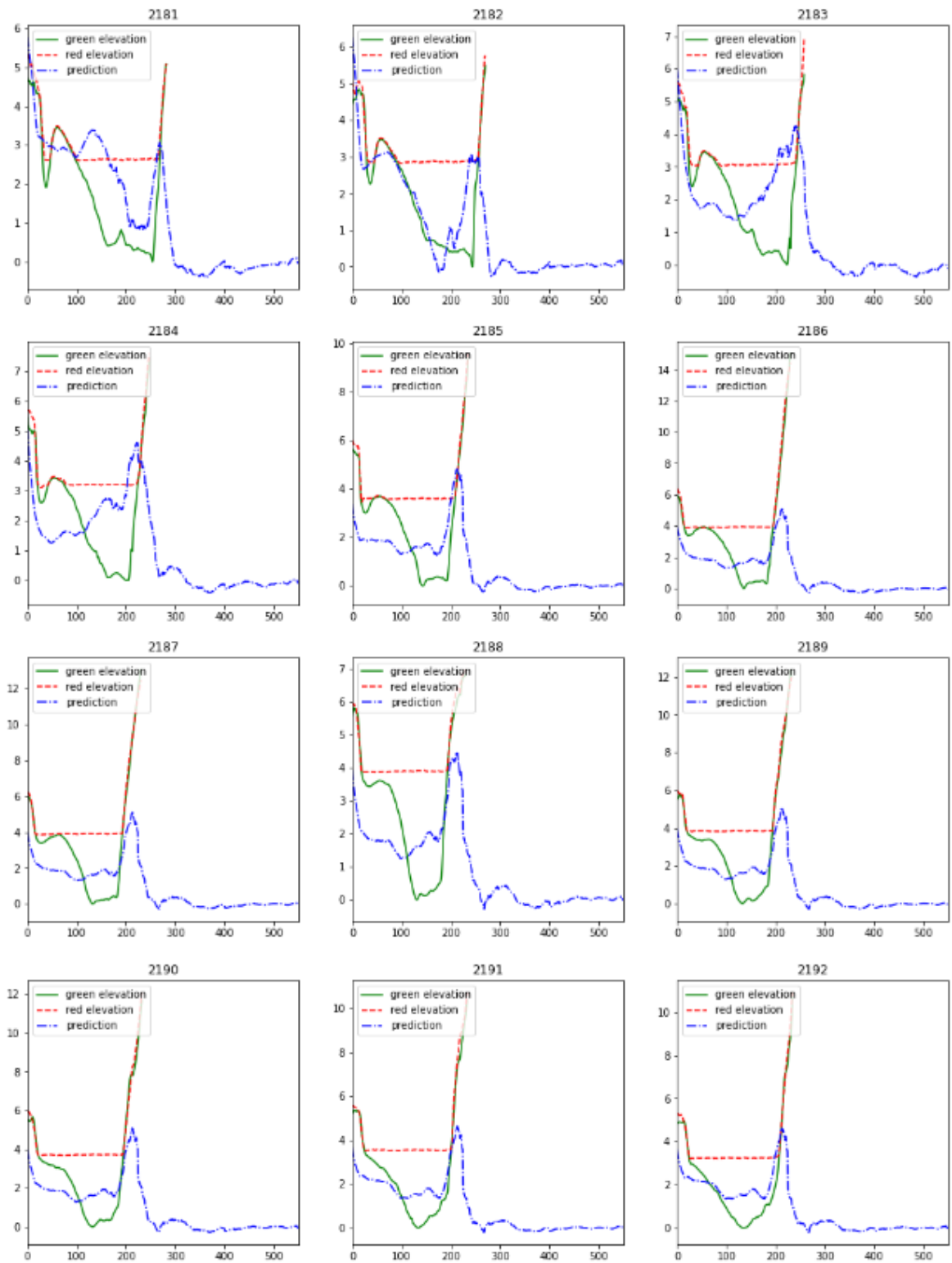
    #input_pr = pd.merge(Left,Right, left_index=True, right_index=True)
    predictions = model.predict(df,batch_size=1,verbose=1)
    predictions = np.transpose(predictions)

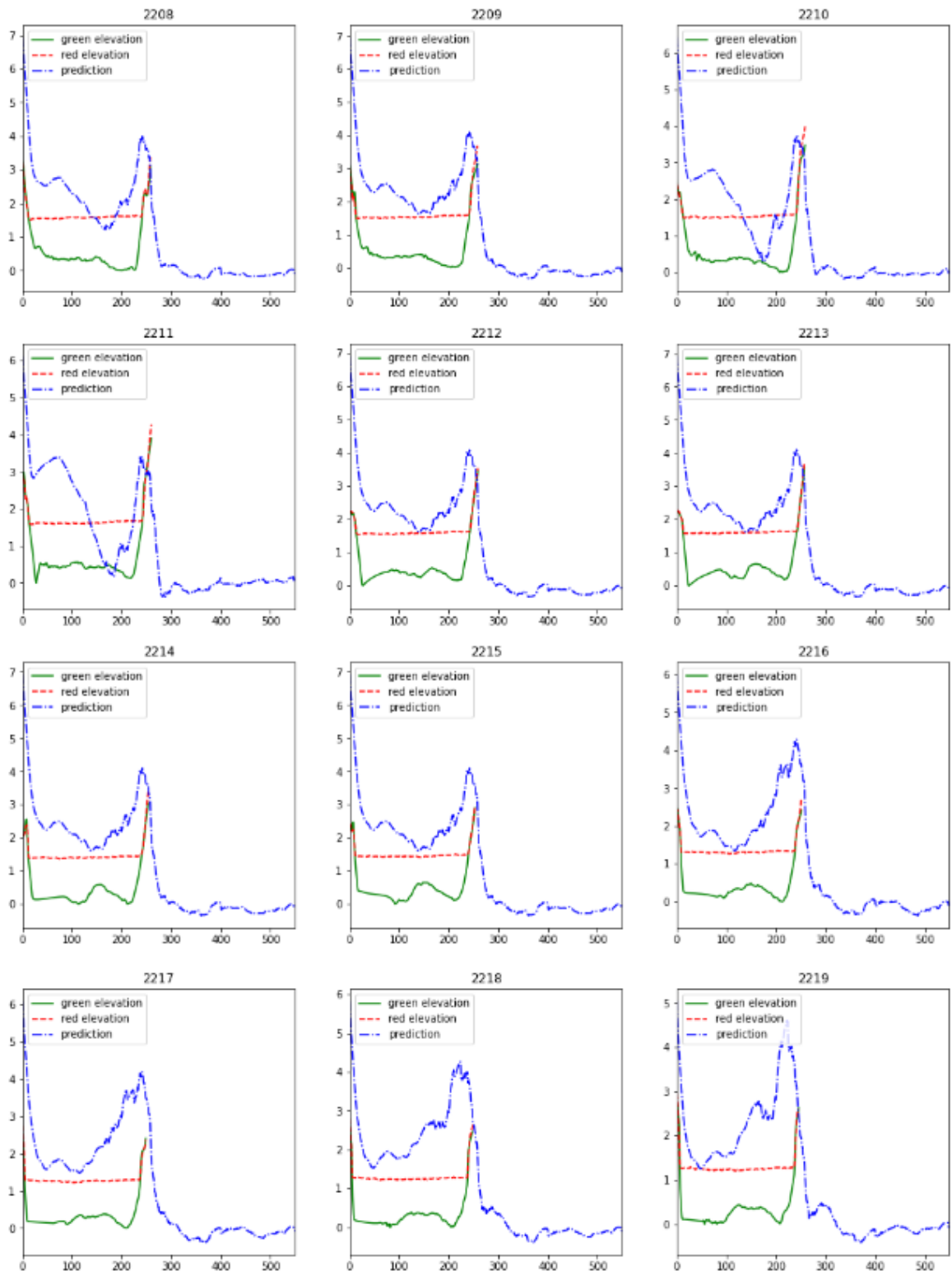
    #print(input_pr)
    pred = pd.DataFrame(predictions)
    ind1 = np.arange(0,863,1)

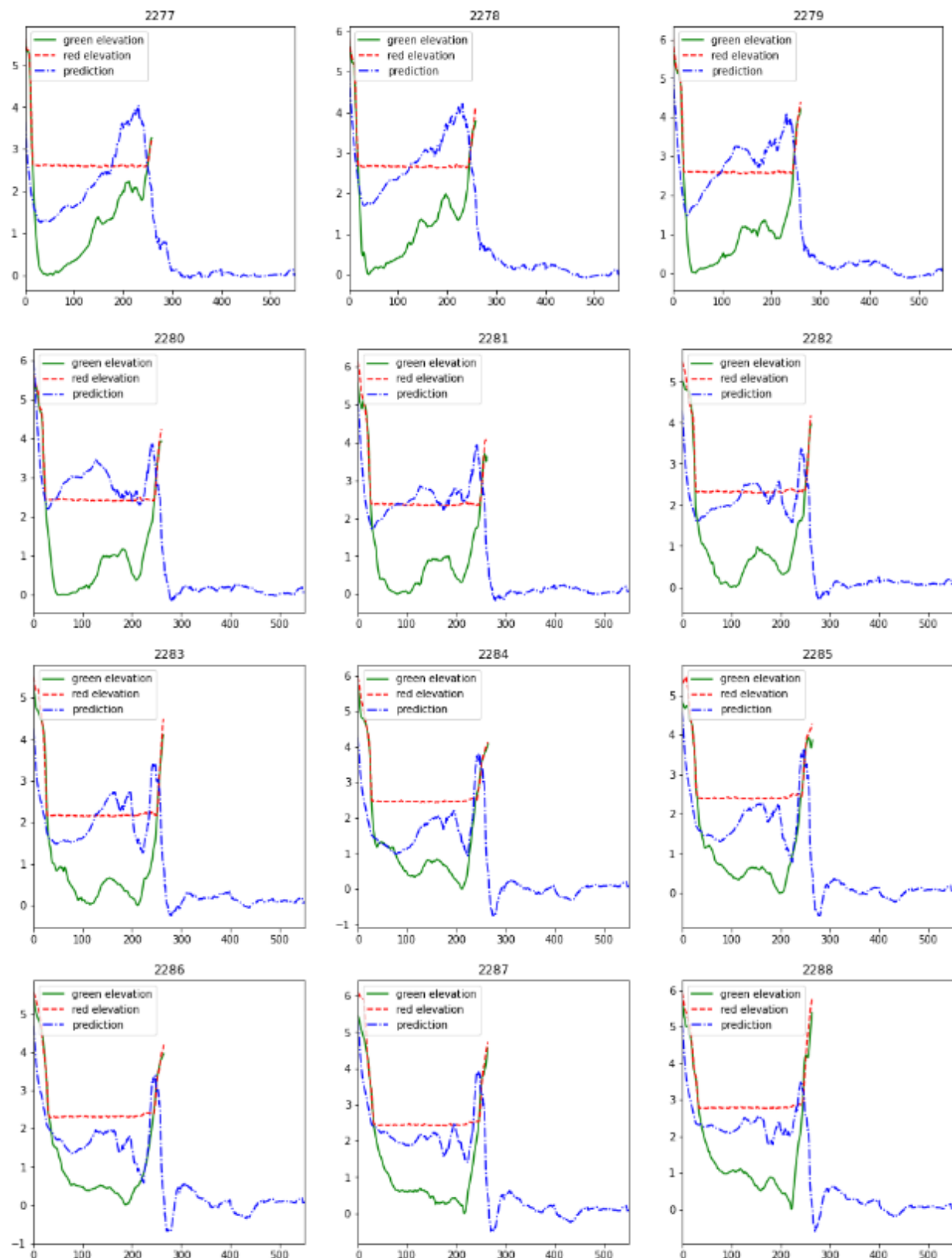
    plt.subplot(3,3,count)
    plt.plot(data_cross["Green_Lida"],label ="green elevation",color = "g",linestyle= "-")
    plt.plot(data_cross["Red_Lidar"],"--r",label ="red elevation")
    plt.plot(ind1,pred[0],label ="prediction",color = "b",linestyle= "-.")
    plt.legend(loc = "upper left", fontsize = 10)
    plt.title(j)
    #plt.ylim([0,16])
    plt.xlim([0,550])
    if count < 9:
        count += 1
    else:
        count = 1
    pdfFile.savefig(fig)
    fig = plt.figure(figsize = [16,16])

pdfFile.close()

```







## Scenario c

```
In [1]: import pandas as pd
Gaula_data = pd.read_csv(r'C:\Users\raffaa\Desktop\ID_model\Gaula_points.csv')

In [2]: Gaula_data
Out[2]:
   OID_  ORIG_FID  ORIG_FID_1  red_elevation  green_elevation  POINT_X  POINT_Y
0      1         1          200     33.745838    33.745838  562748.8648  7.001246e+08
1      2         1          200     33.736206    33.736206  562748.1769  7.001246e+08
2      3         1          200     33.730690    33.730690  562747.8889  7.001246e+08
3      4         1          200     33.711281    33.711281  562747.2010  7.001246e+08
4      5         1          200     33.695003    33.695003  562746.7130  7.001246e+08
...
1045880 1045881 2818          200     13.830121    13.830121  564226.5692  7.020697e+08
1045881 1045882 2818          200     13.754012    13.754012  564227.0542  7.020697e+08
1045882 1045883 2818          200     13.770851    13.770851  564227.5392  7.020697e+08
1045883 1045884 2818          200     13.831068    13.831068  564228.0242  7.020697e+08
1045884 1045885 2818          200     13.825141    13.825141  564228.5092  7.020698e+08

1045885 rows × 7 columns
```

```
In [3]: z= 400 #change

In [4]: import numpy as np
import pandas as pd

Red_frame = pd.DataFrame(0, index= np.arange(0,2300,1), columns = [np.arange(0,400,1)]) #change

sample = np.arange(1,2301,1)
list = []
count = 0
for j in sample:
    data_cross = Gaula_data.loc[Gaula_data["ORIG_FID"] == j]
    data_cross = data_cross.reset_index(drop=True)
    Min = data_cross['green_elevation'].min()
    data_cross["green_elevation"] = data_cross["green_elevation"] - Min
    data_cross["red_elevation"] = data_cross["red_elevation"] - Min
    Red = data_cross["red_elevation"]

    list.append(len(Red))

    if len(Red)== z-1:
        new_row = Red.iloc[z-2]
        Red.loc[z-1] = new_row

    Red_frame.iloc[count,0:len(Red)] = Red.values
    #print(Len(Red))
    count= count +1
# print(max(List))
# print(min(List))
```

```
In [6]: import numpy as np
import pandas as pd

Green_frame = pd.DataFrame(0, index= np.arange(0,2300,1), columns = [np.arange(0,400,1)]) #change

sample = np.arange(1,2301,1)
list = []
count = 0
for j in sample:
    data_cross = Gaula_data.loc[Gaula_data["ORIG_FID"] == j]
    data_cross = data_cross.reset_index(drop=True)
    Min = data_cross['green_elevation'].min()
    data_cross["green_elevation"] = data_cross["green_elevation"] - Min
    data_cross["red_elevation"] = data_cross["red_elevation"] - Min
    Green = data_cross["green_elevation"]

    list.append(len(Green))

    if len(Green)== z-1:
        new_row = Green.iloc[z-2]
        Green.loc[z-1] = new_row

    Green_frame.iloc[count,0:len(Green)] = Green.values
    #print(Len(Green))
    count= count +1
# print(max(List))
# print(min(List))
```

```
In [8]: import tensorflow as tf
from keras.models import Sequential
from tensorflow.keras.layers import Activation, Dense
from tensorflow.keras.optimizers import Adam
from tensorflow.keras.metrics import categorical_crossentropy
```

```
In [9]: # model creation & adding layers
model = Sequential([
    Dense(164, activation= "sigmoid", input_shape=(400,)),
    Dense(164, activation= "sigmoid"),
    Dense(400, activation= "linear"),
])
model.summary()
```

```
Model: "sequential"
-----  
Layer (type)          Output Shape         Param #
-----  
dense (Dense)        (None, 164)           65764  
dense_1 (Dense)      (None, 164)           27060  
dense_2 (Dense)      (None, 400)            66000  
-----  
Total params: 158,824  
Trainable params: 158,824  
Non-trainable params: 0
```

```
In [10]: # compile model
model.compile(optimizer ="rmsprop",
              loss= "mse")
model.summary()
```

```
Model: "sequential"
-----  
Layer (type)          Output Shape         Param #
-----  
dense (Dense)        (None, 164)           65764  
dense_1 (Dense)      (None, 164)           27060  
dense_2 (Dense)      (None, 400)            66000  
-----  
Total params: 158,824  
Trainable params: 158,824  
Non-trainable params: 0
```

```
In [11]: # Tranning
history=model.fit(
Red_frame,
Green_frame,
batch_size=1,
epochs=250, verbose=2,
callbacks=None,
validation_split=0.2,
validation_data=None,
shuffle=True,
class_weight=None,
sample_weight=None,
initial_epoch=0)
```

## Gaula Sigmoid

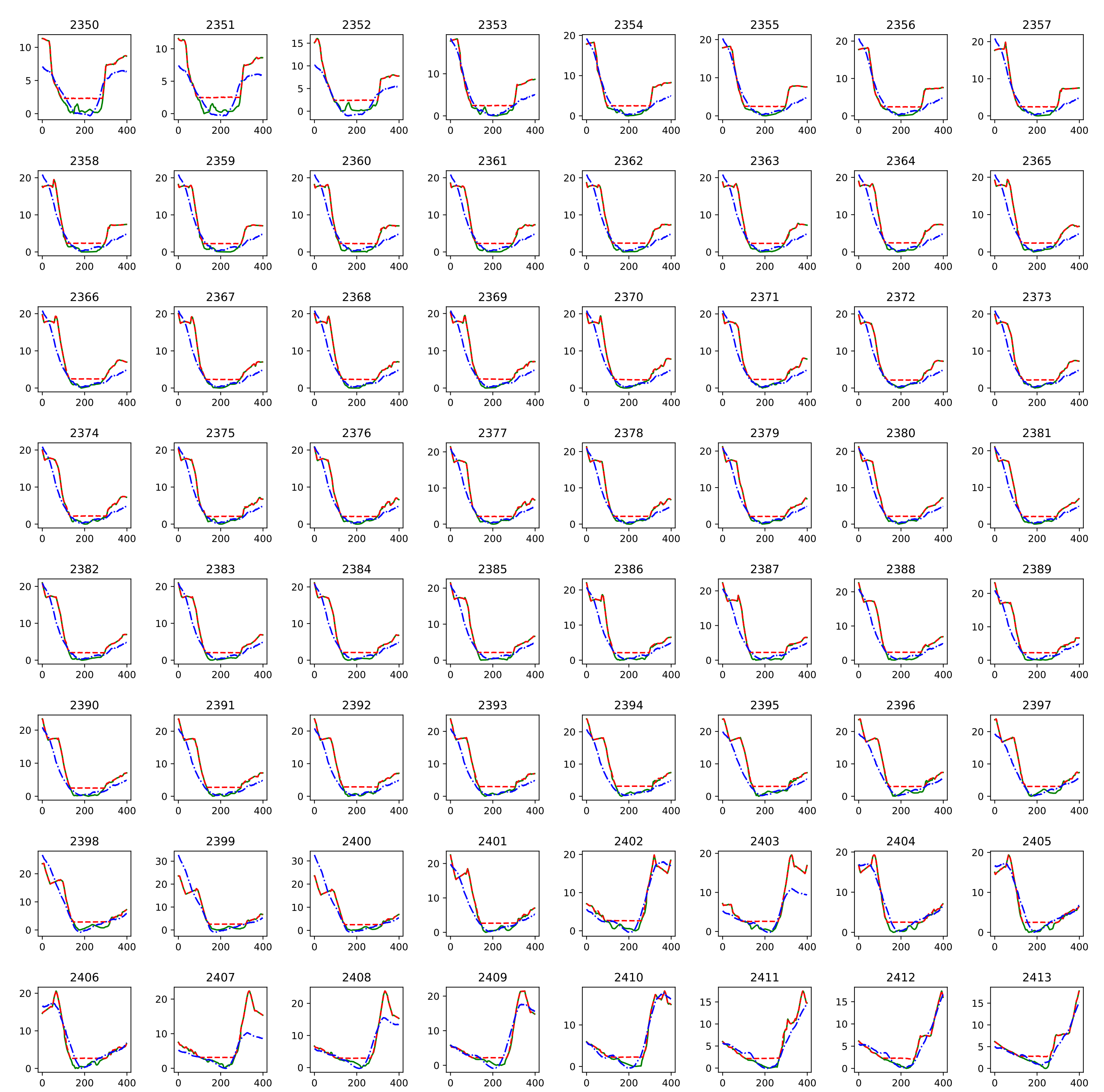
In the next pages, all the cross sections predicted for Gaula outside the range of training are shown using Sigmoid activation function.

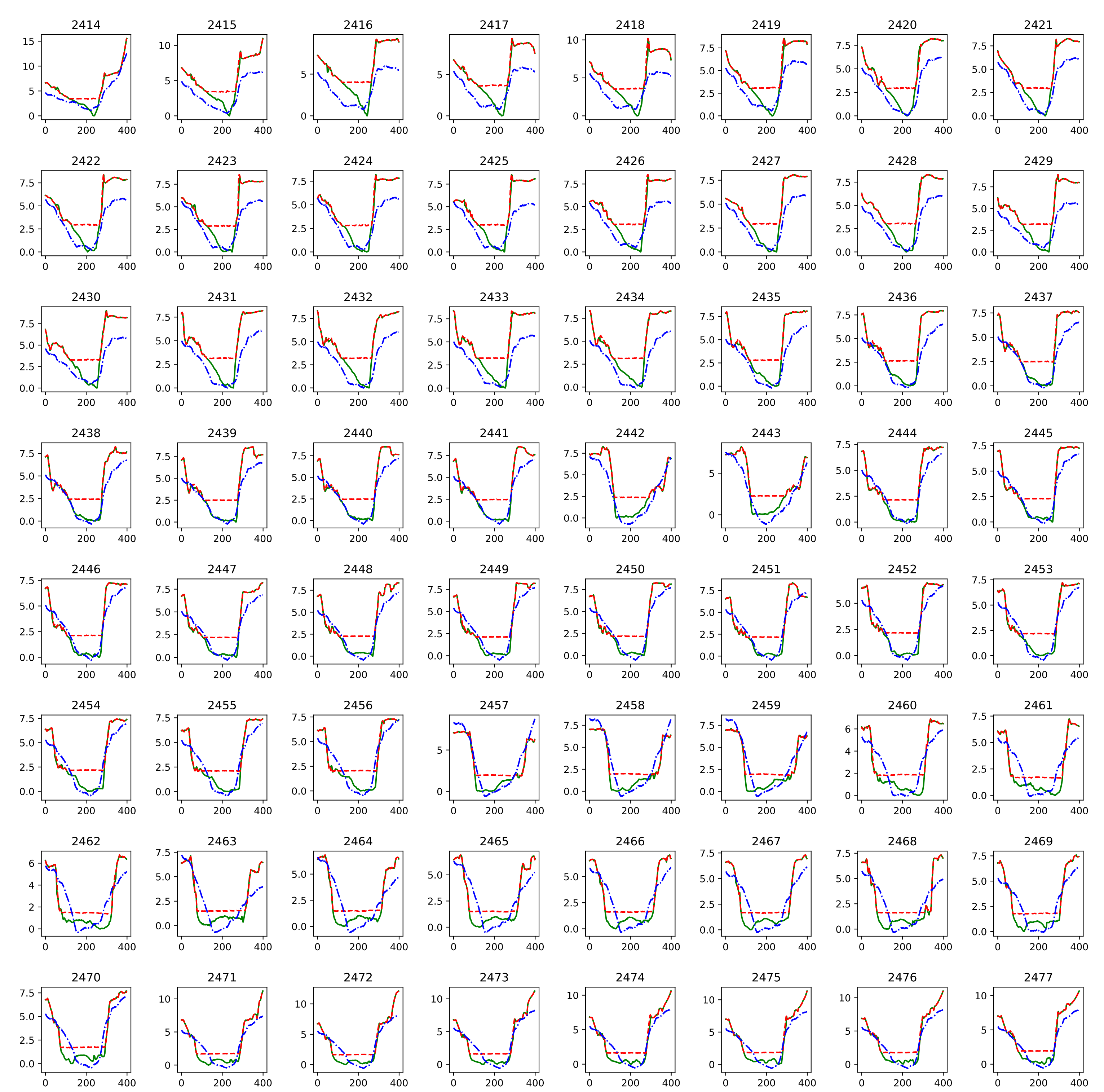
The legend for all the graphs as follow:

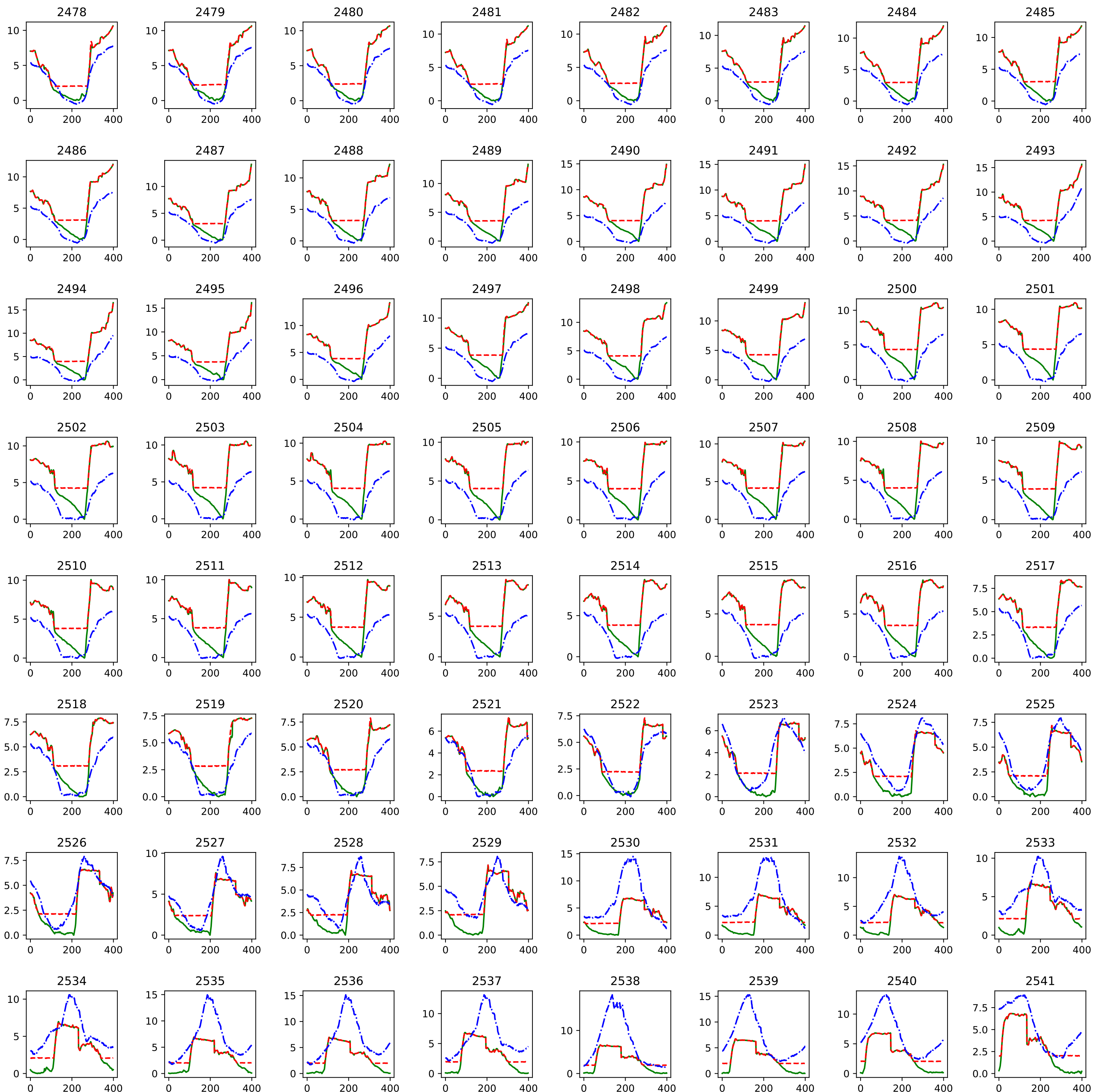
 Green LiDAR

 Red LiDAR

 Prediction







## Driva Sigmoid

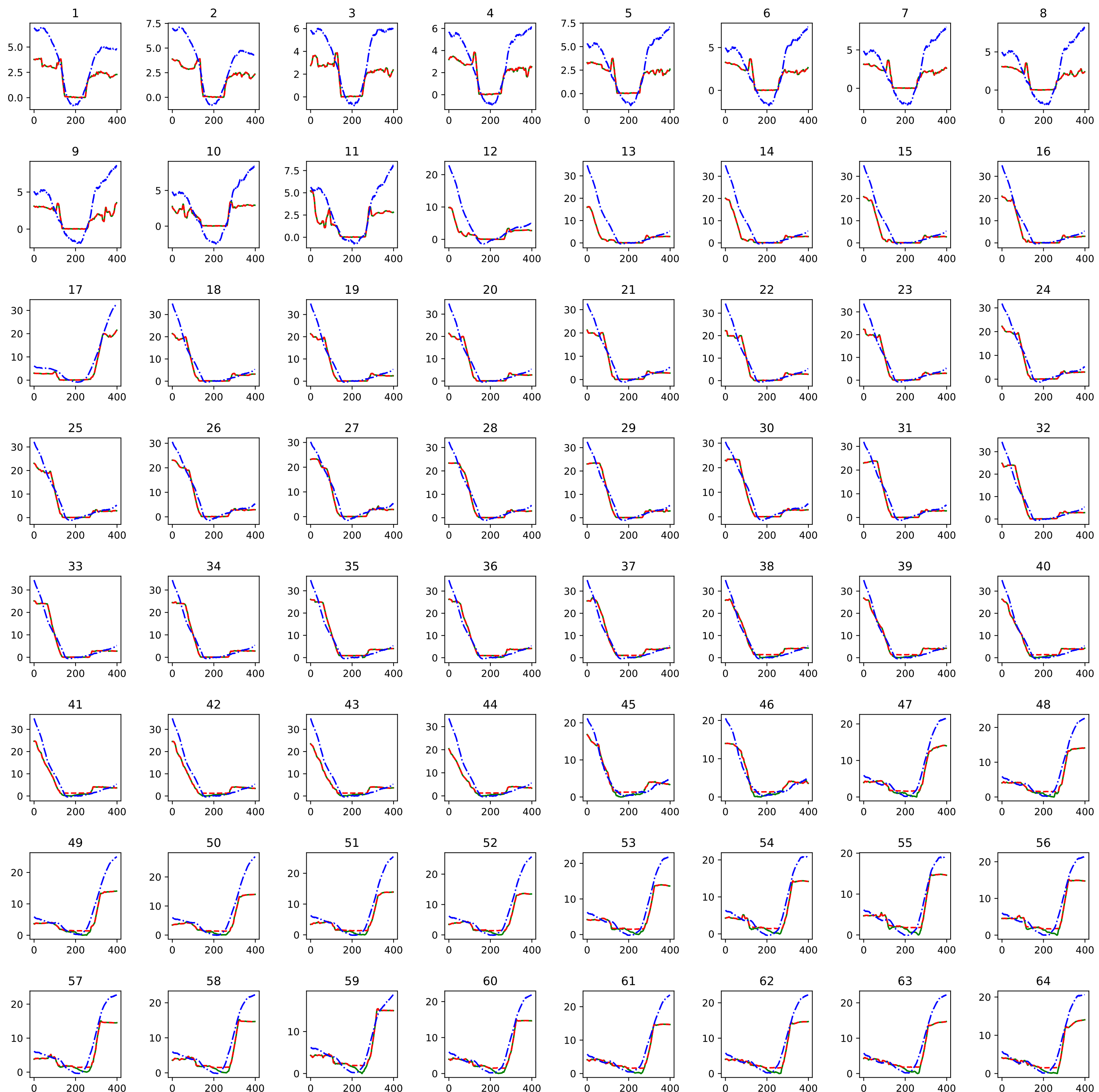
In the next pages, all the cross sections predicted for Driva are shown using Sigmoid activation function.

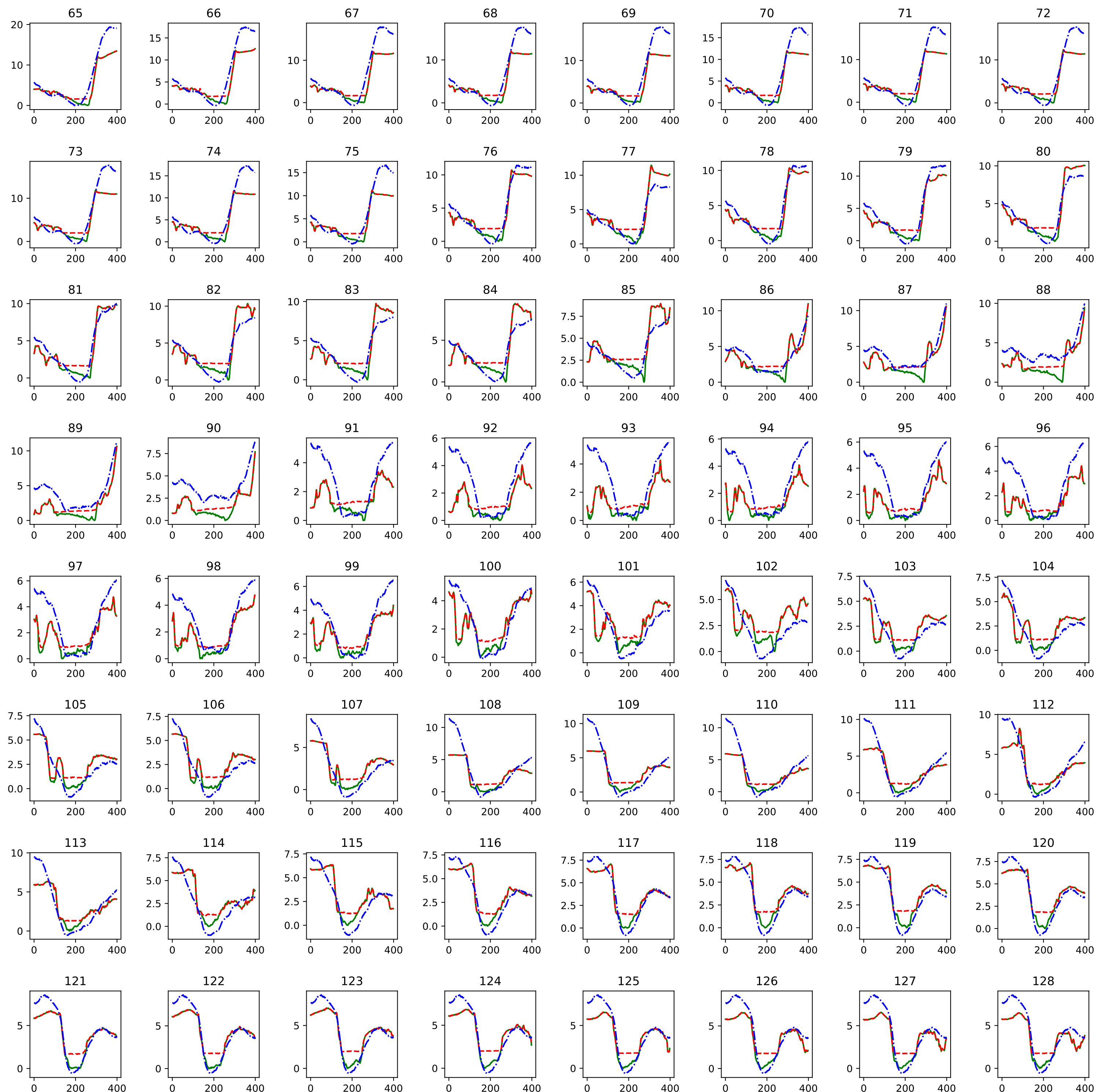
The legend for all the graphs as follow:

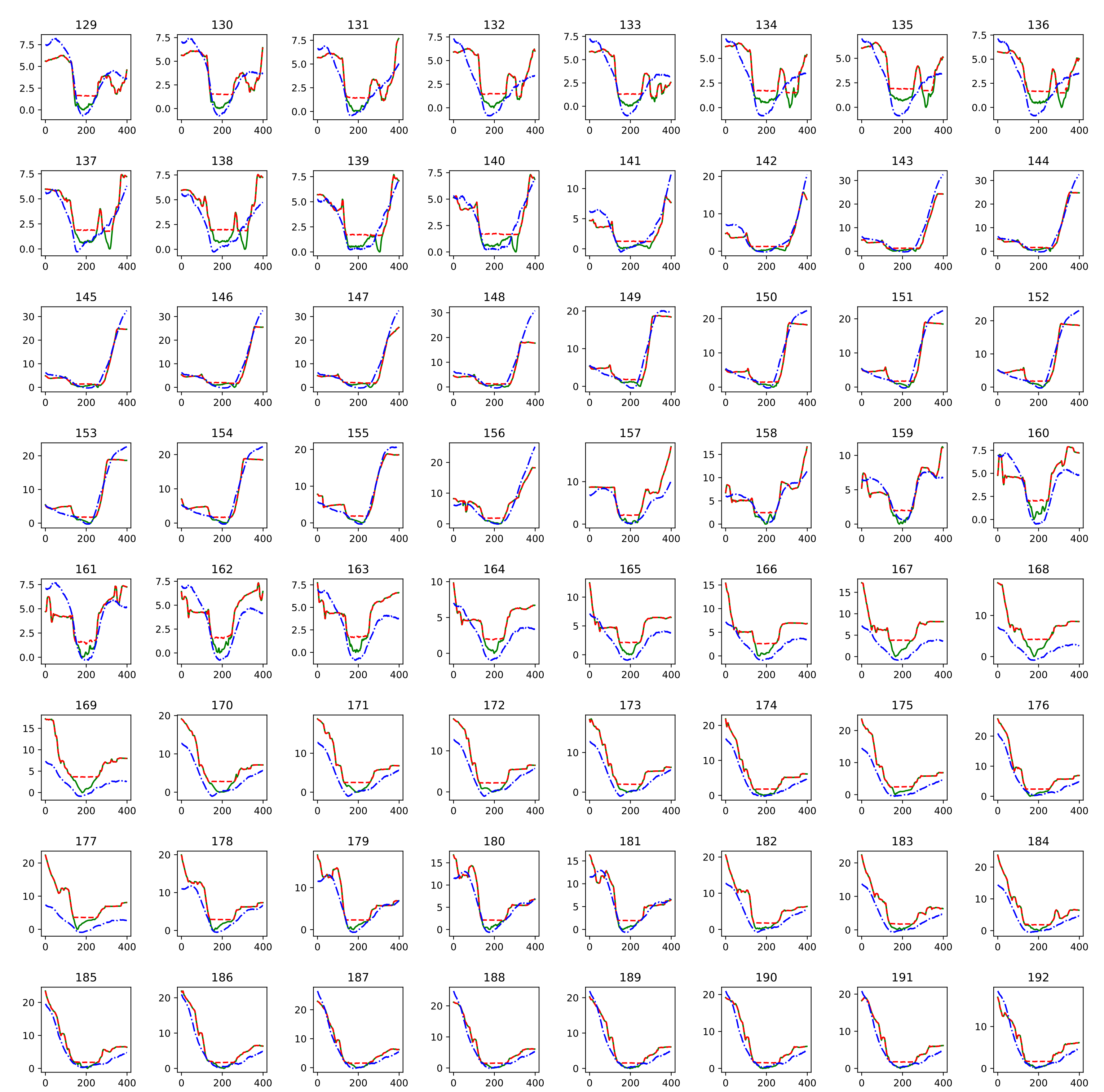
 Green LiDAR

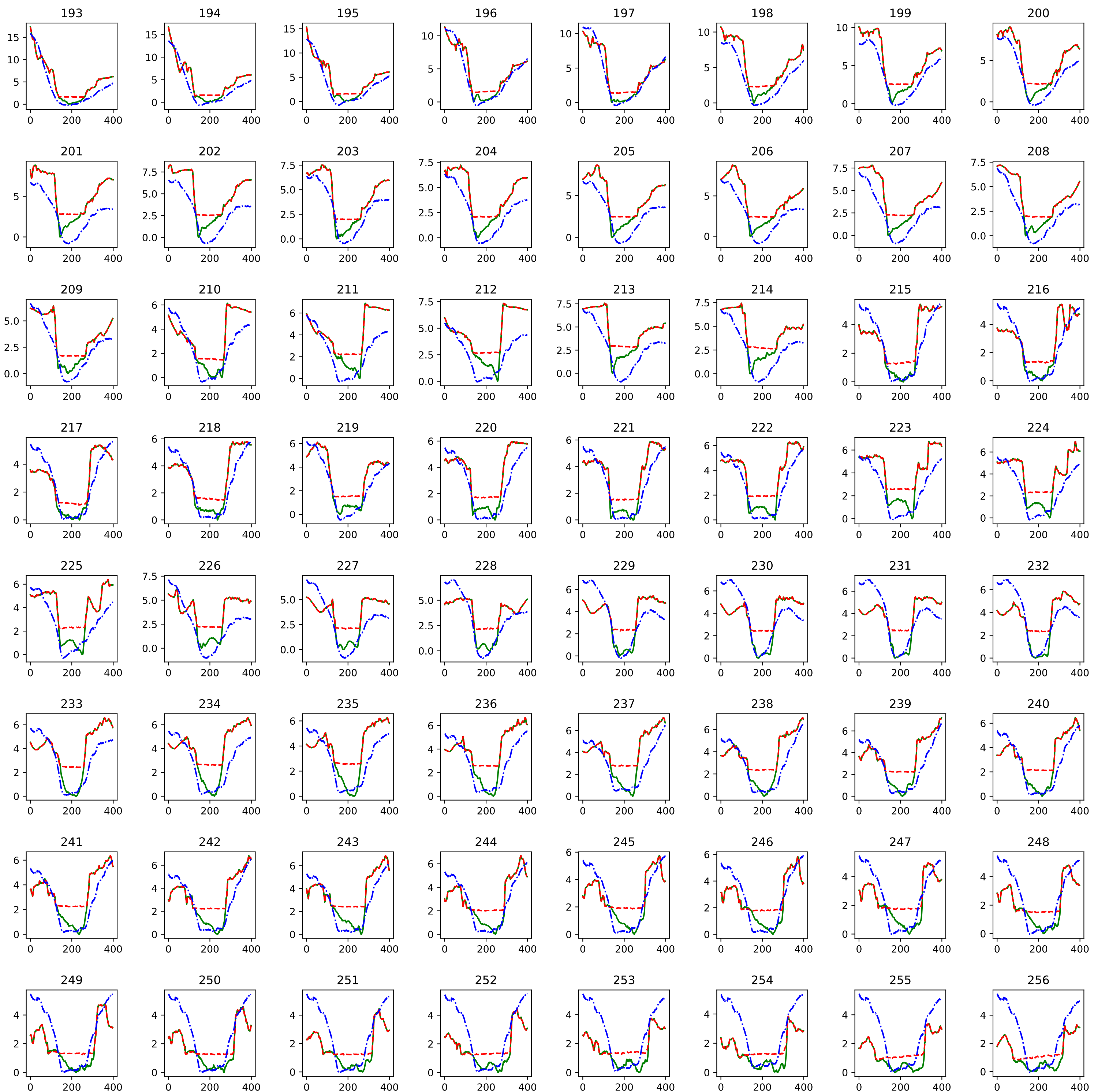
 Red LiDAR

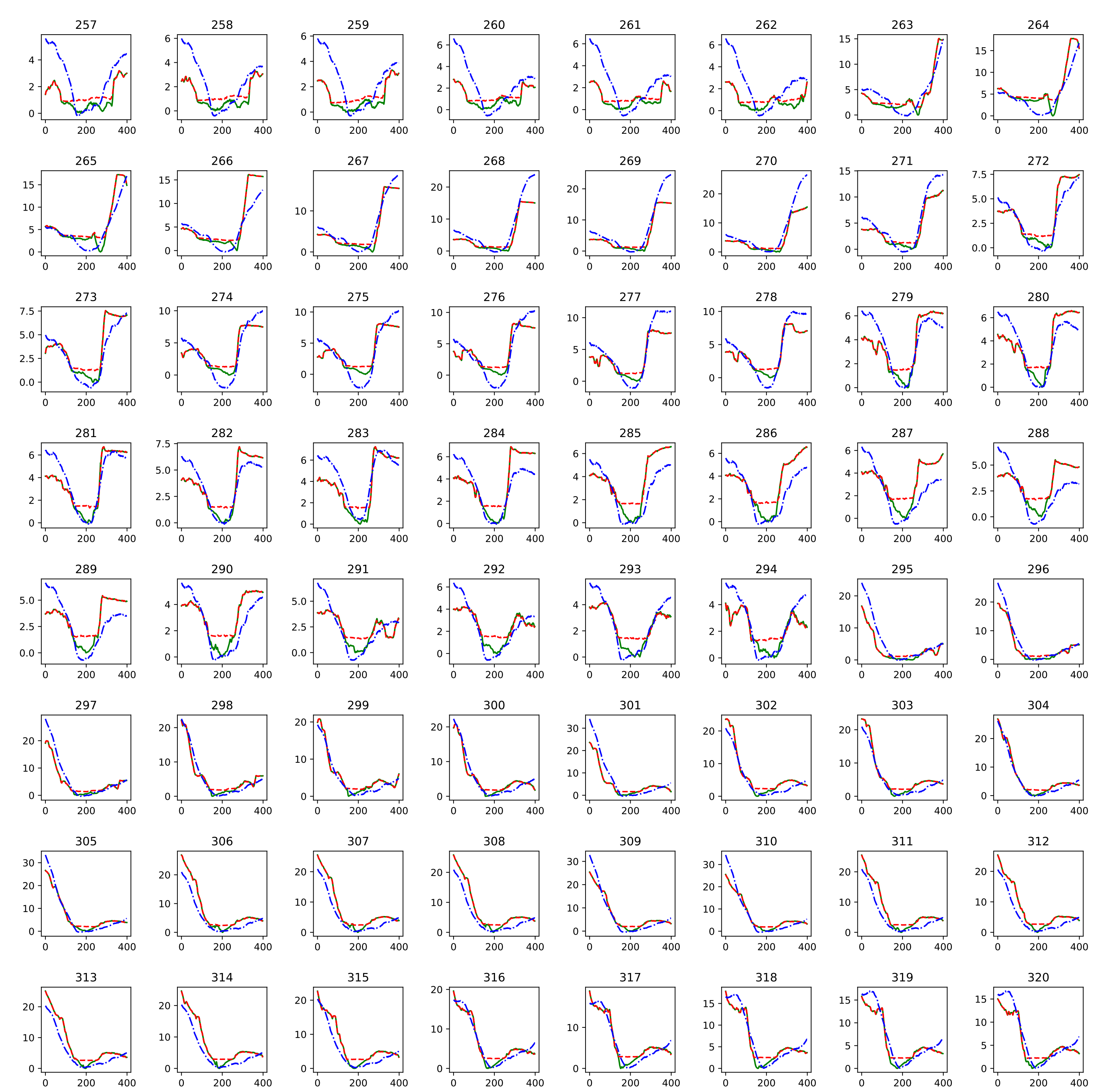
 Prediction

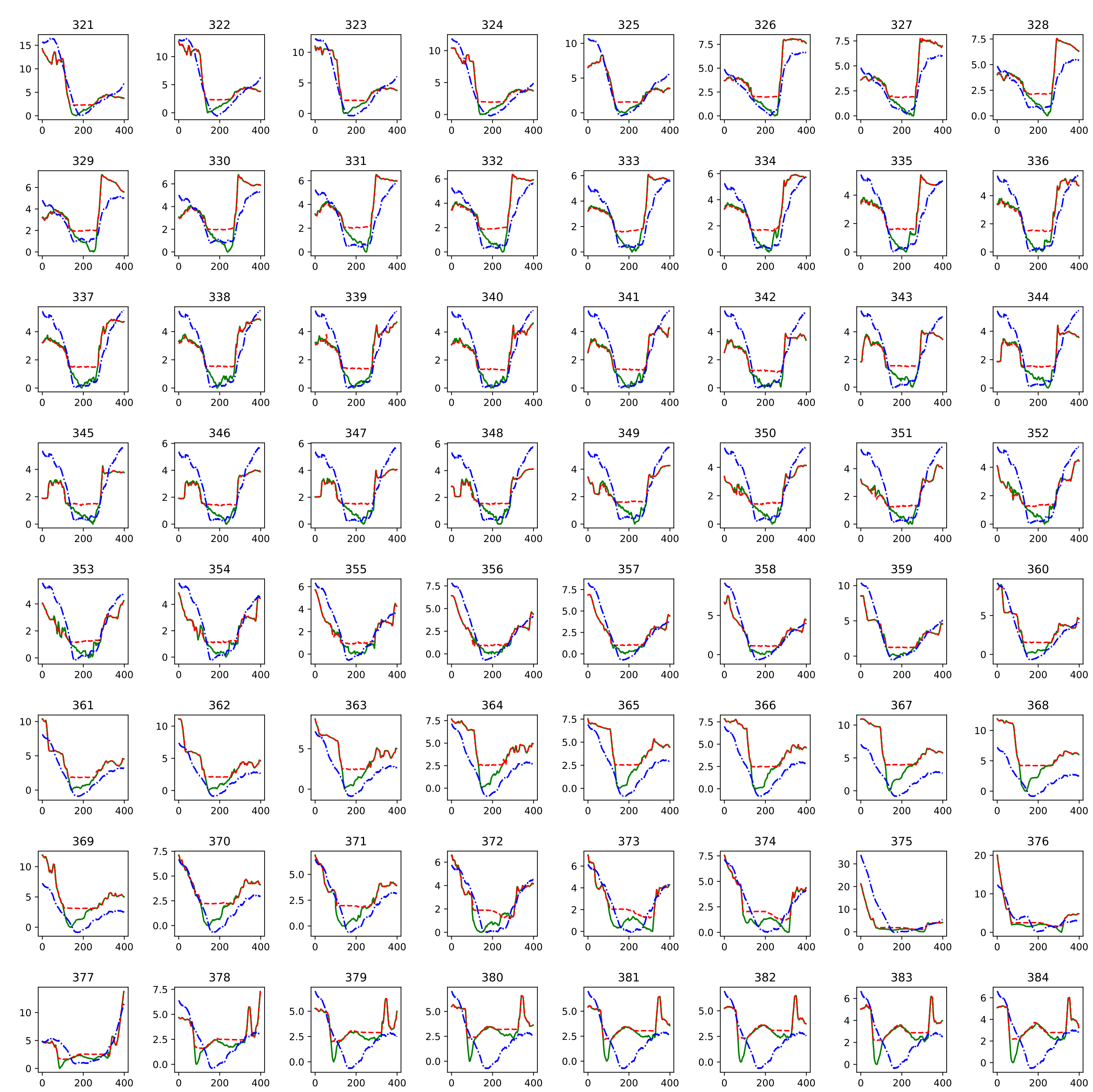


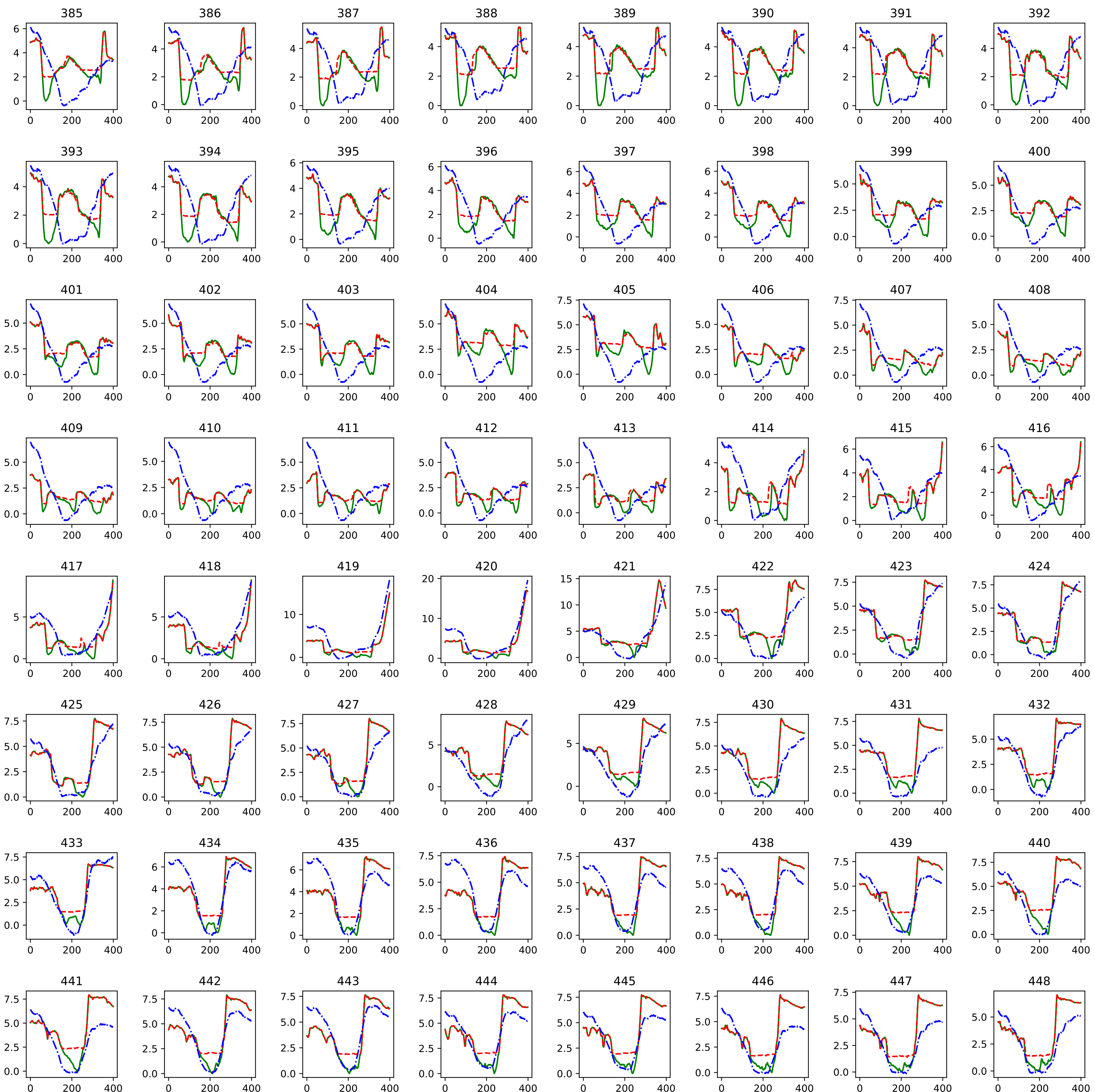


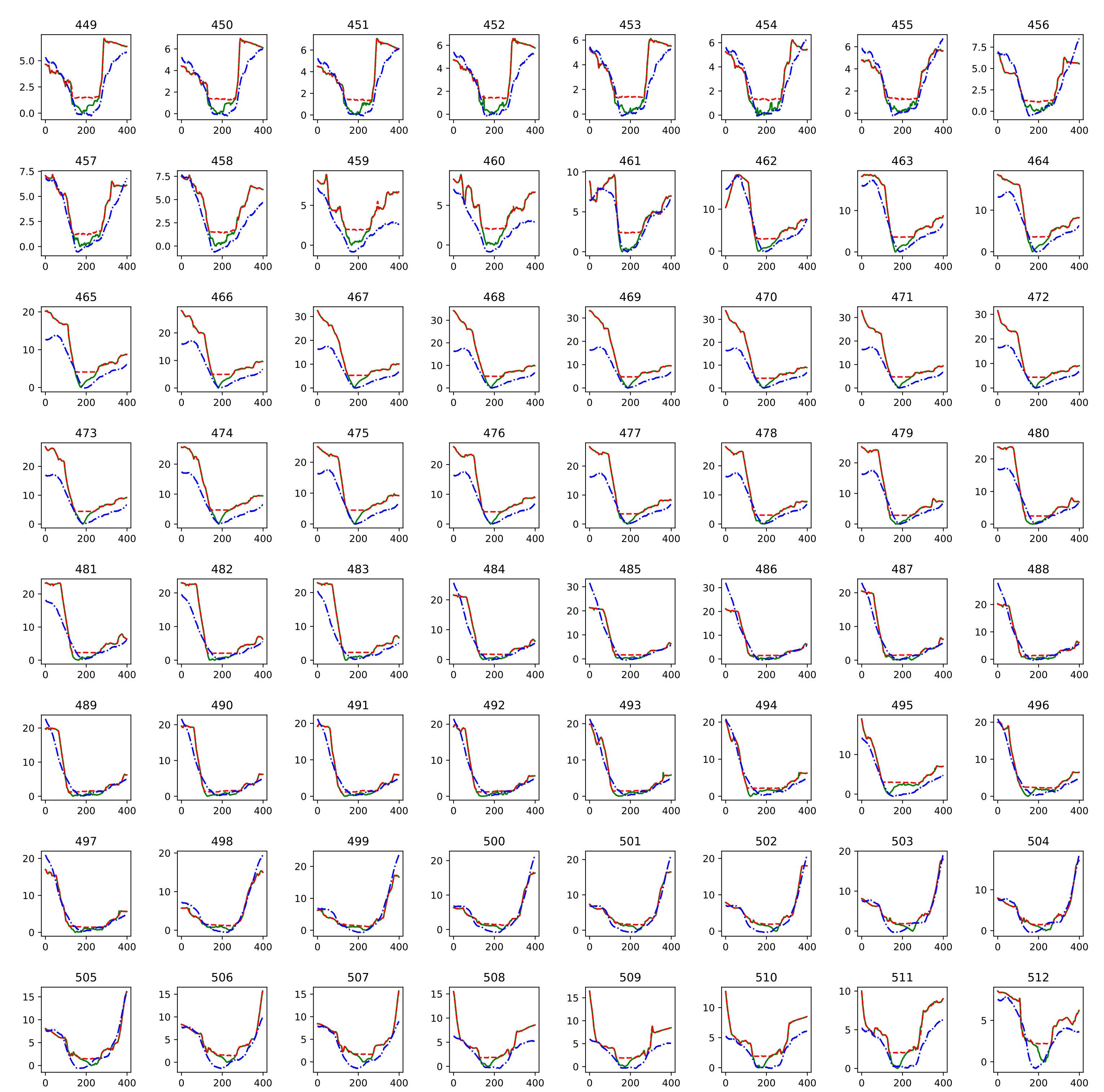


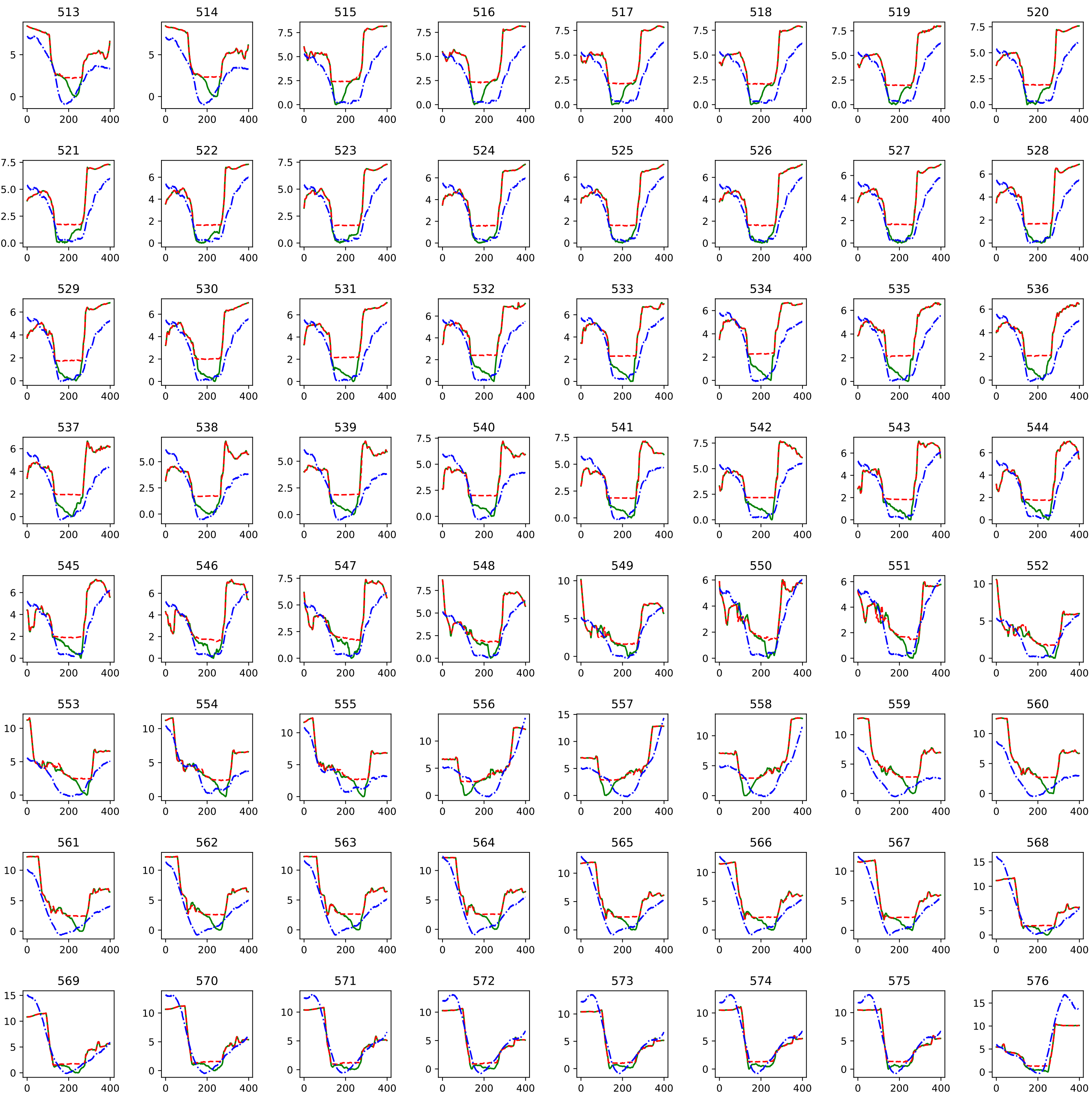


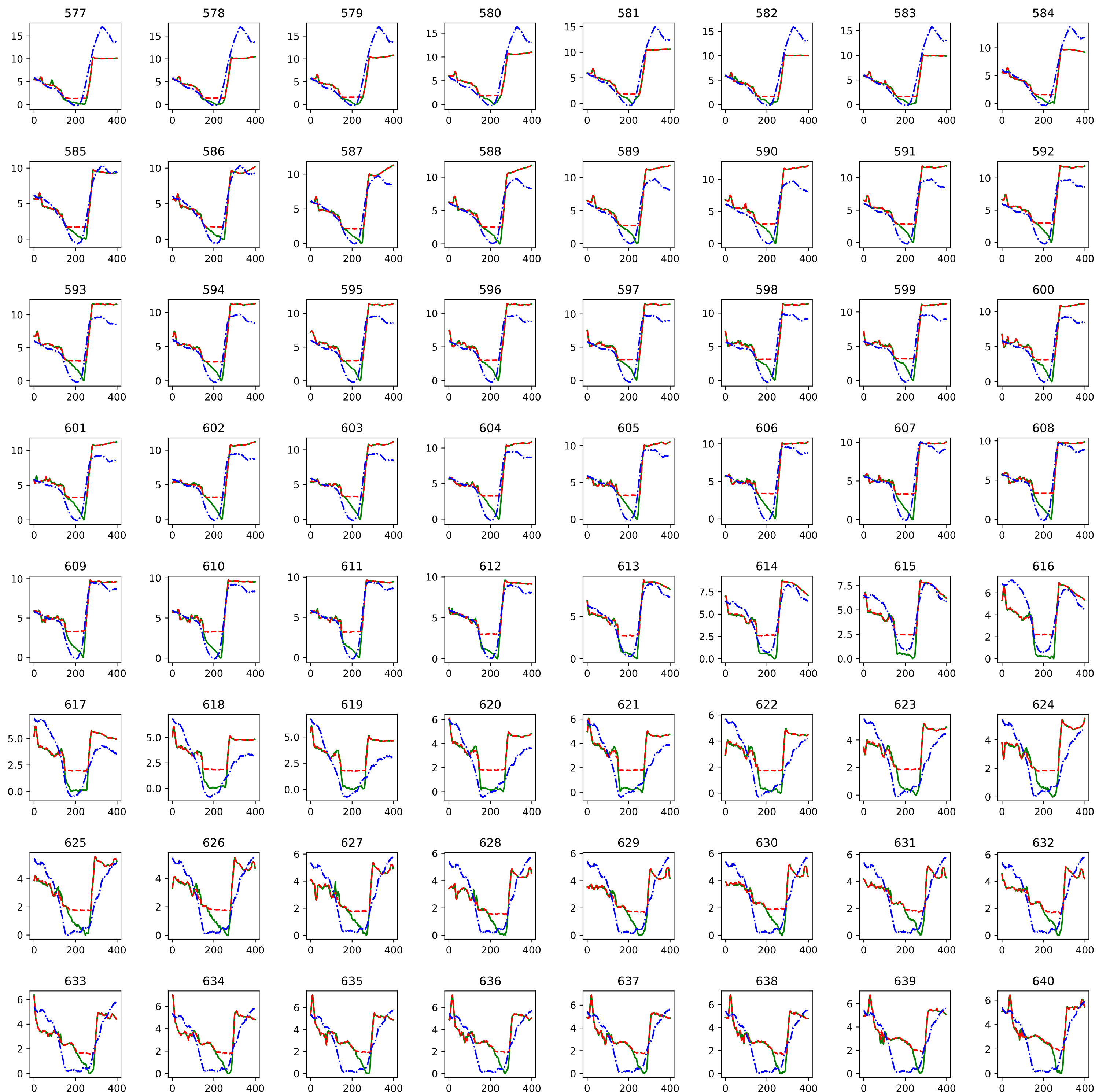


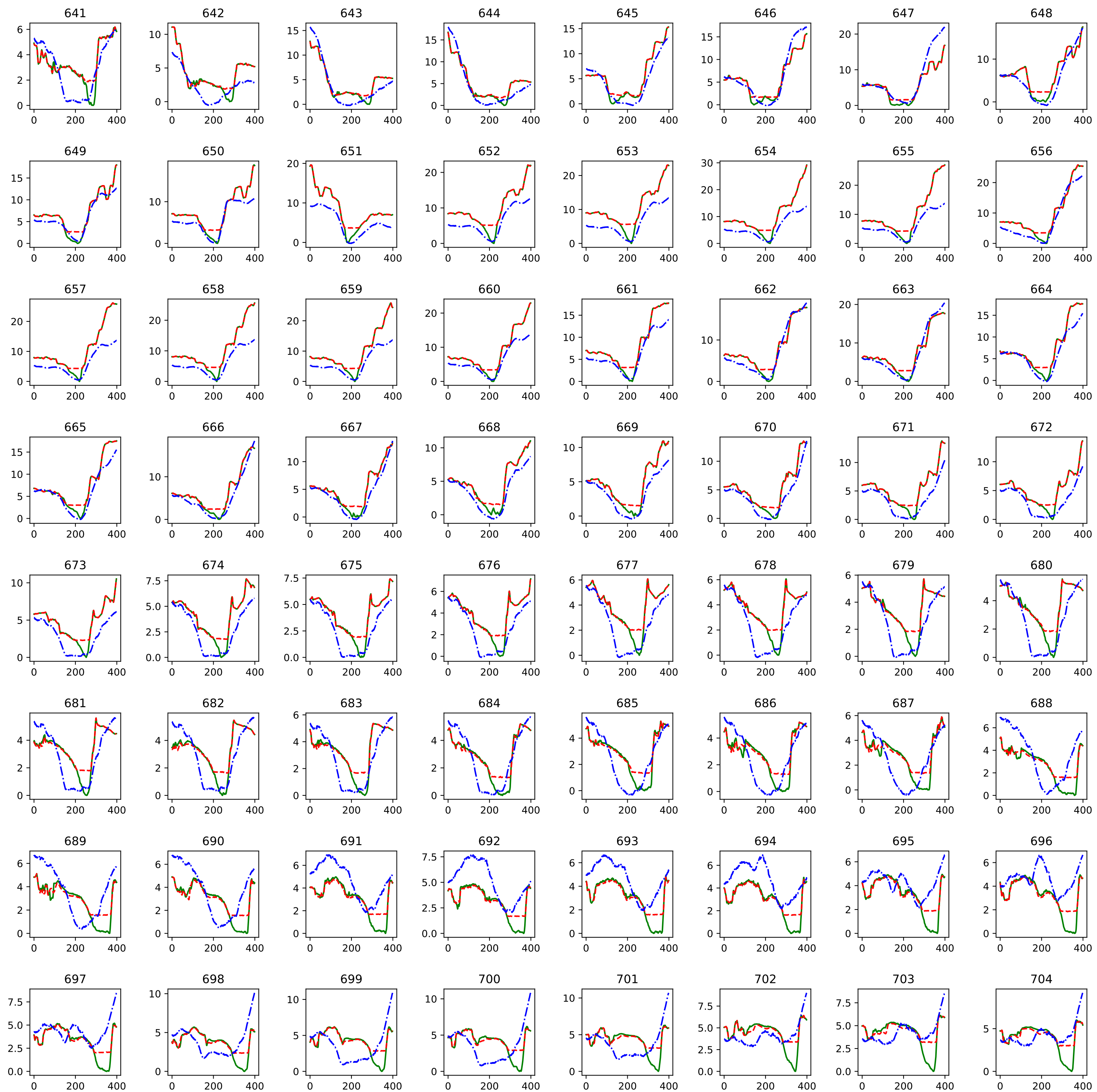


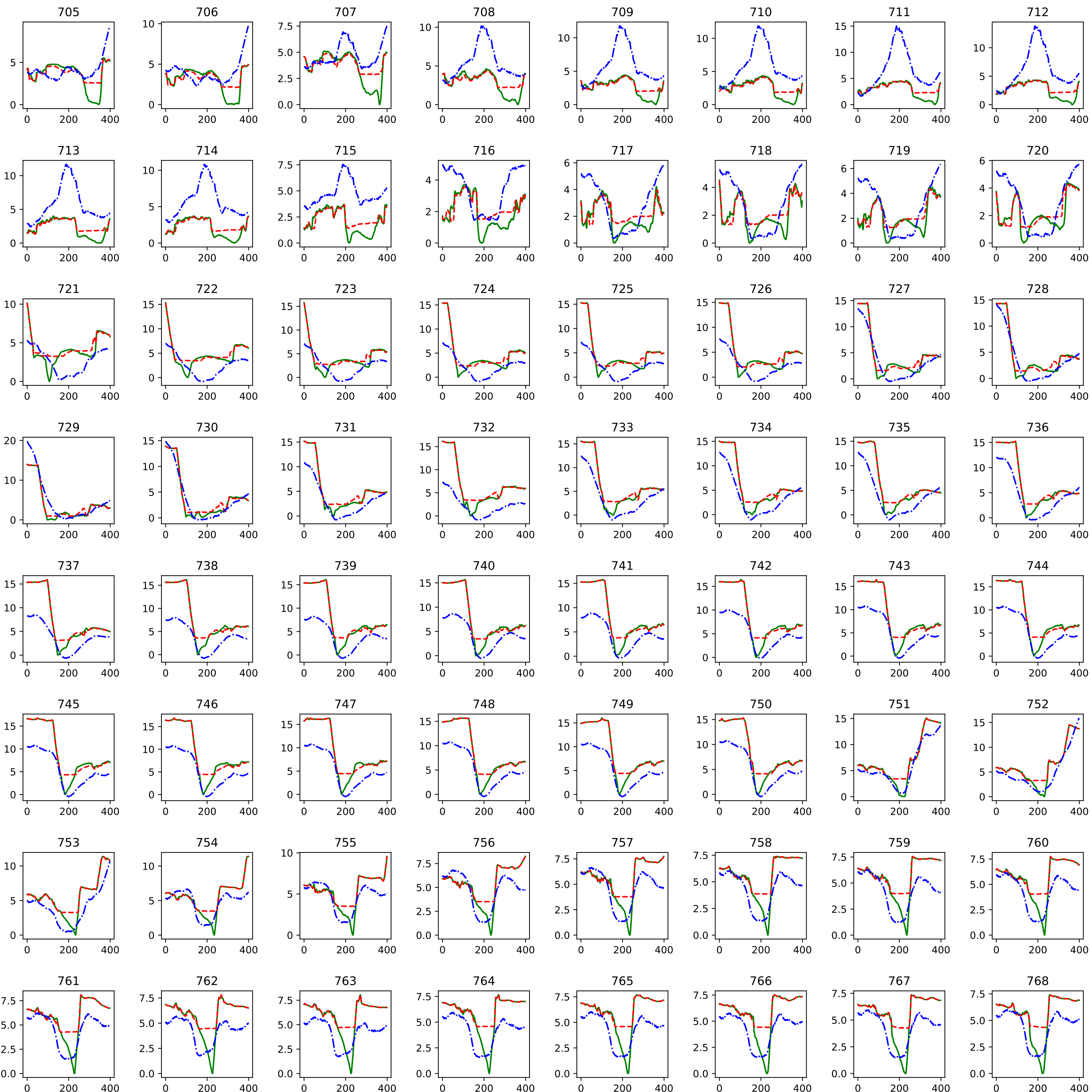


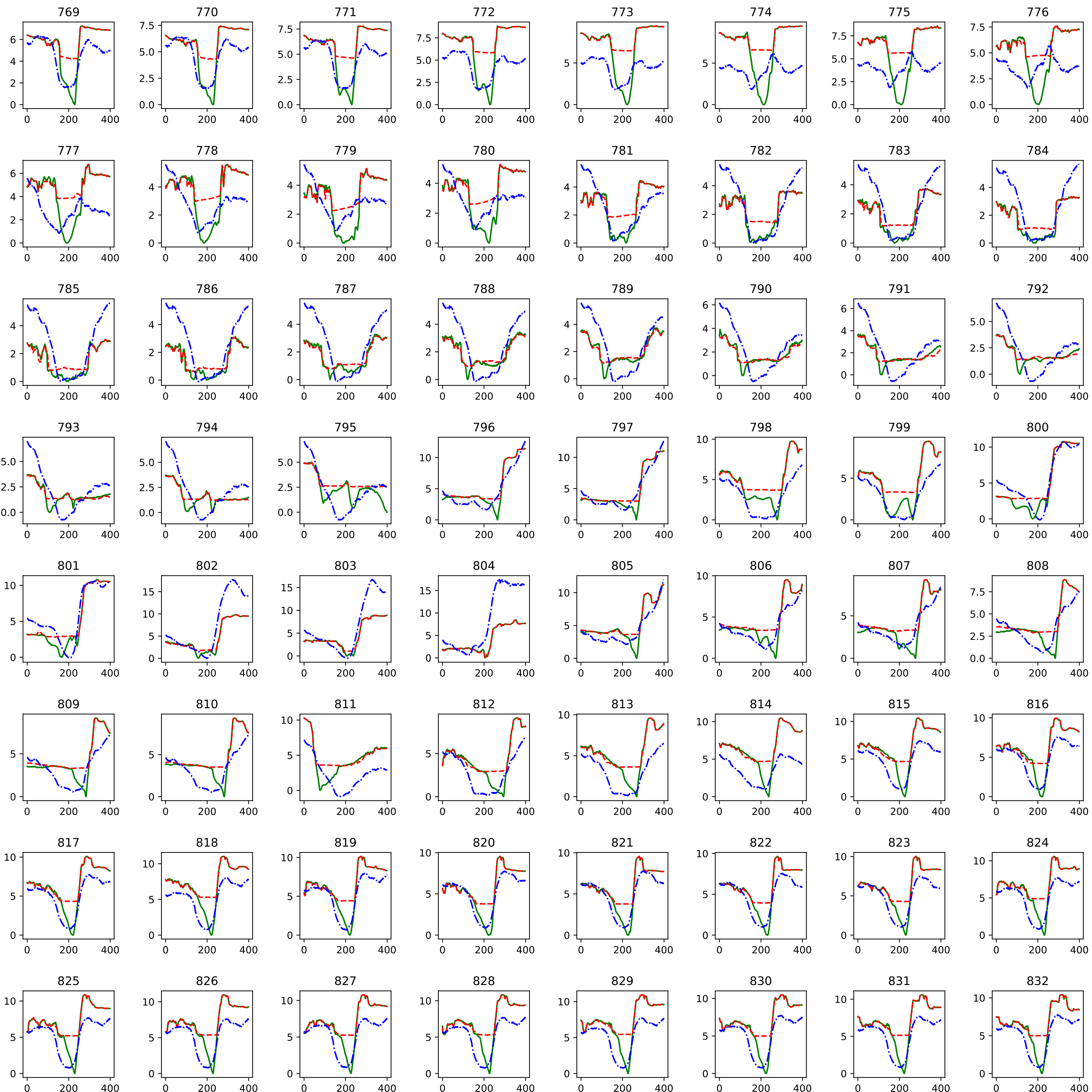


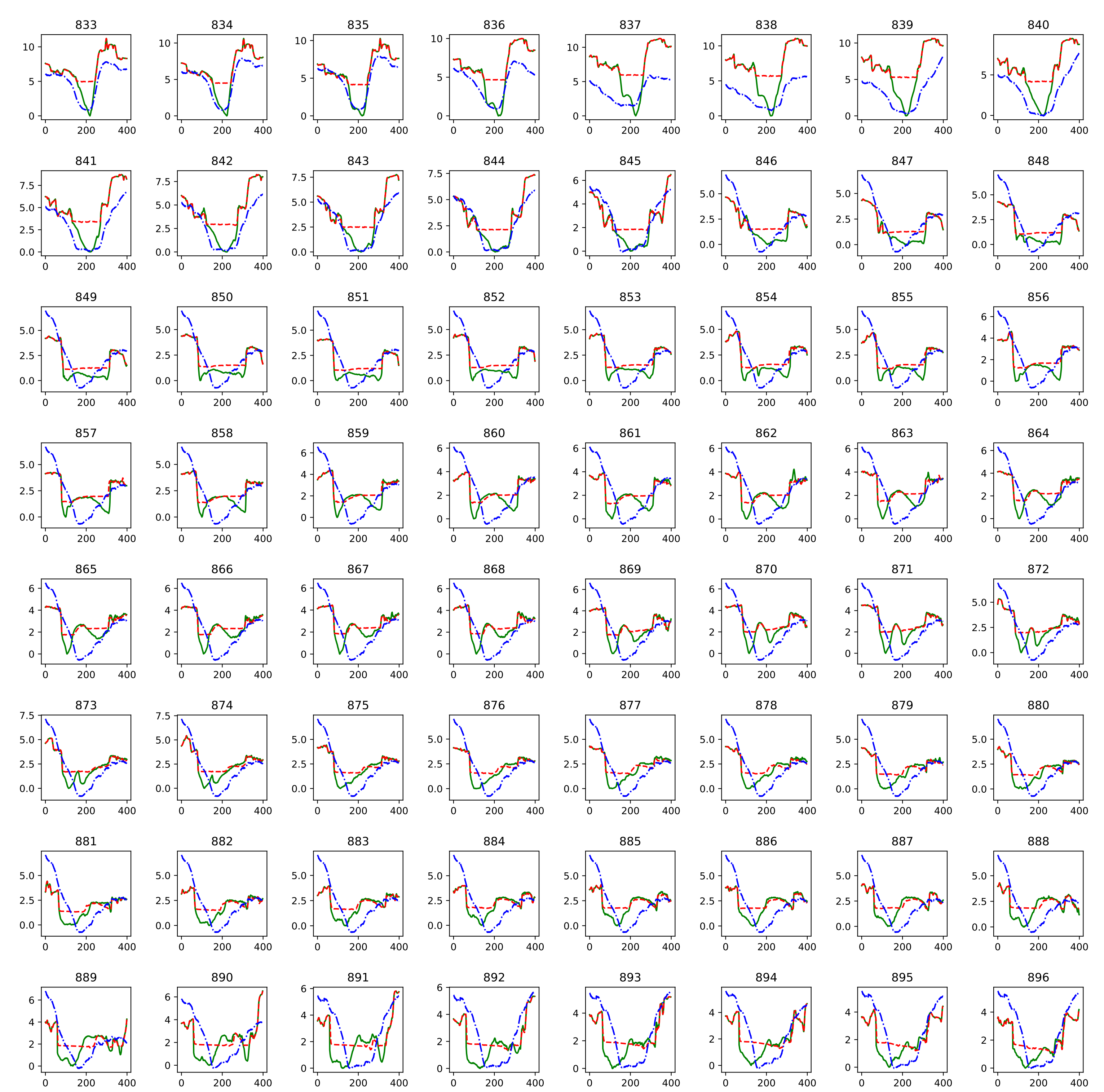


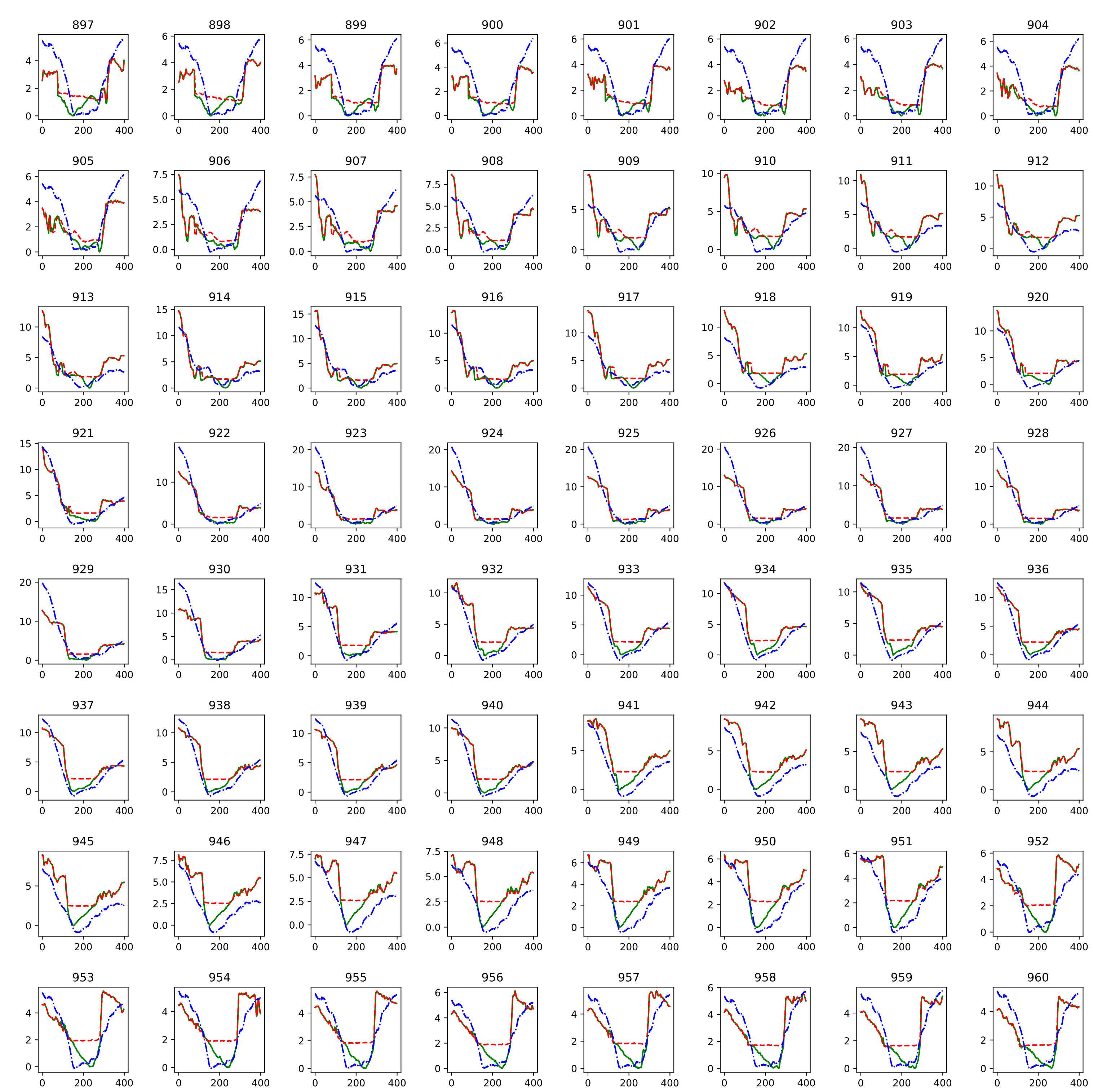


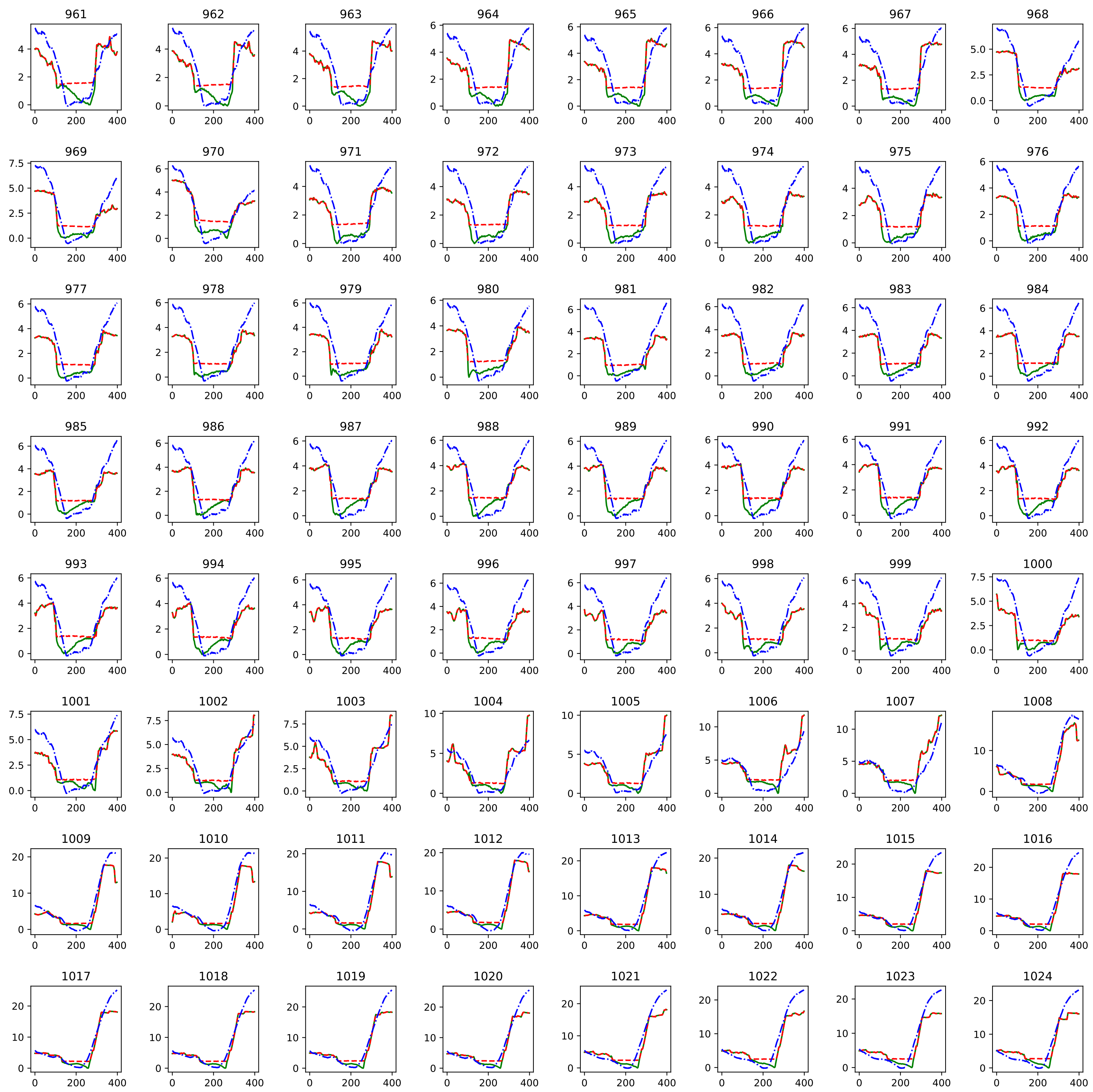


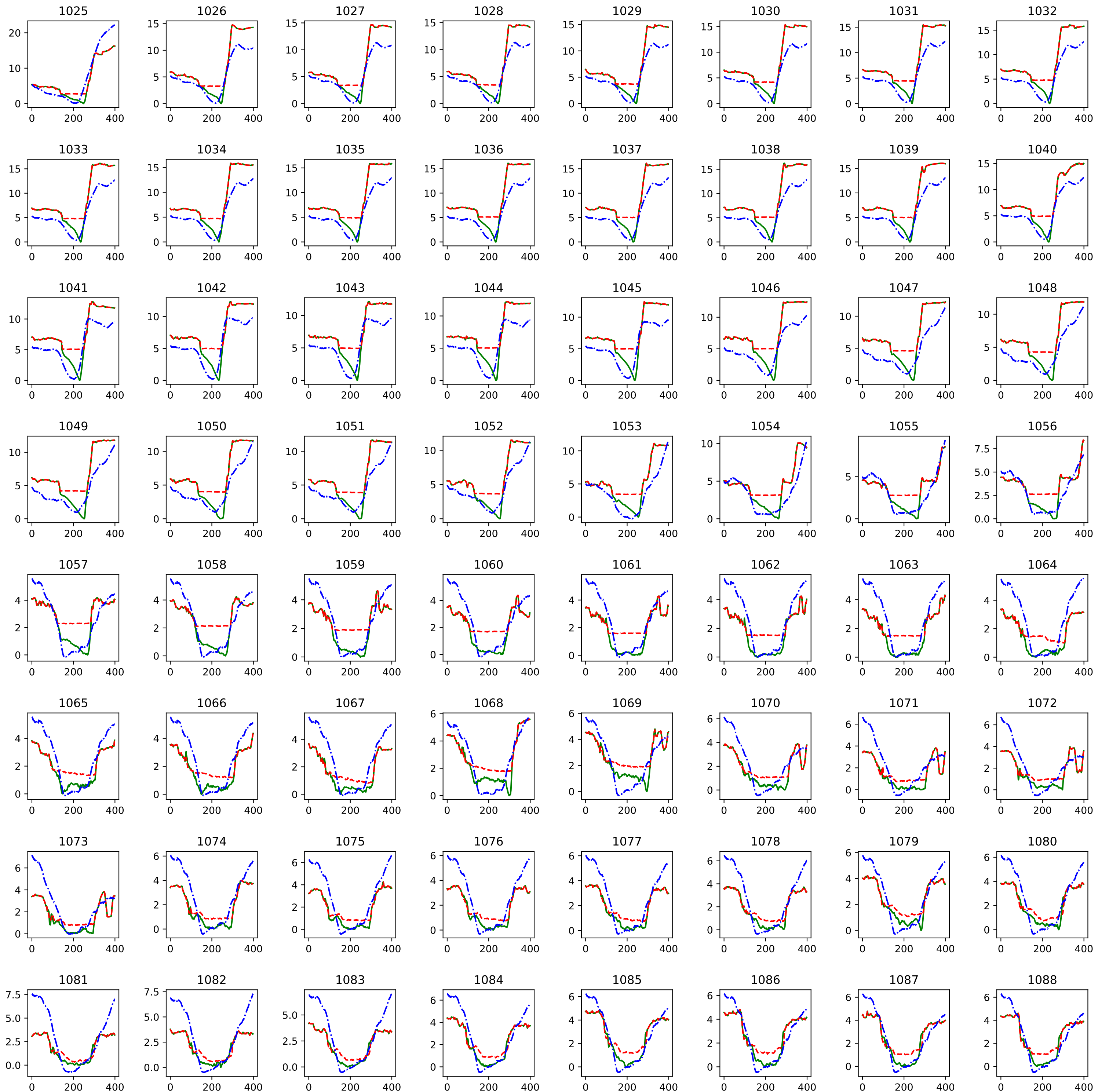


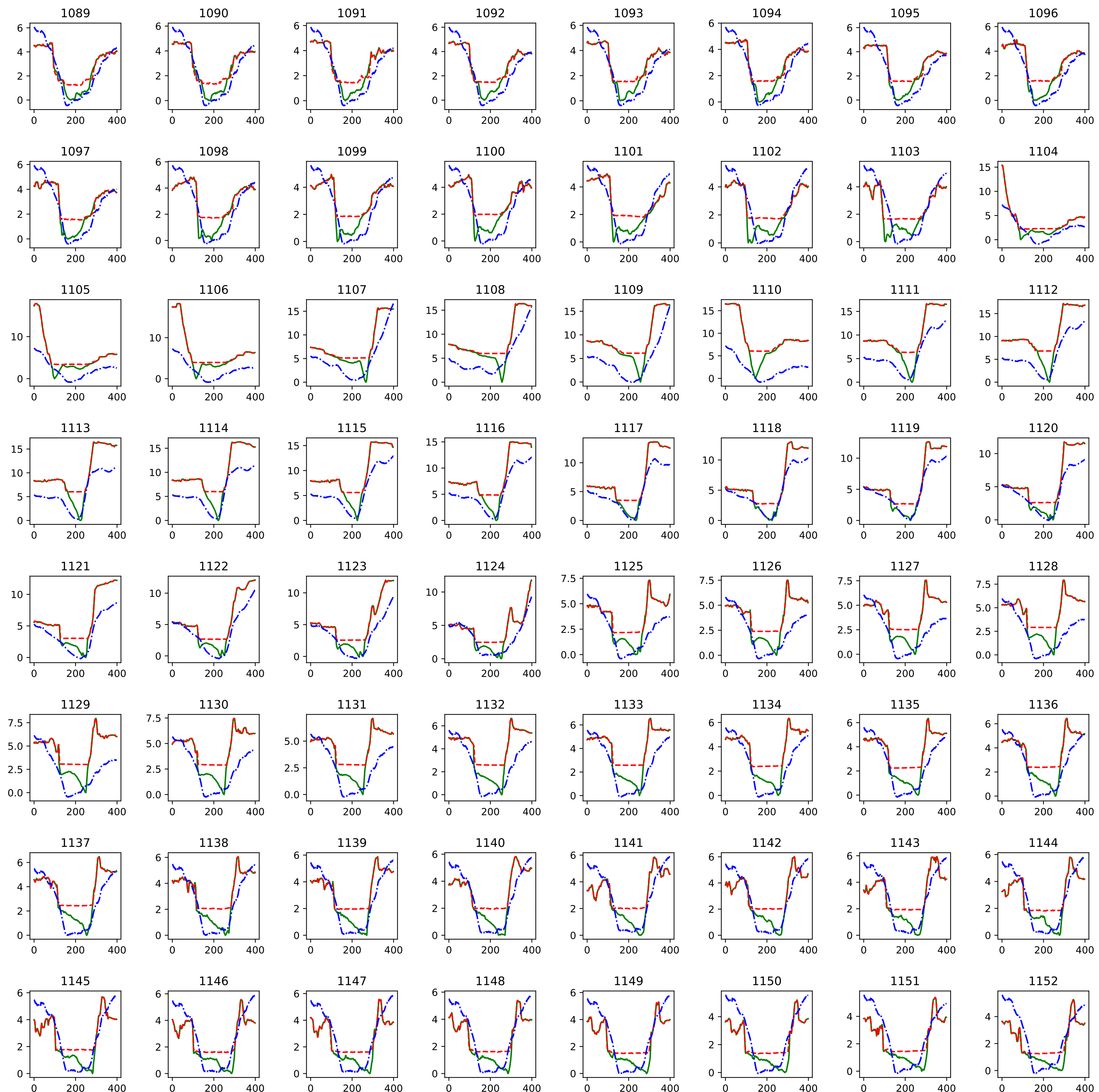












## Surna Sigmoid

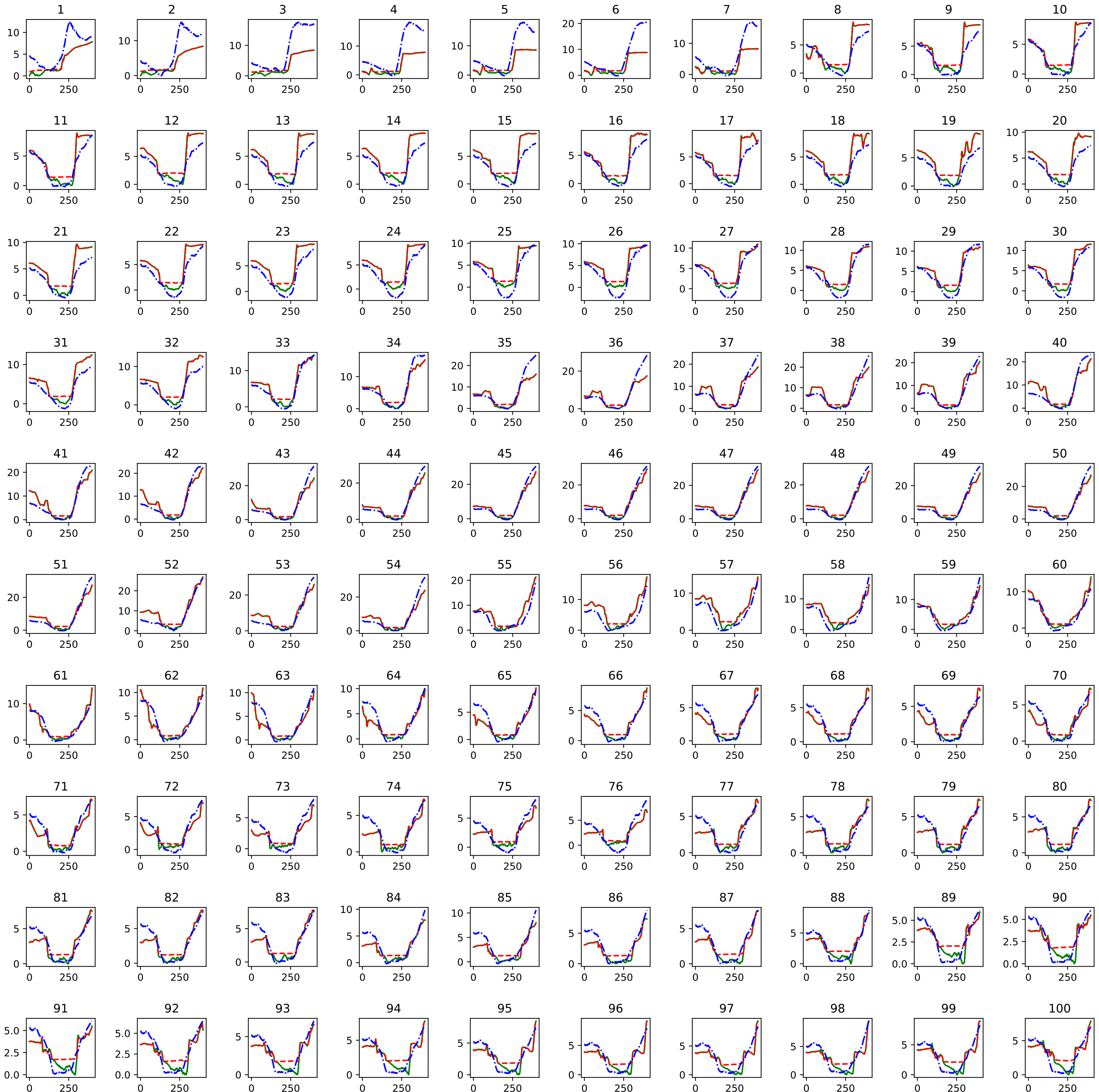
In the next pages, all the cross sections predicted for Surna are shown using Sigmoid activation function.

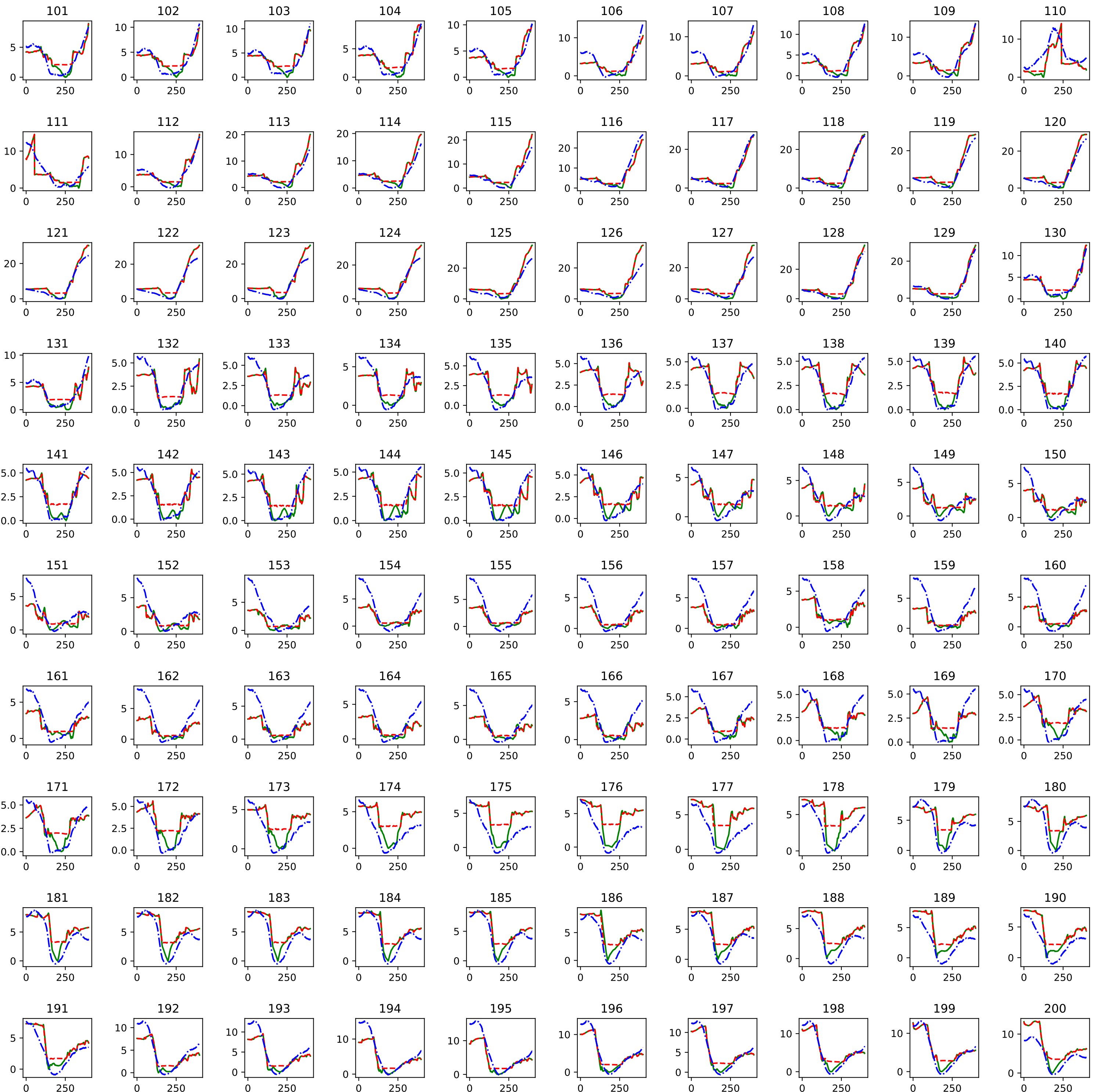
The legend for all the graphs as follow:

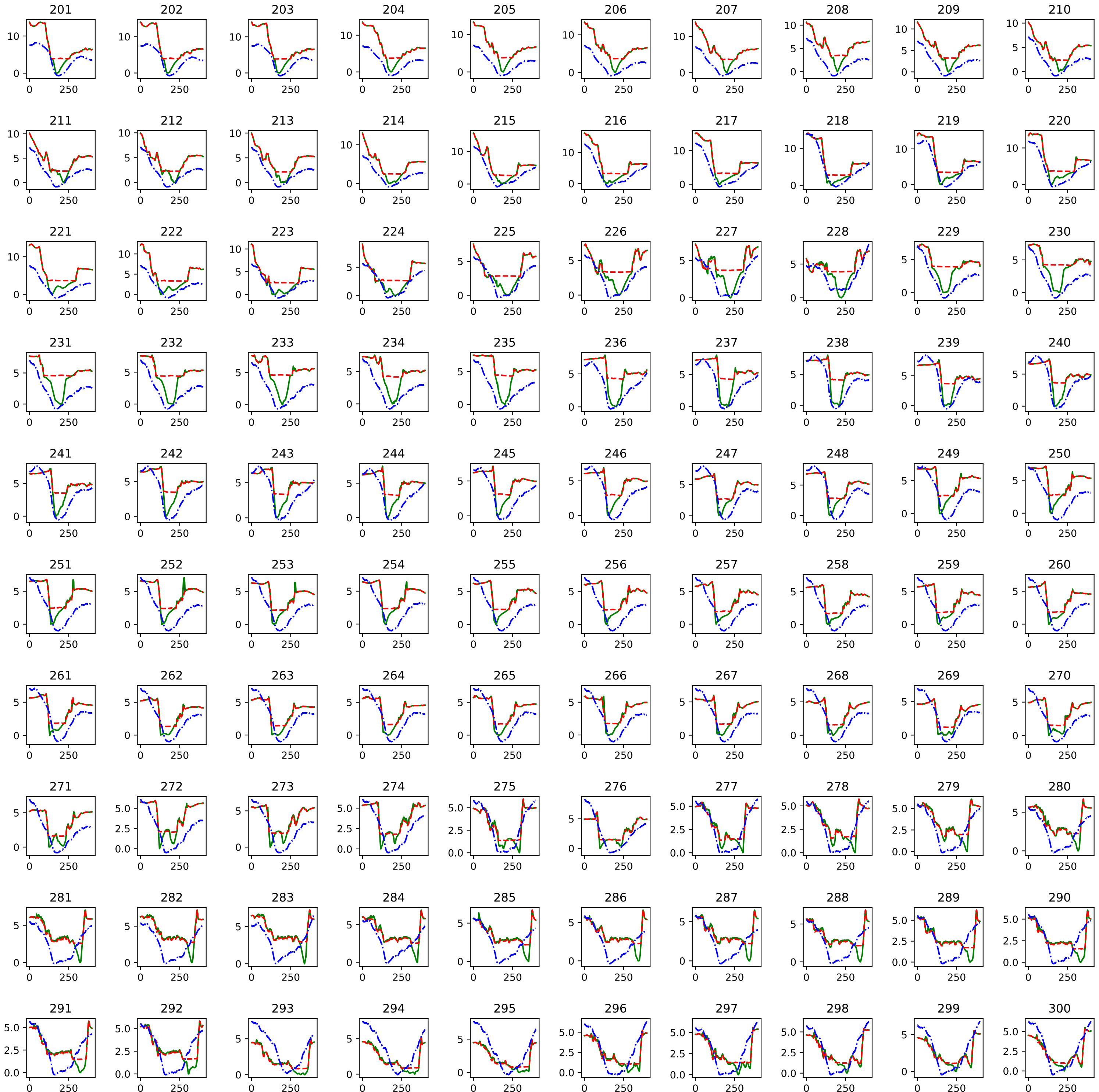
 Green LiDAR

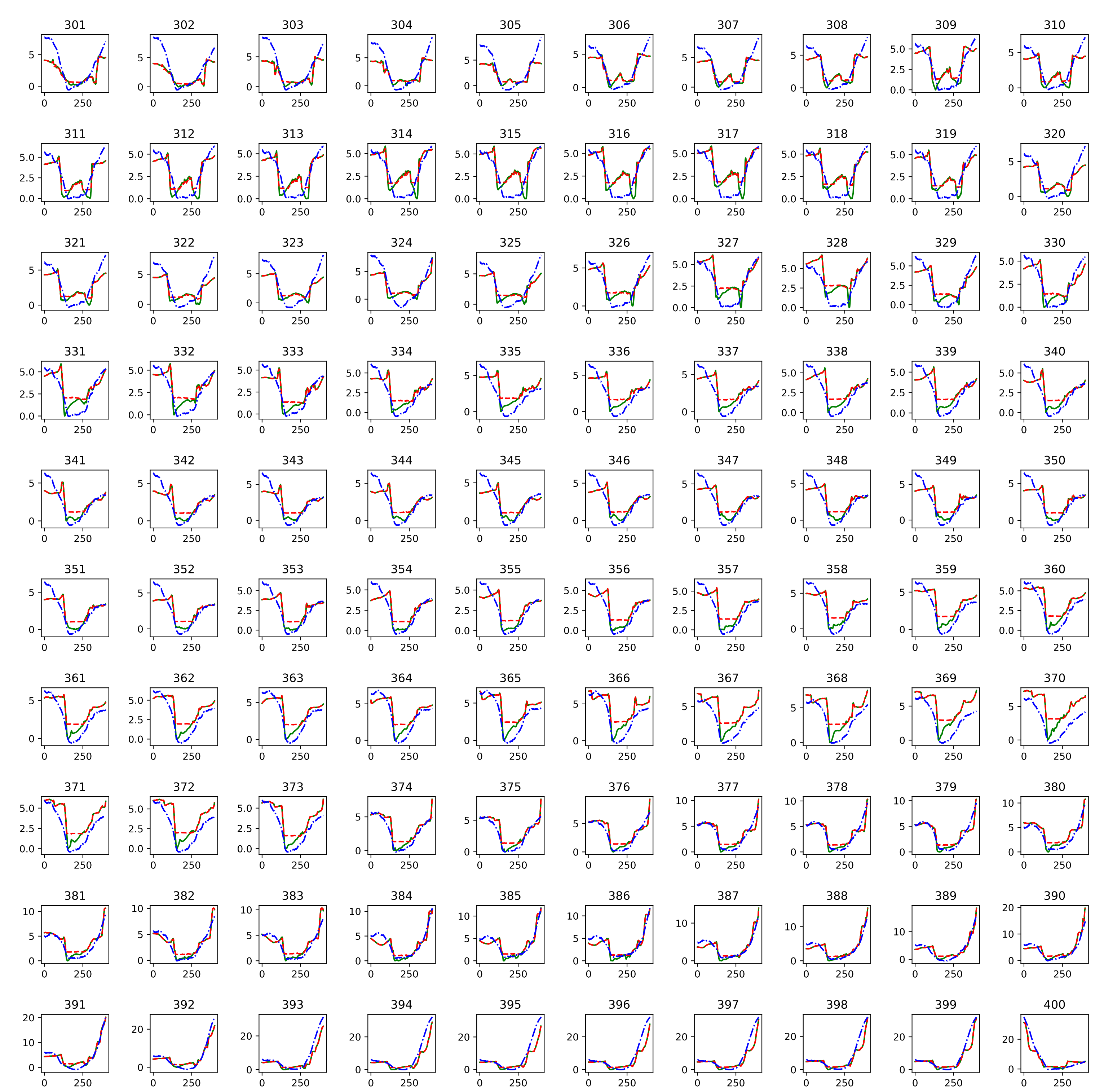
 Red LiDAR

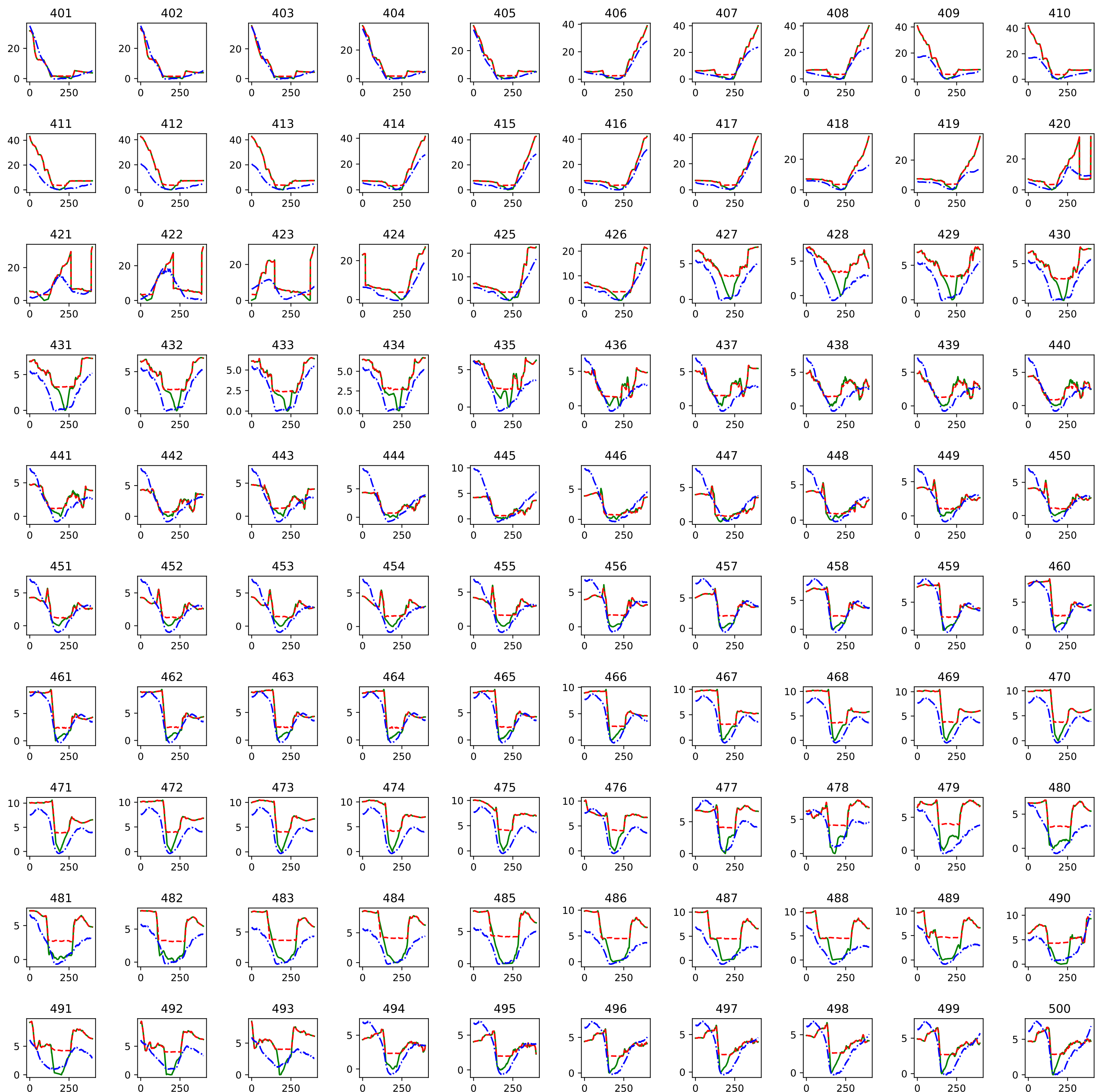
 Prediction

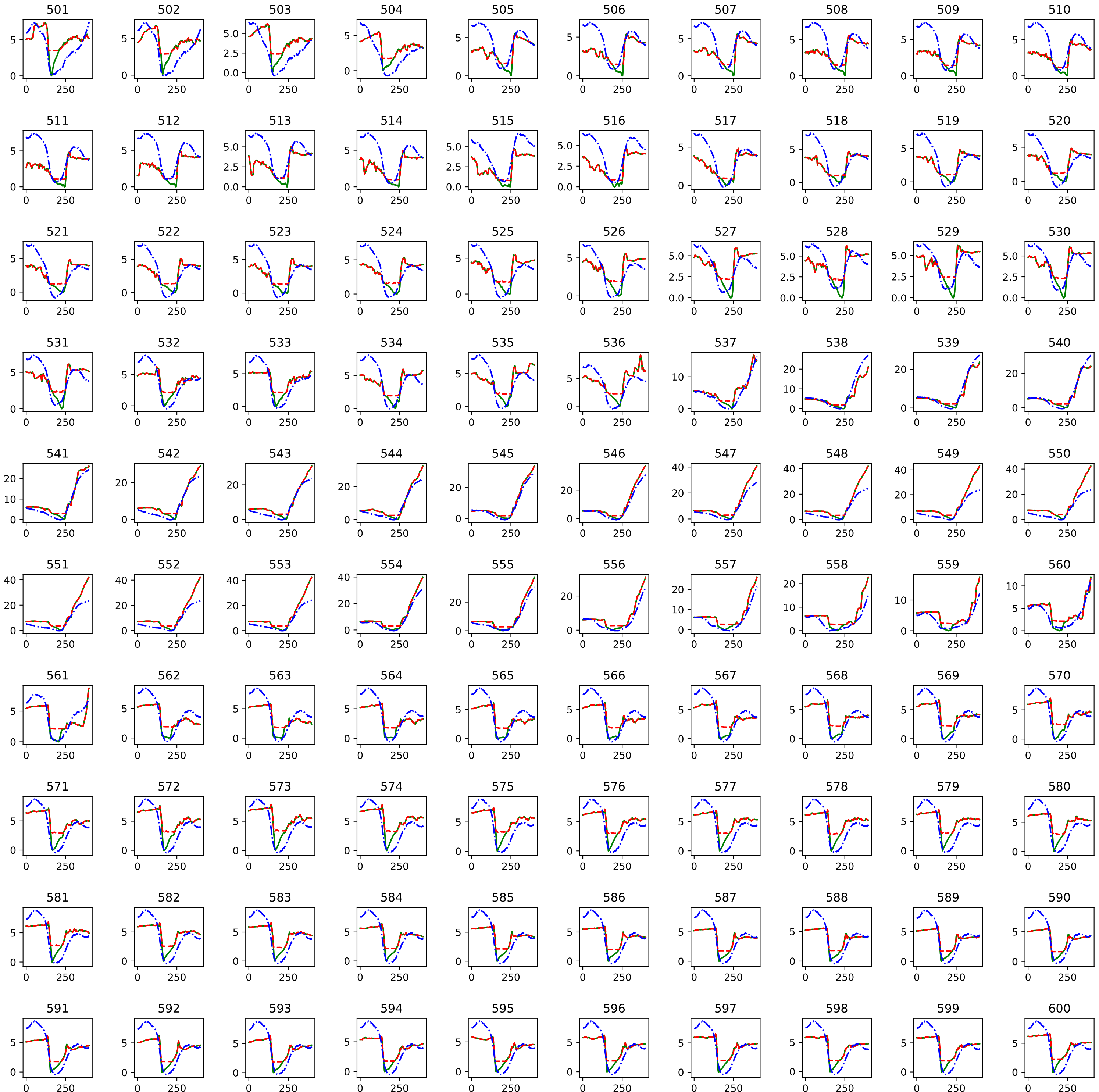


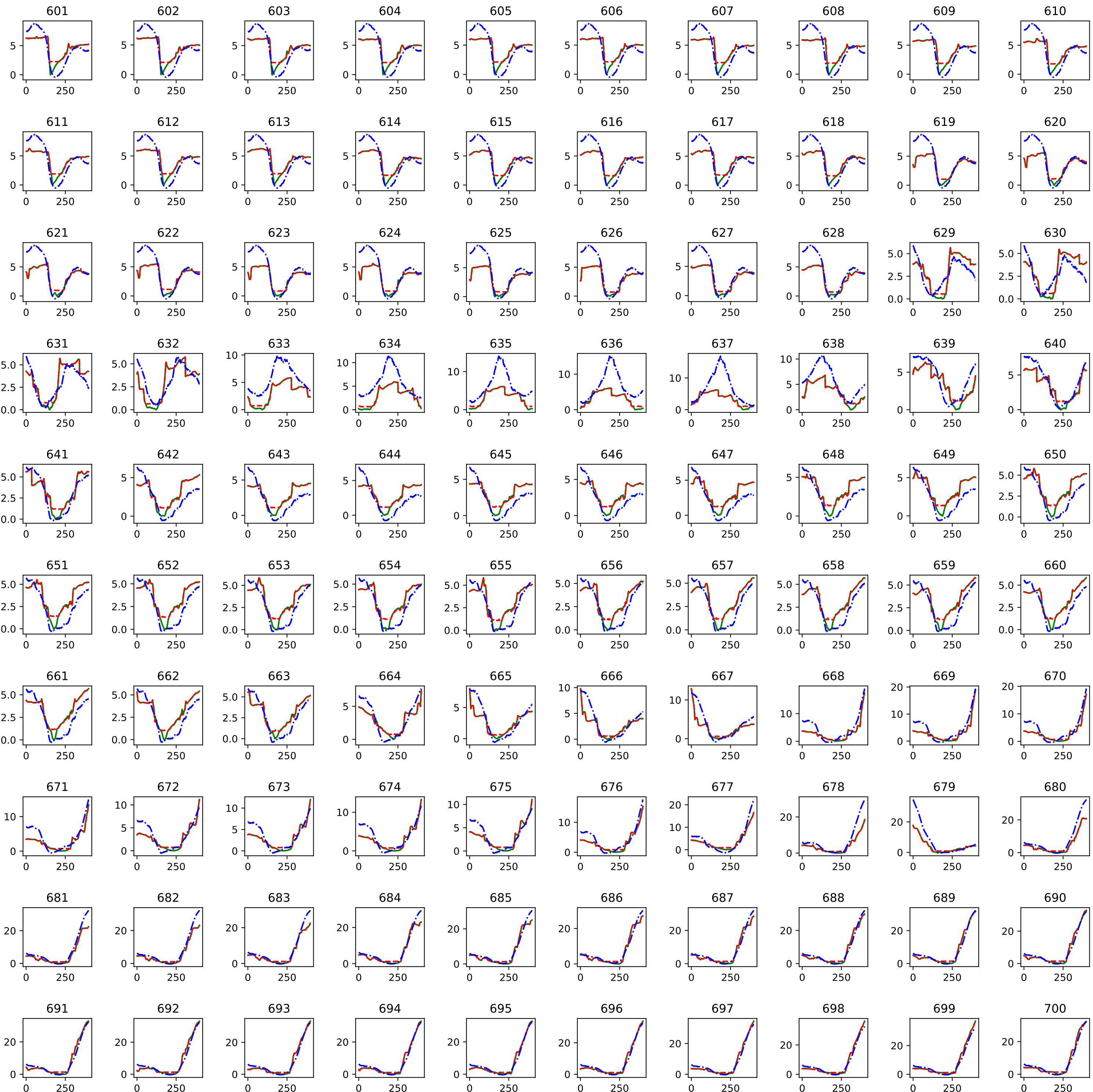


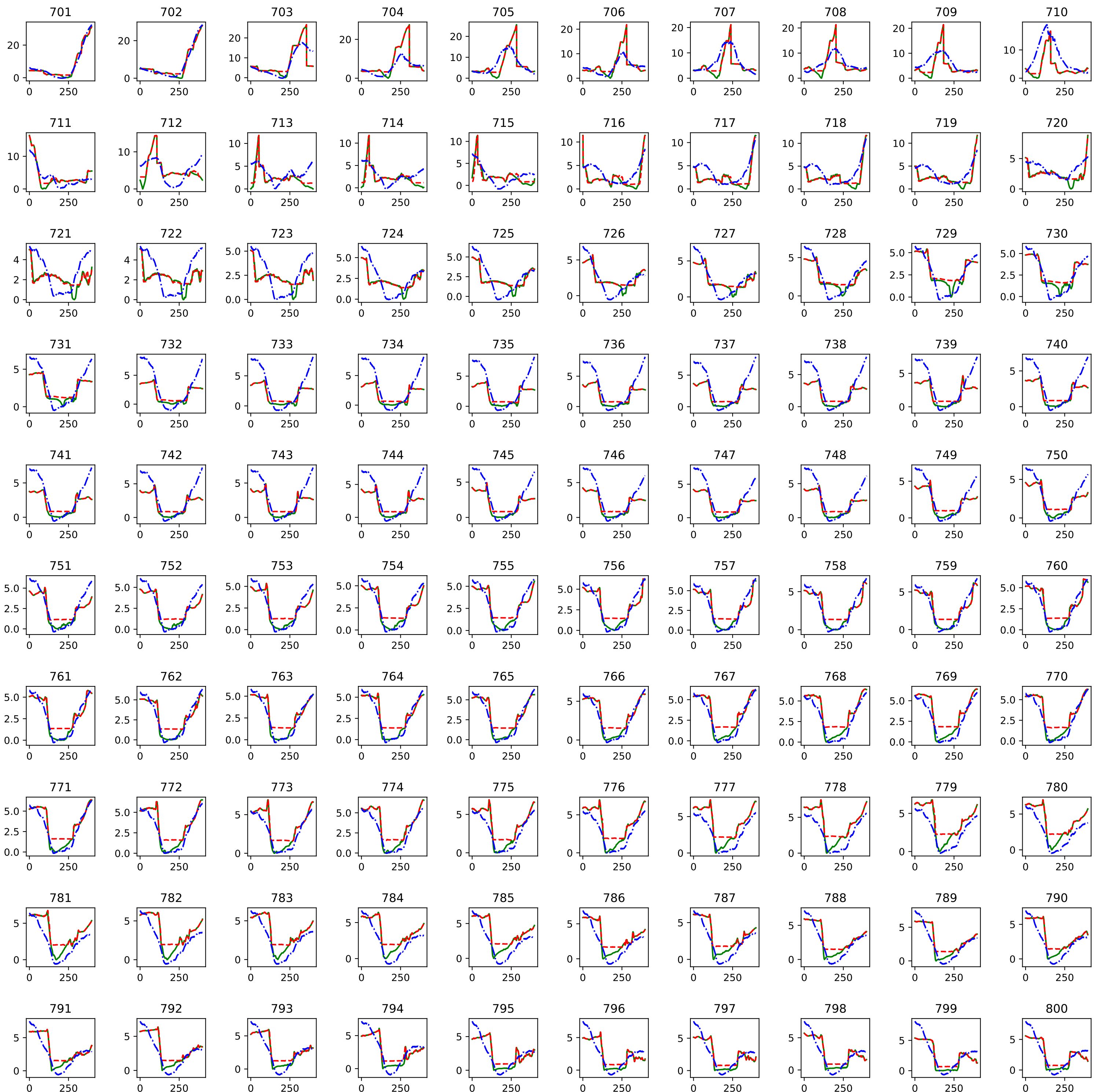


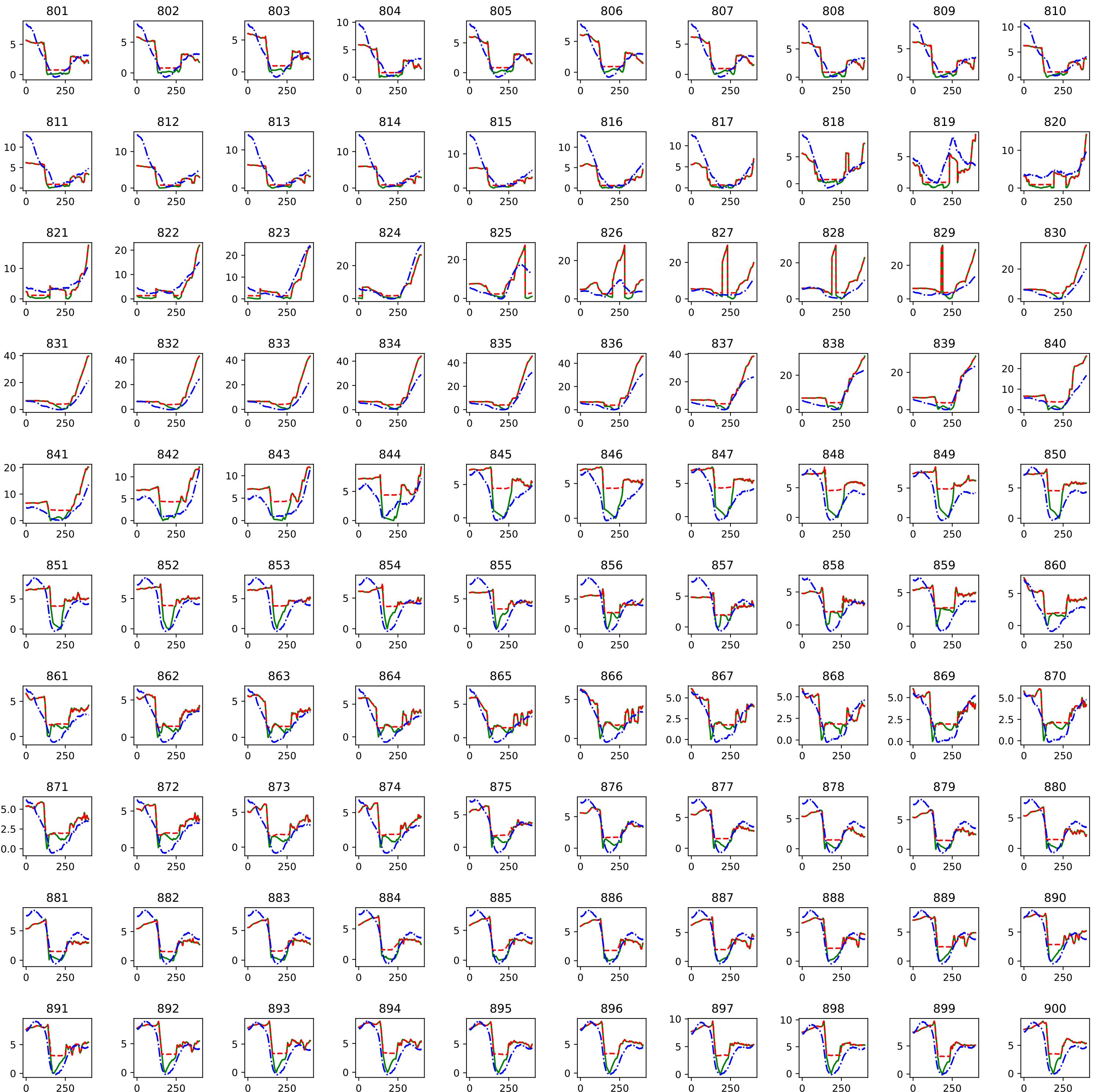


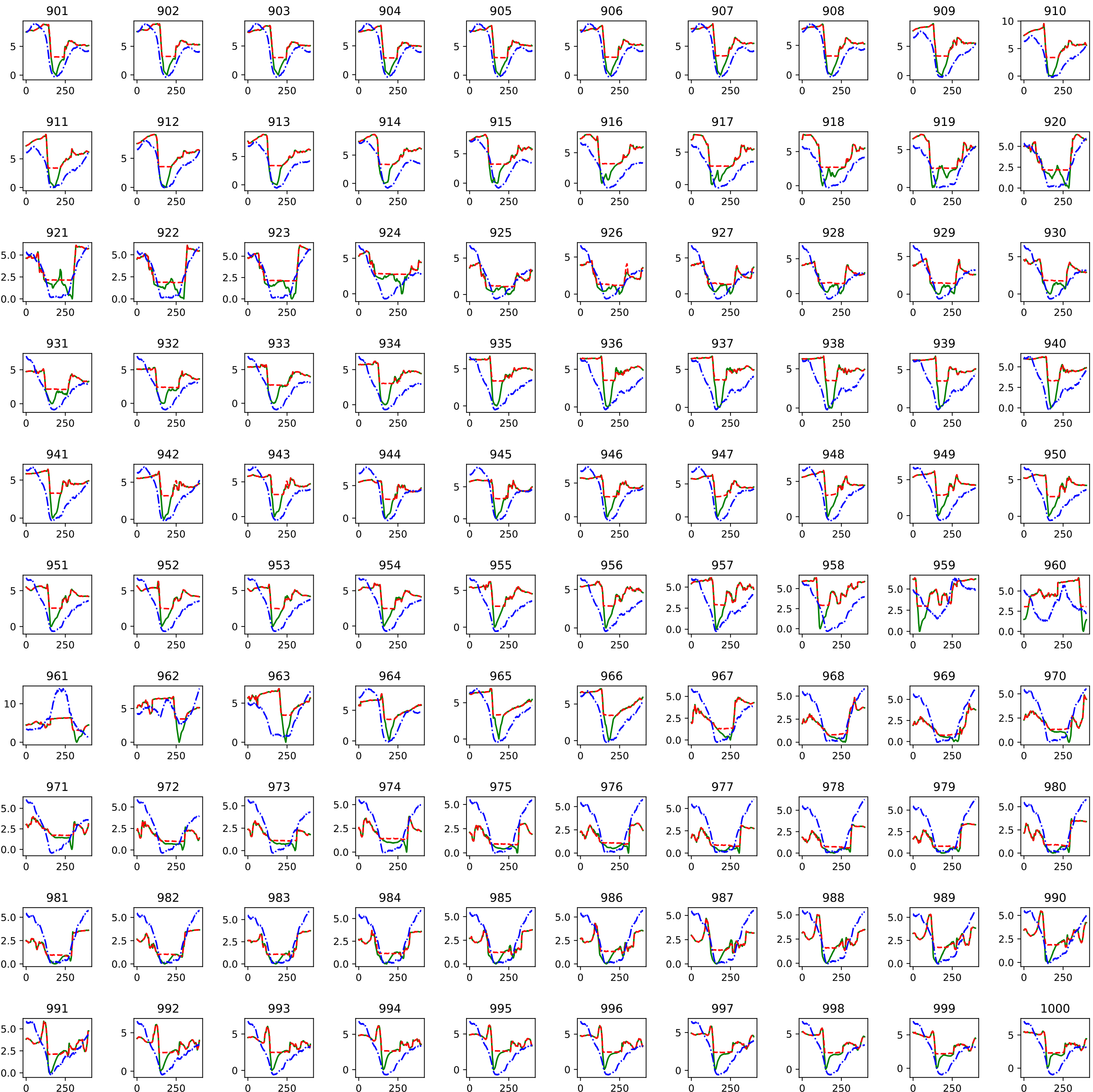


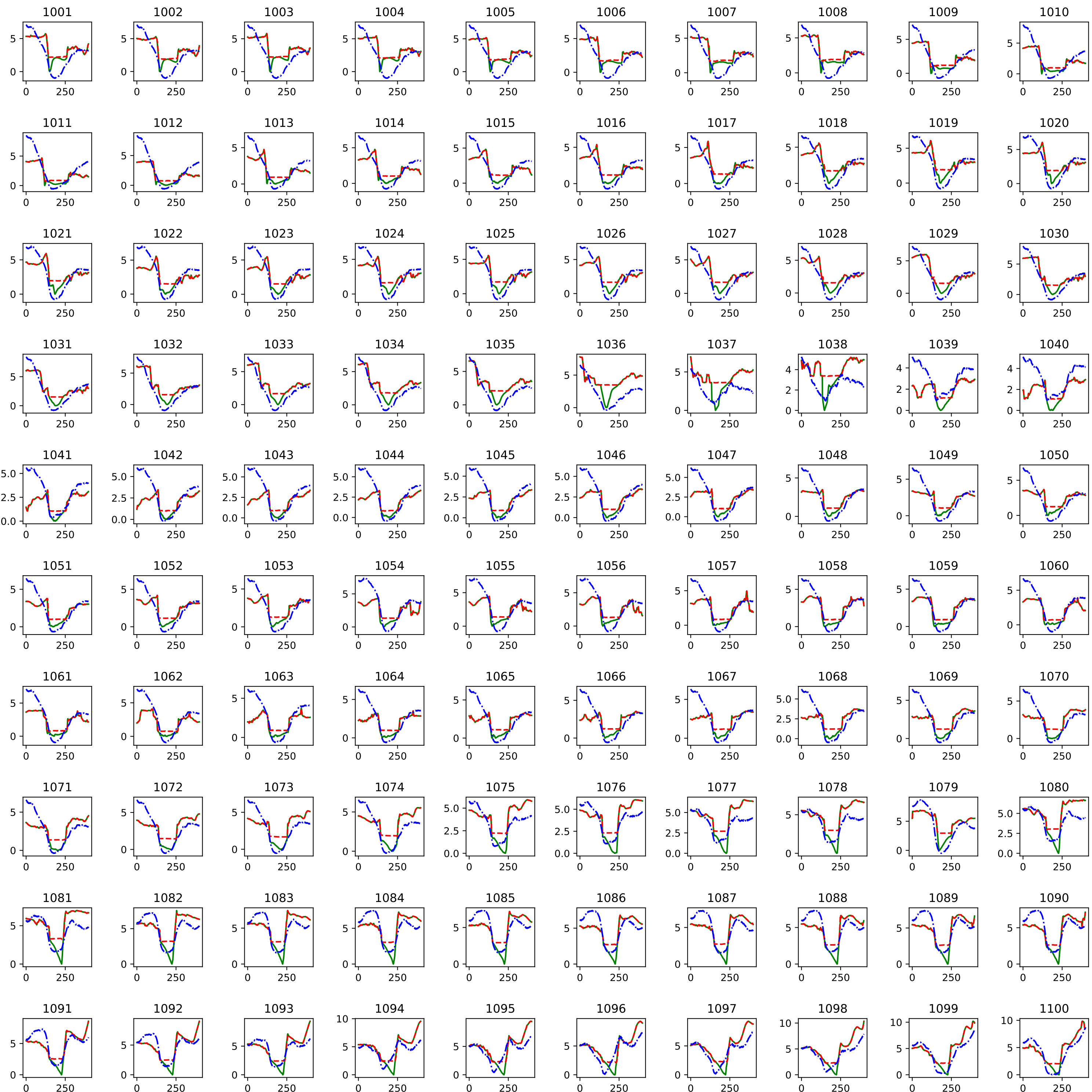


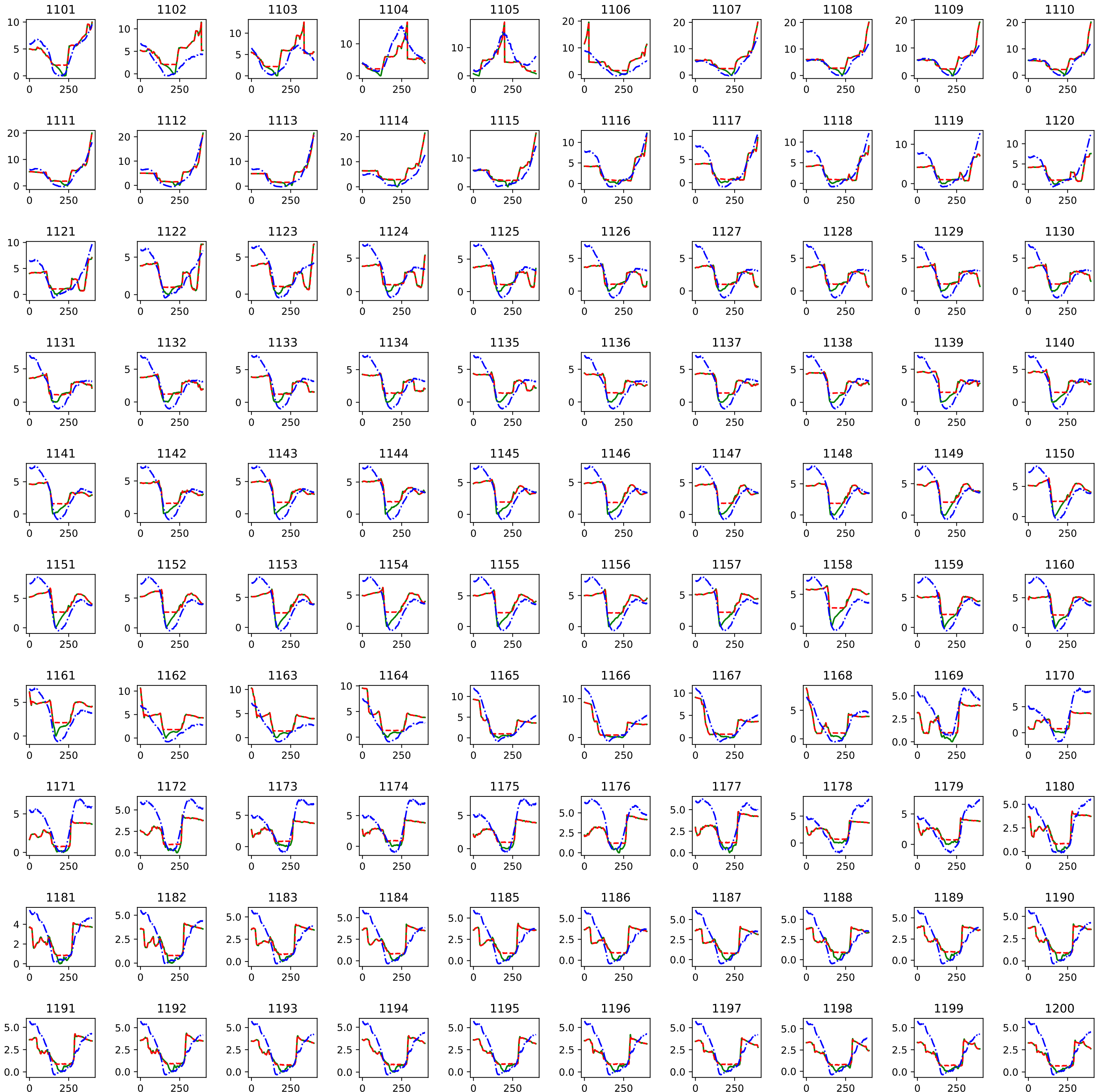


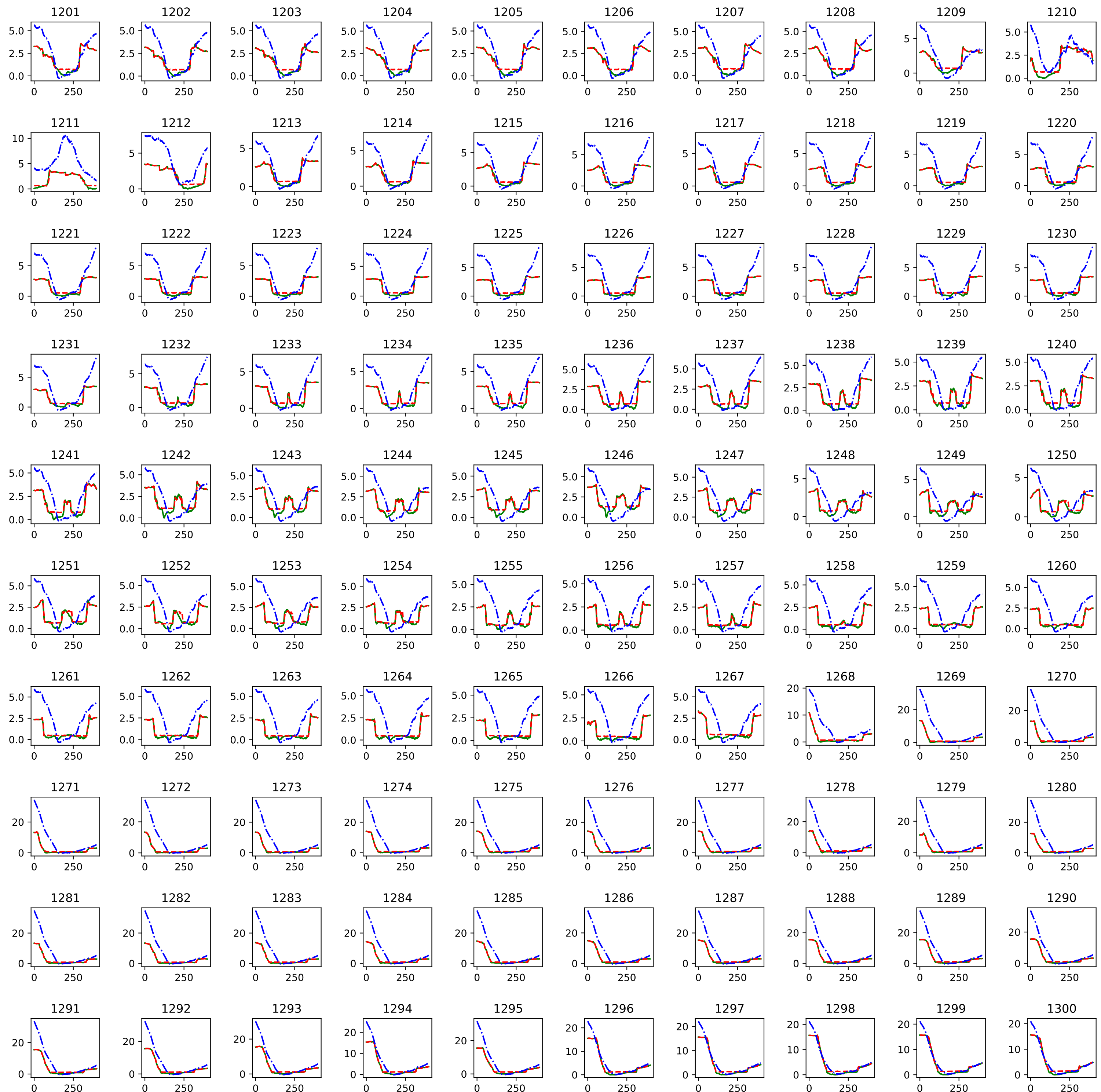


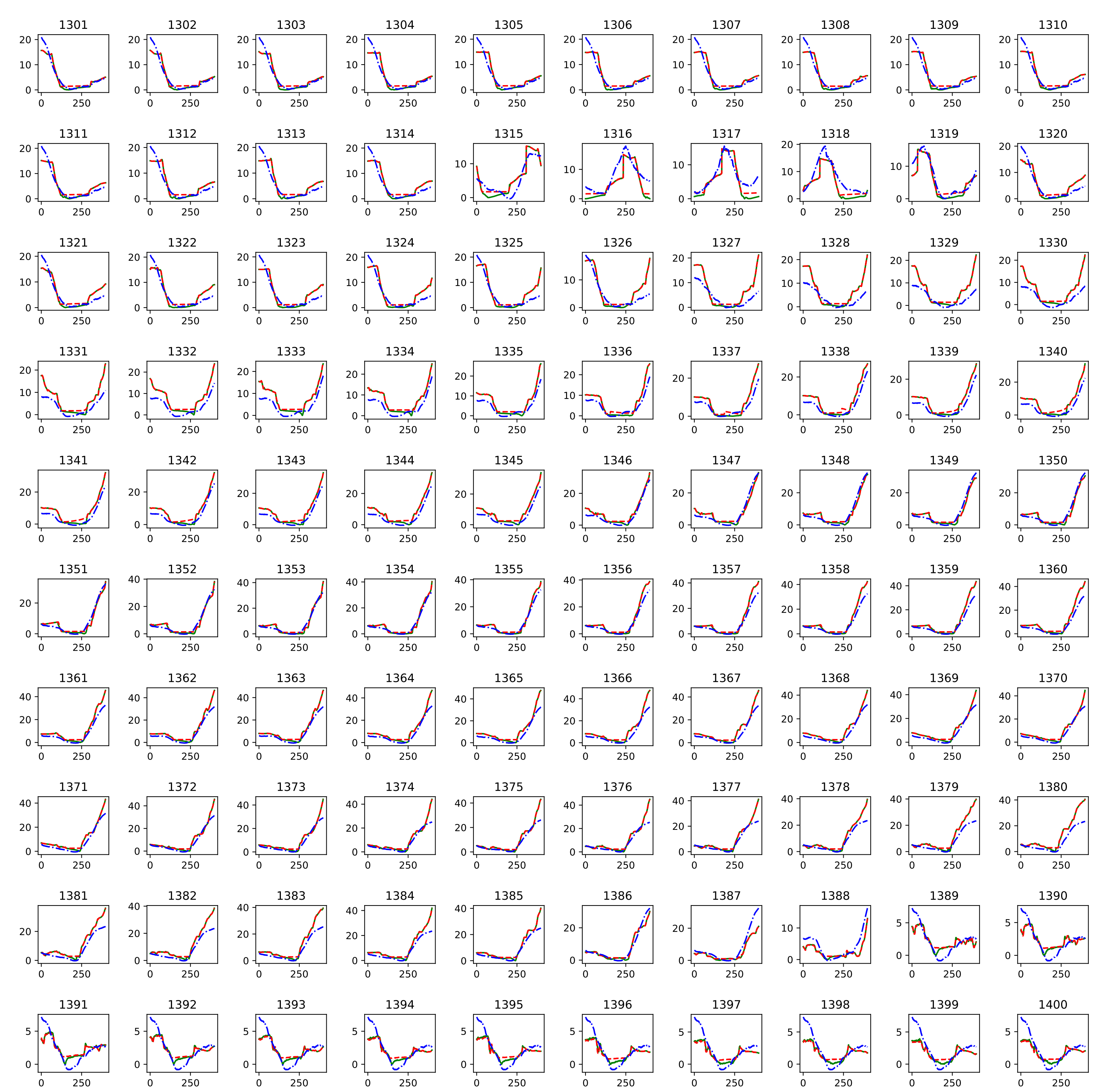


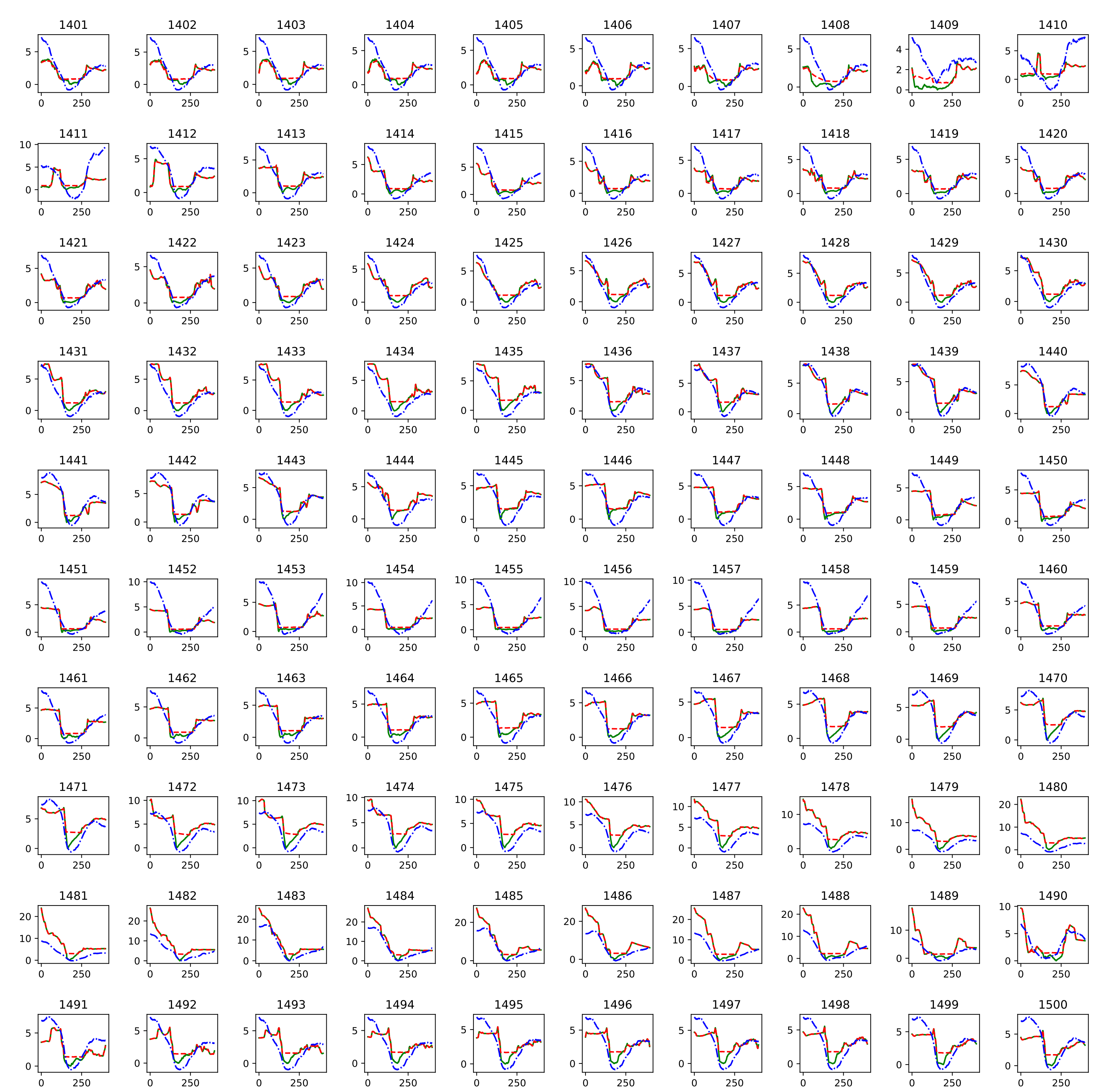


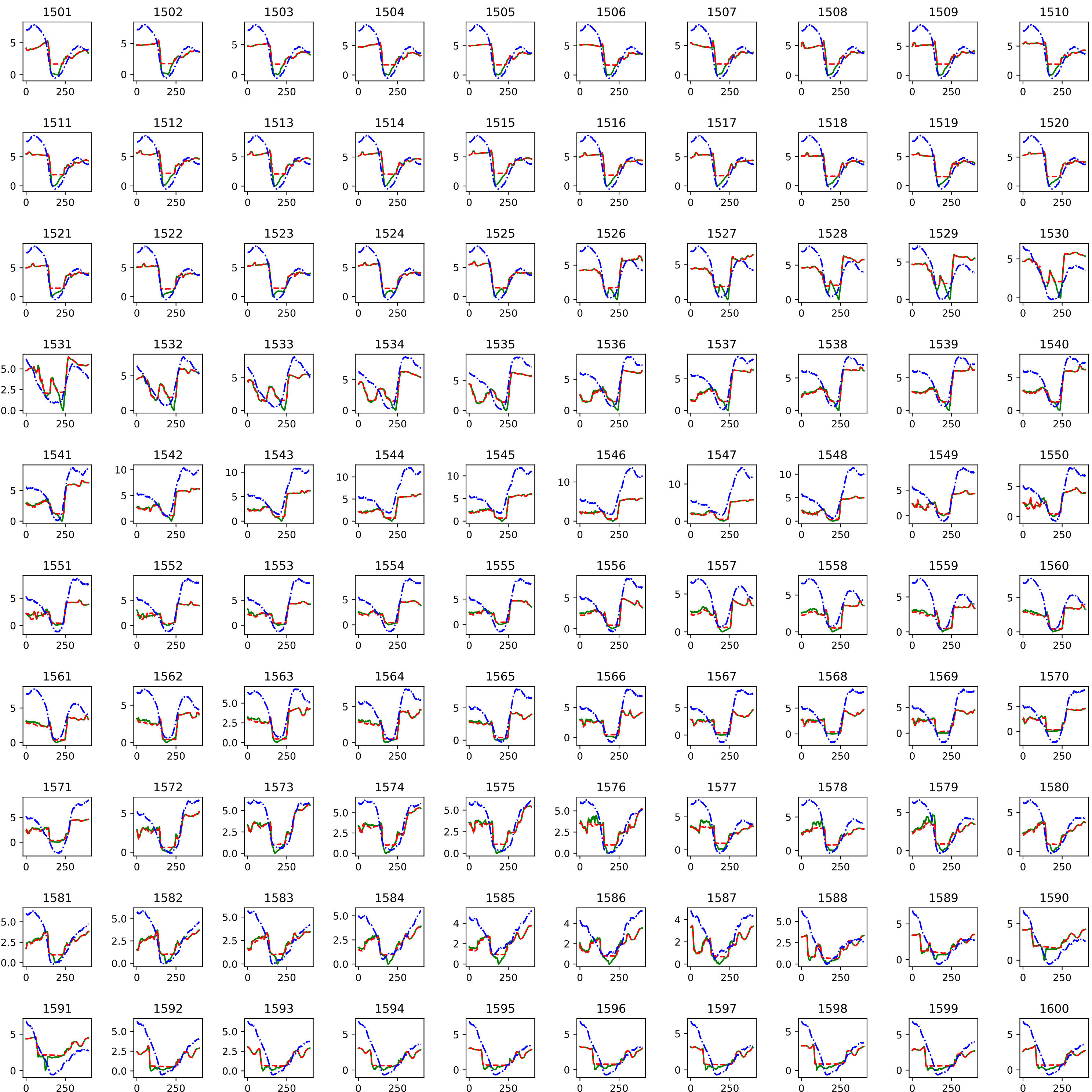


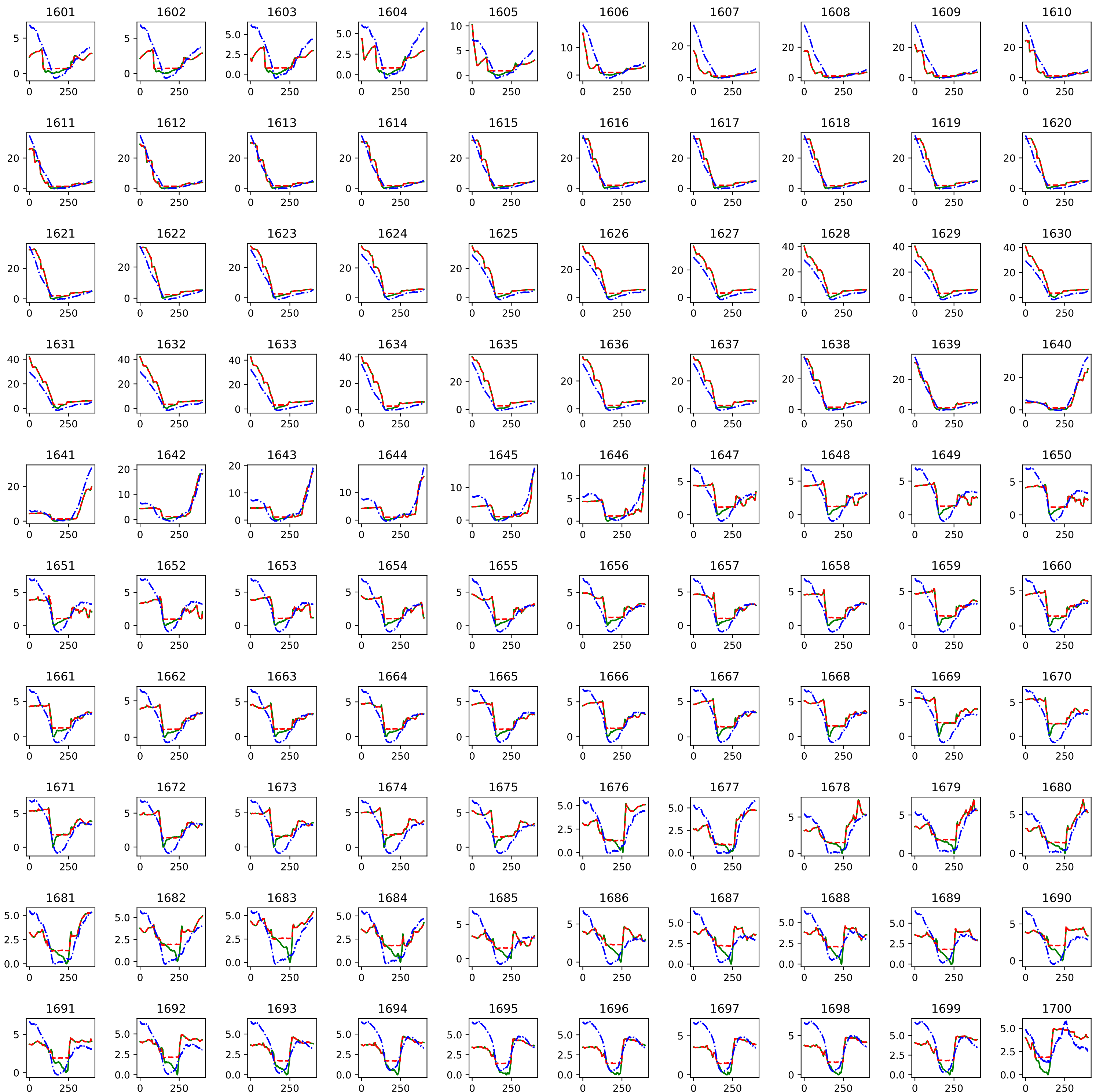


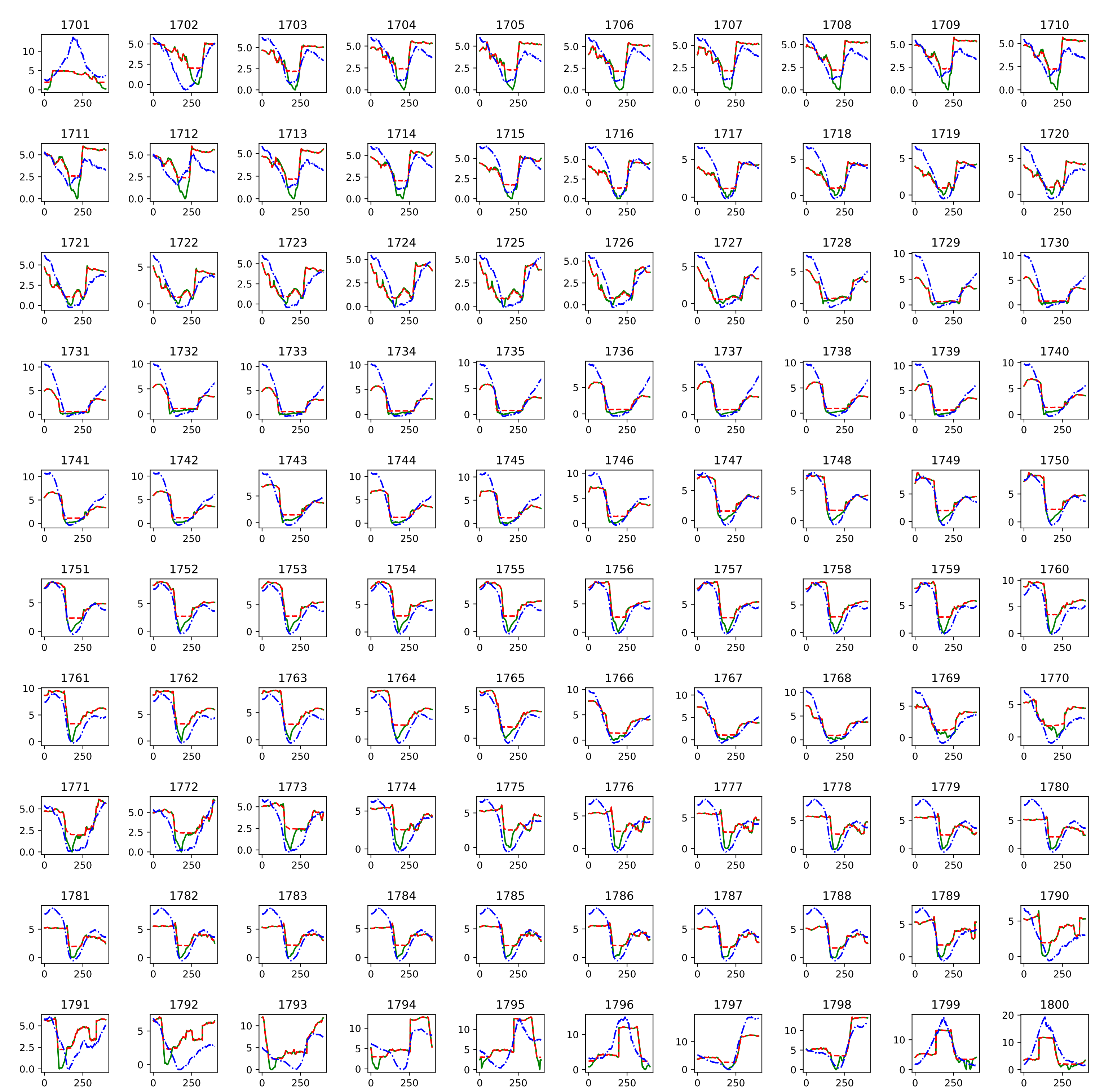












## Gaula ReLU

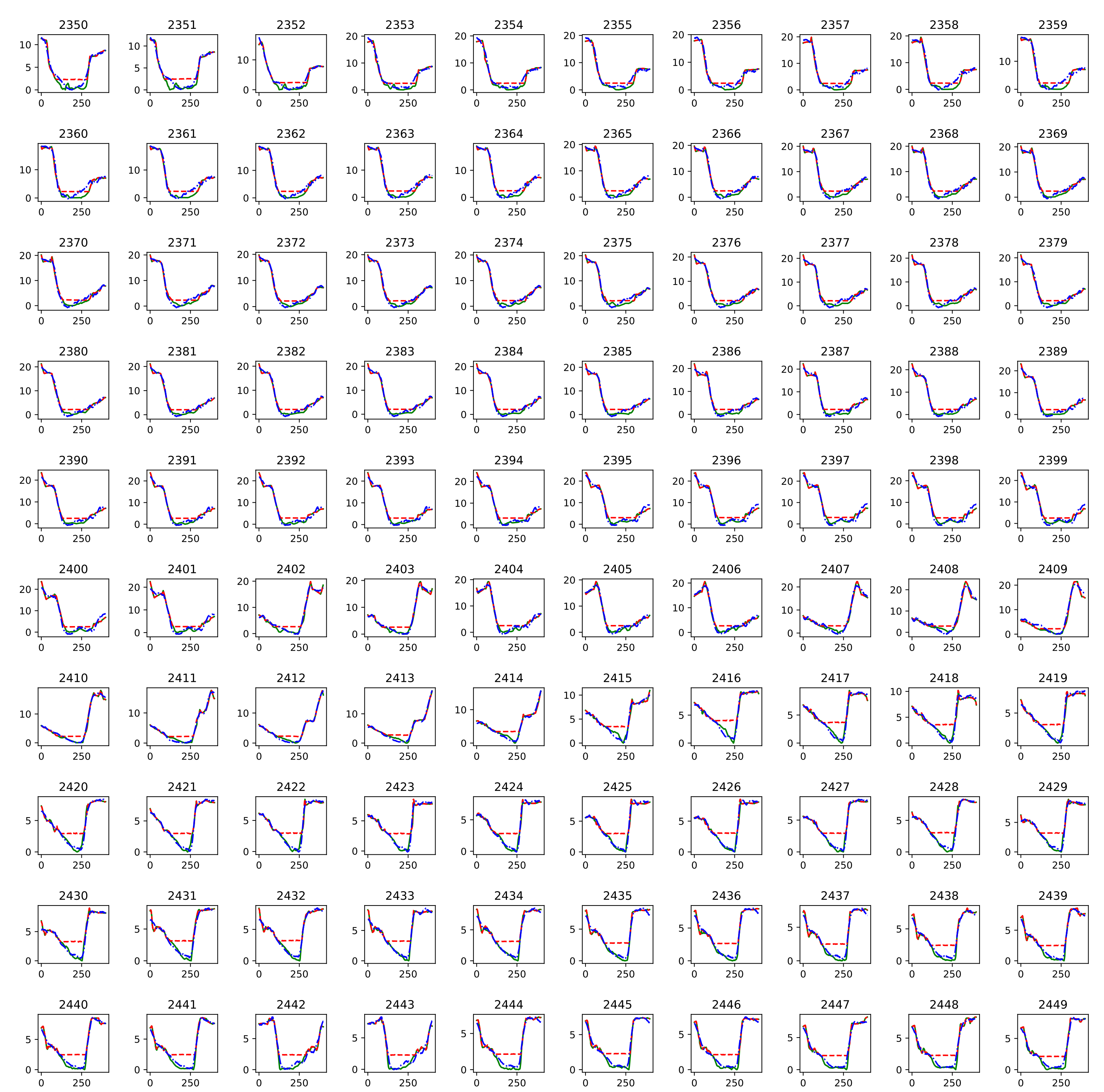
In the next pages, all the cross sections predicted for Gaula outside the range of training are shown using ReLU activation function.

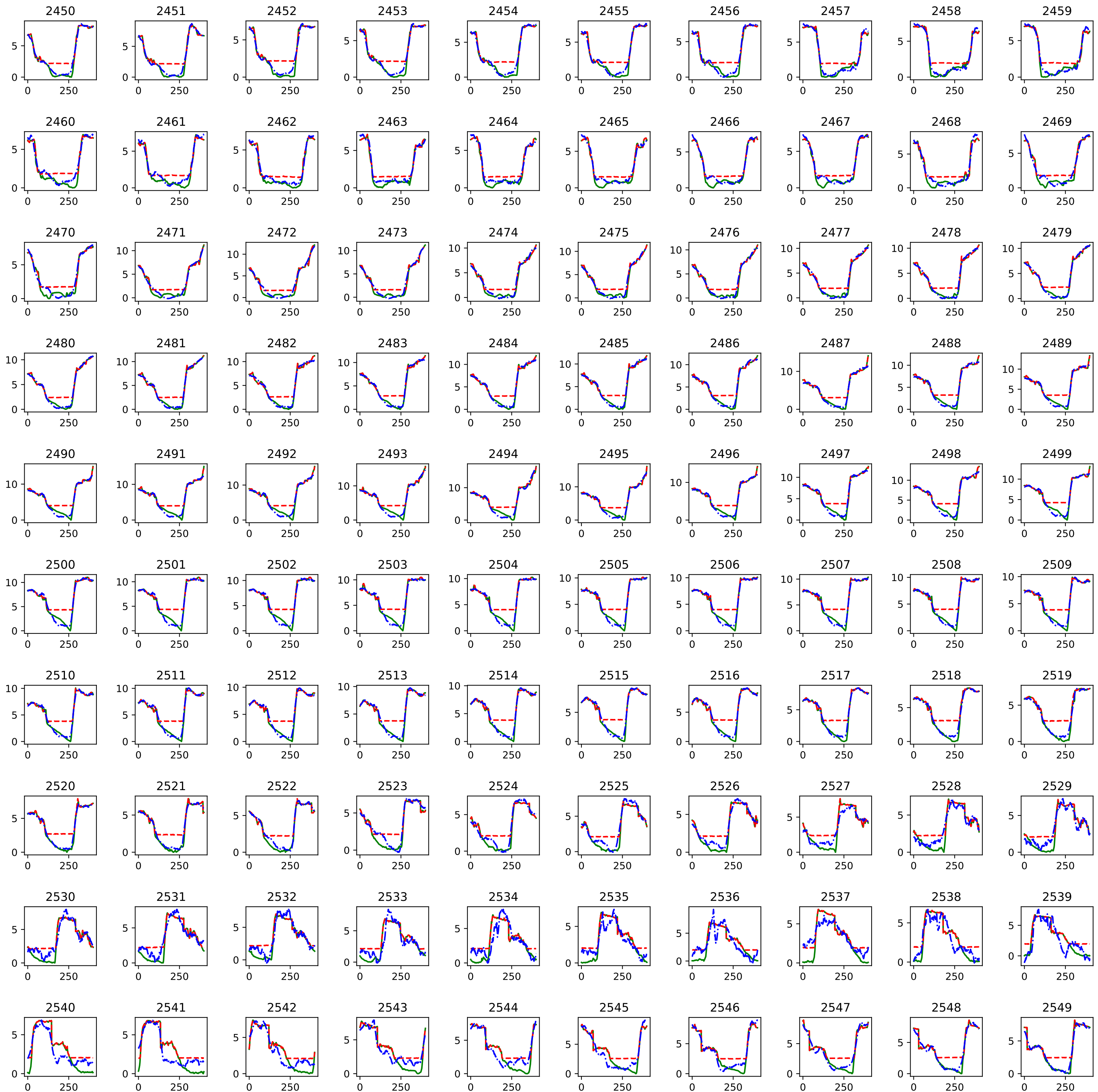
The legend for all the graphs as follow:

 Green LiDAR

 Red LiDAR

 Prediction





## Driva ReLU

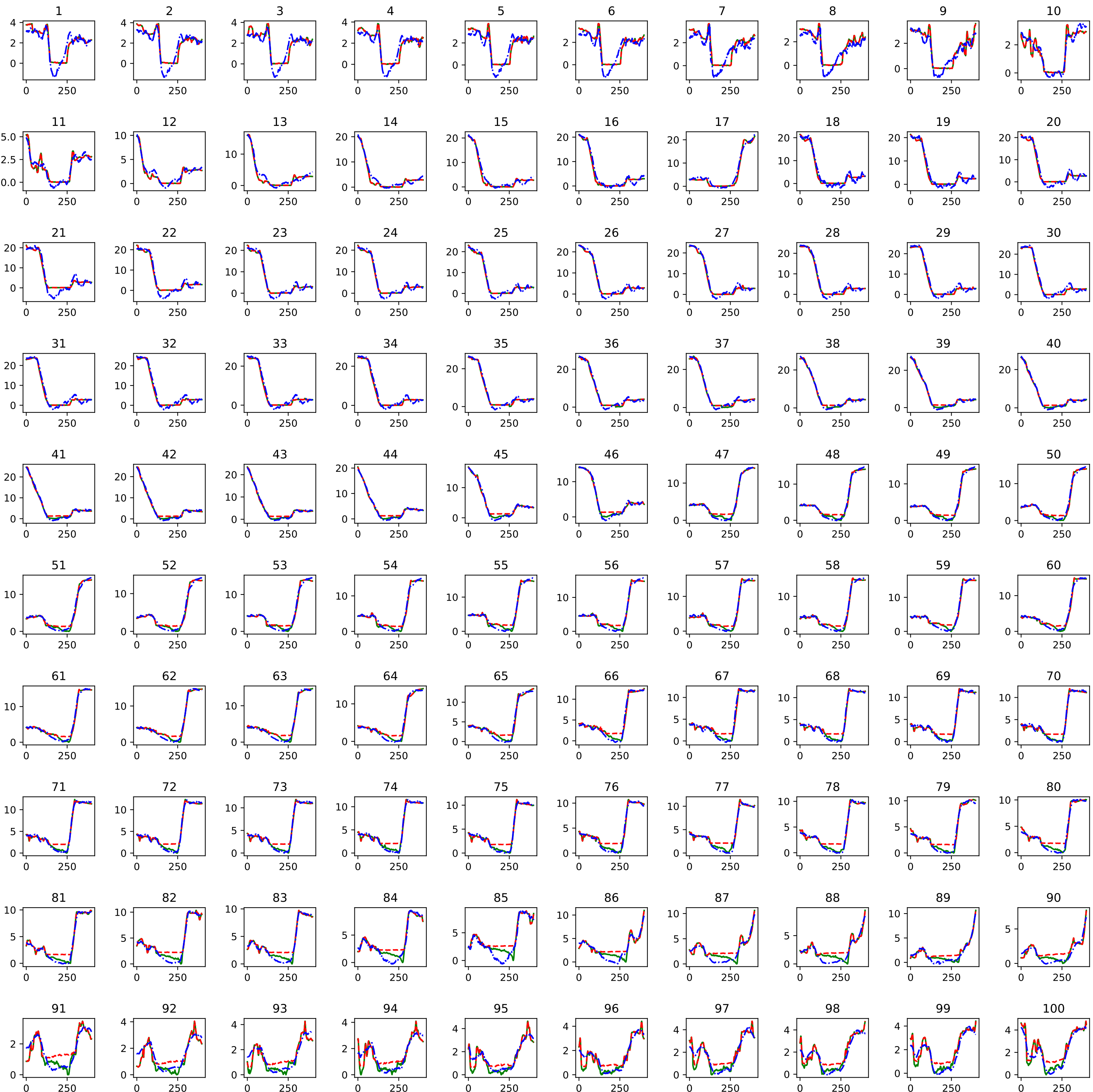
In the next pages, all the cross sections predicted for Driva are shown using ReLU activation function.

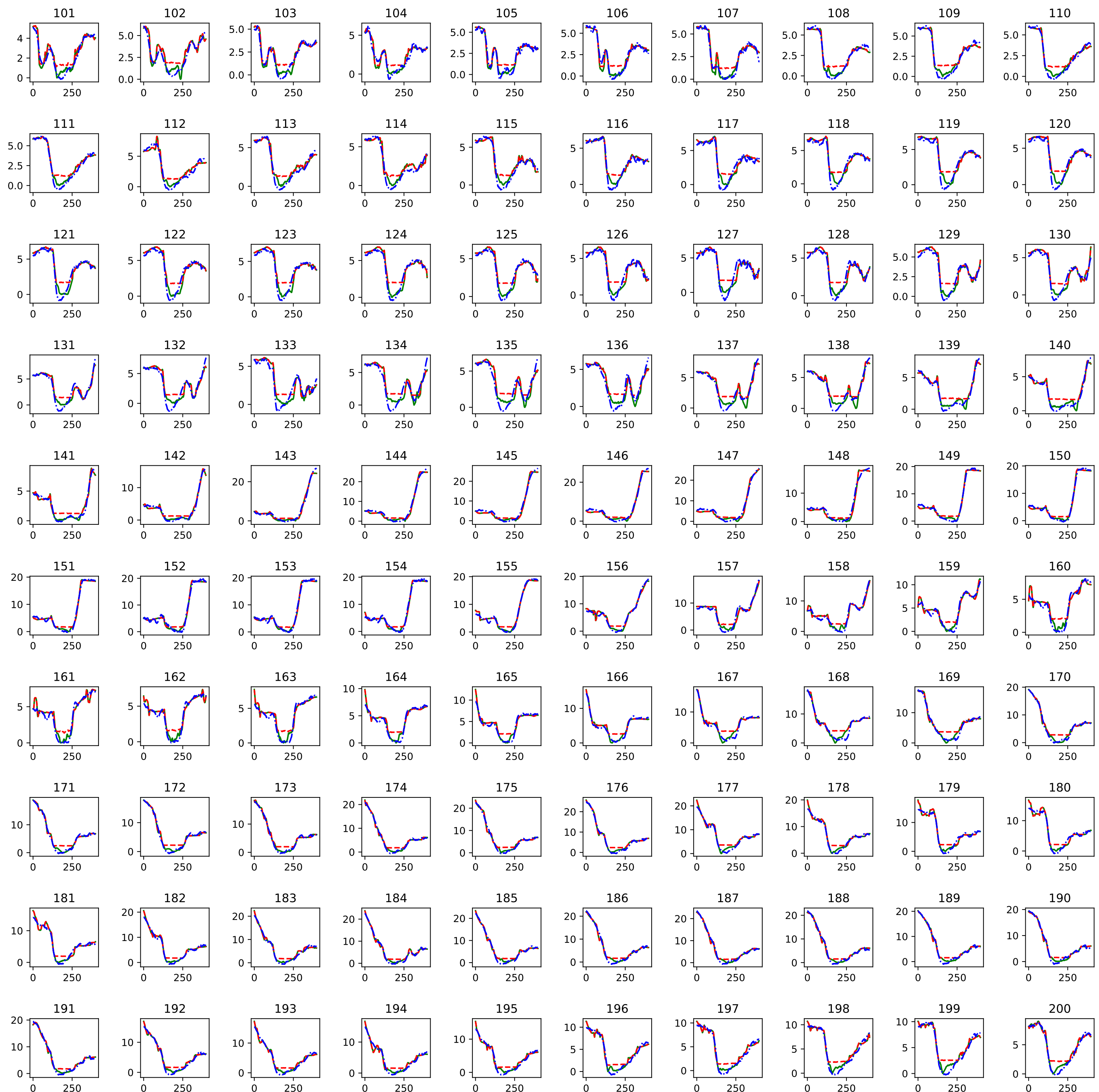
The legend for all the graphs as follow:

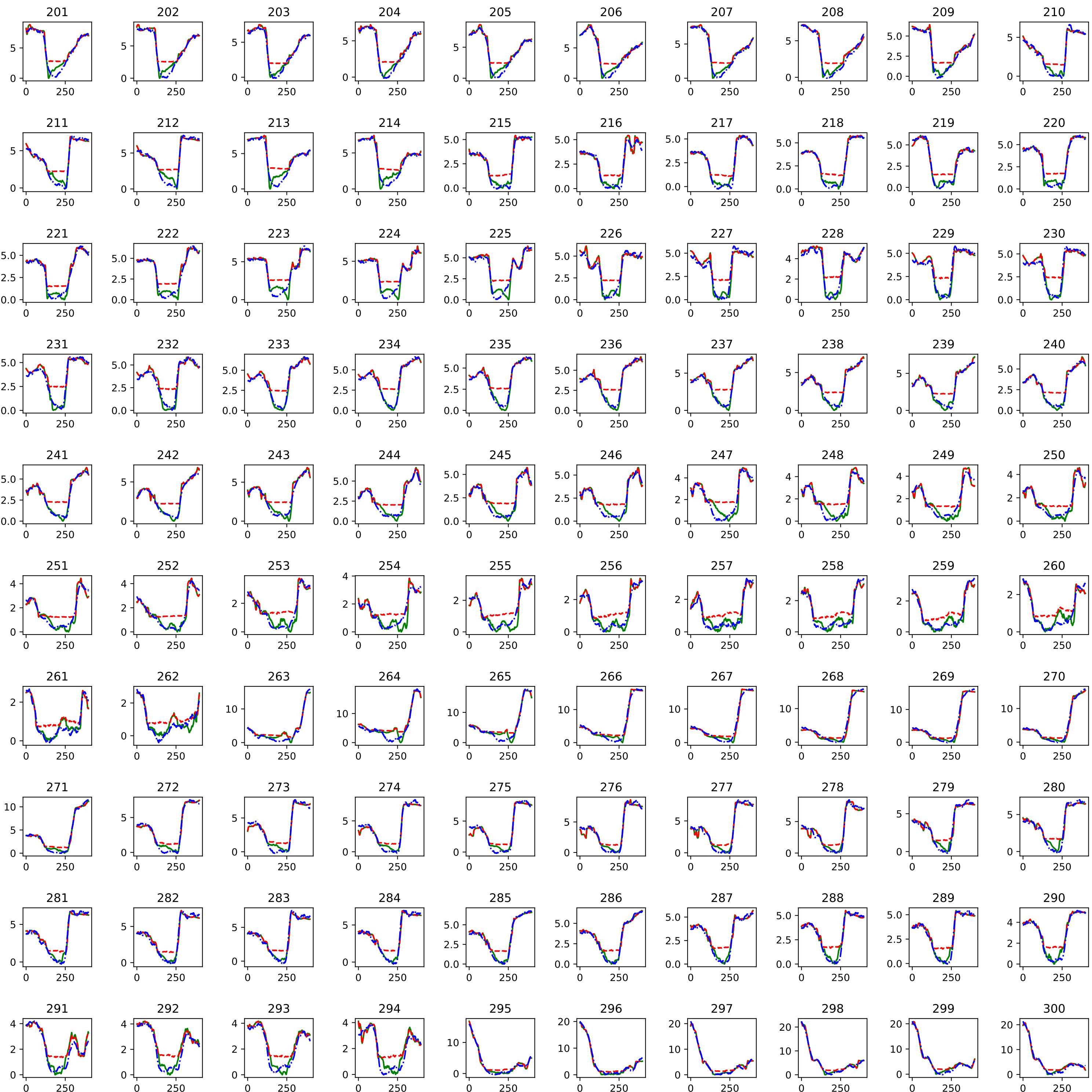
 Green LiDAR

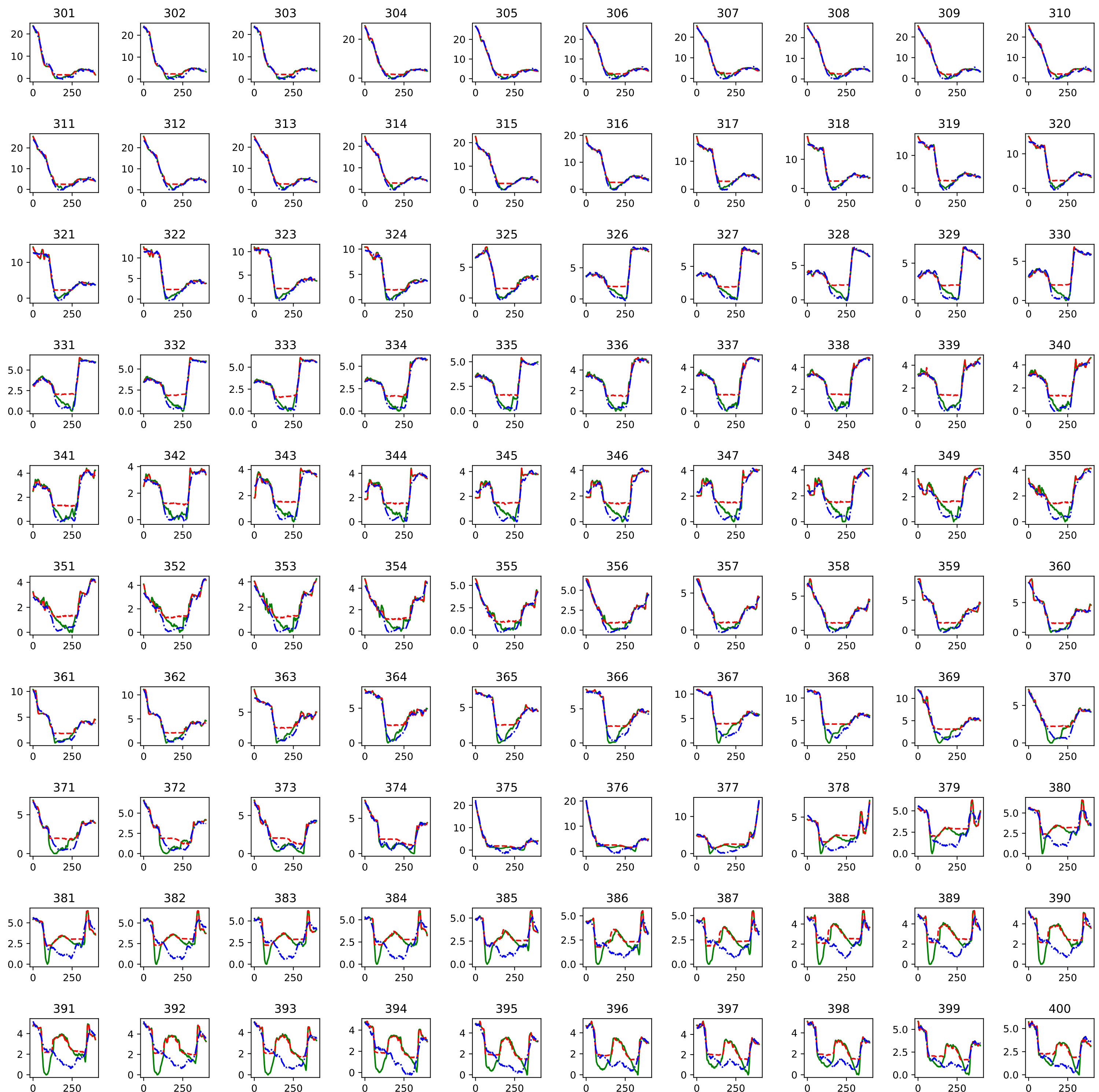
 Red LiDAR

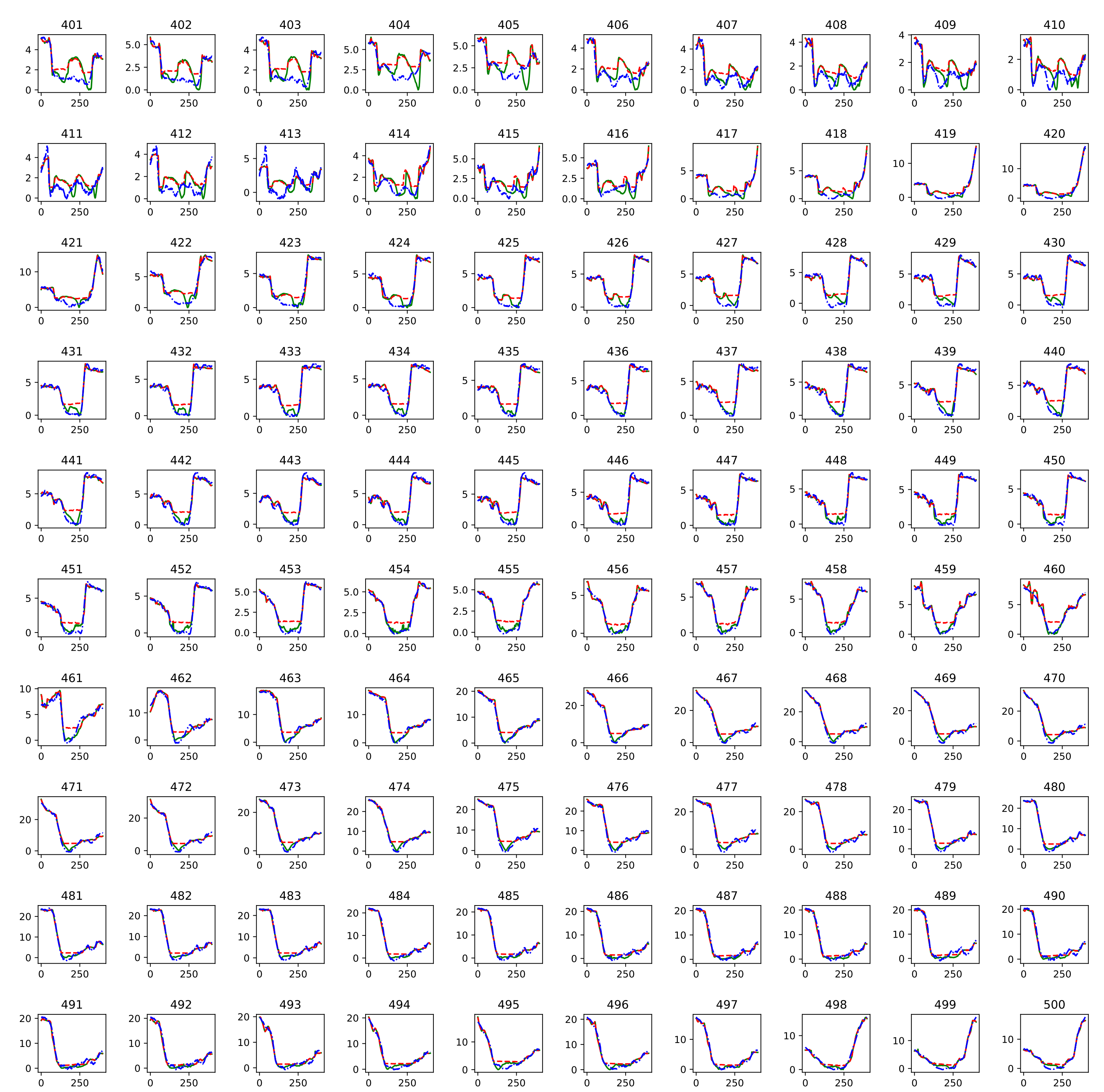
 Prediction

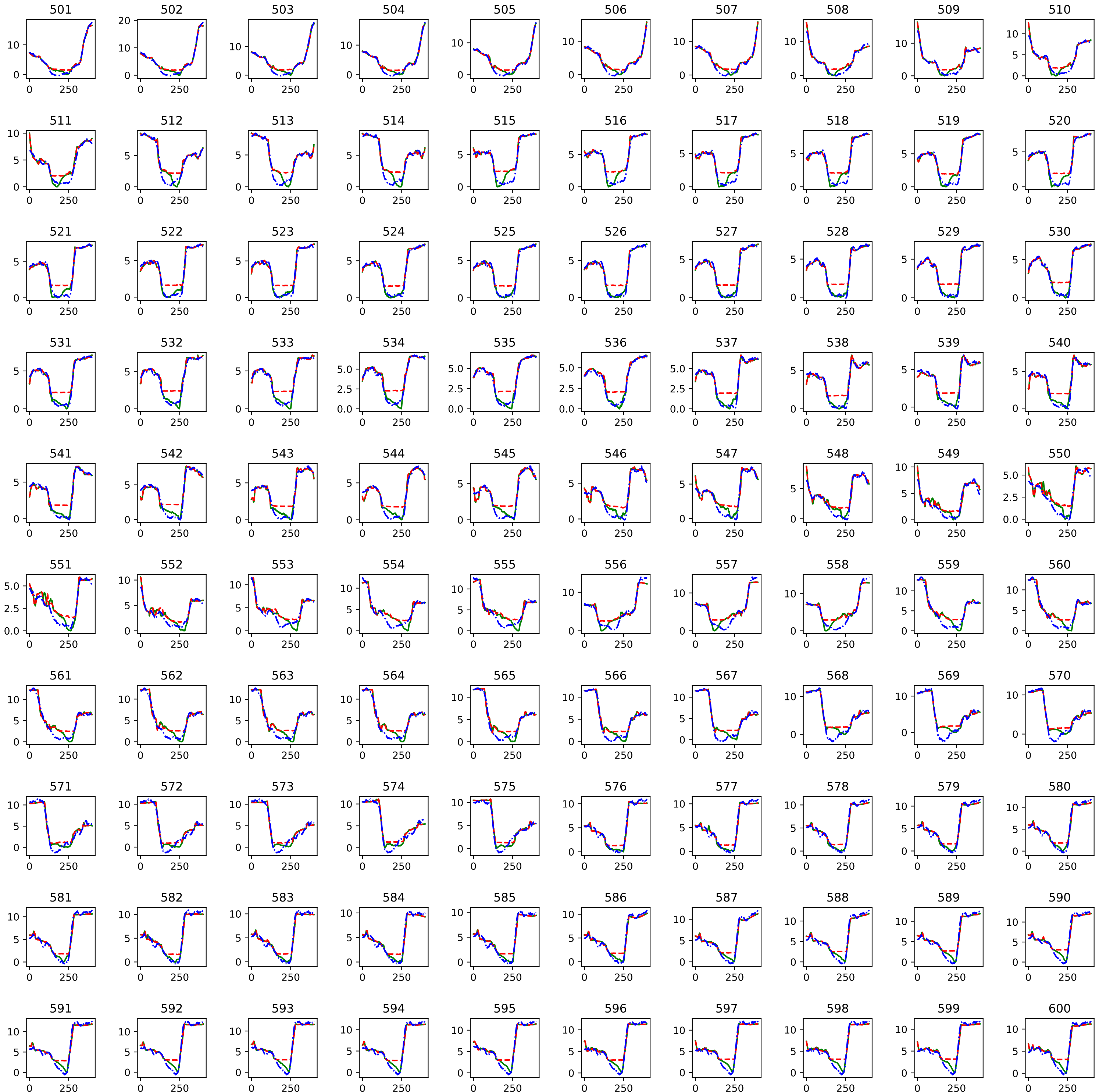


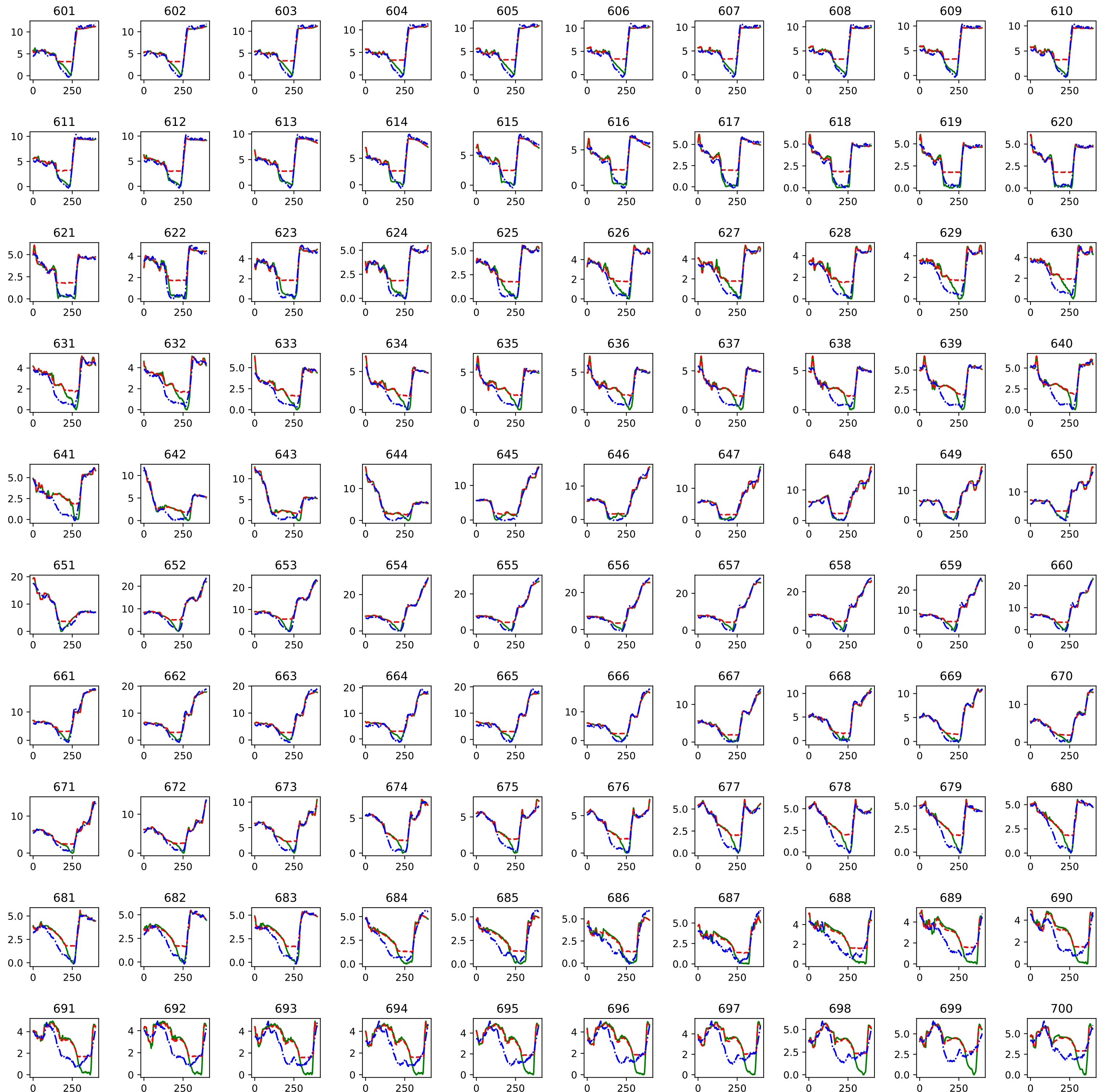


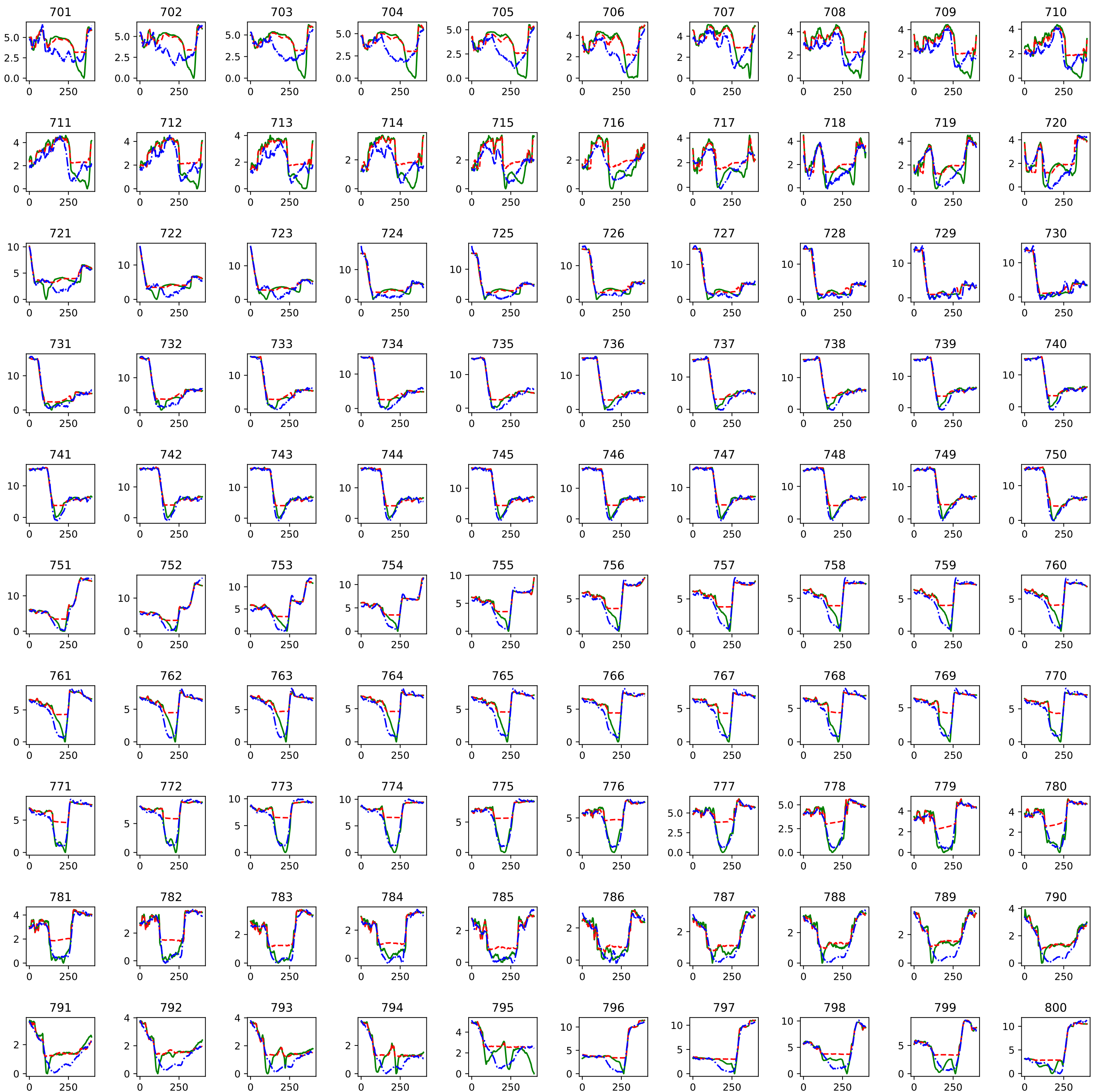


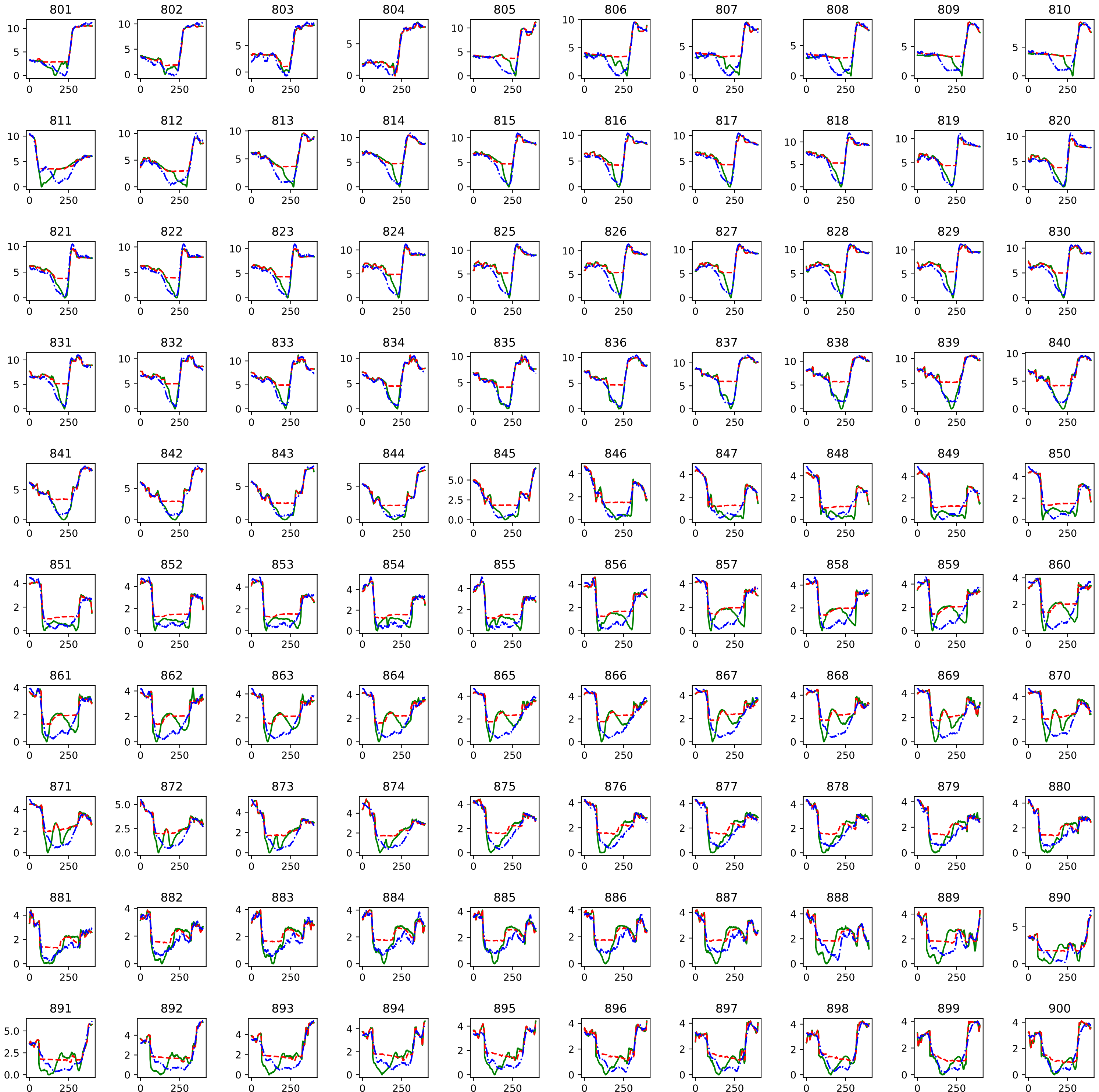


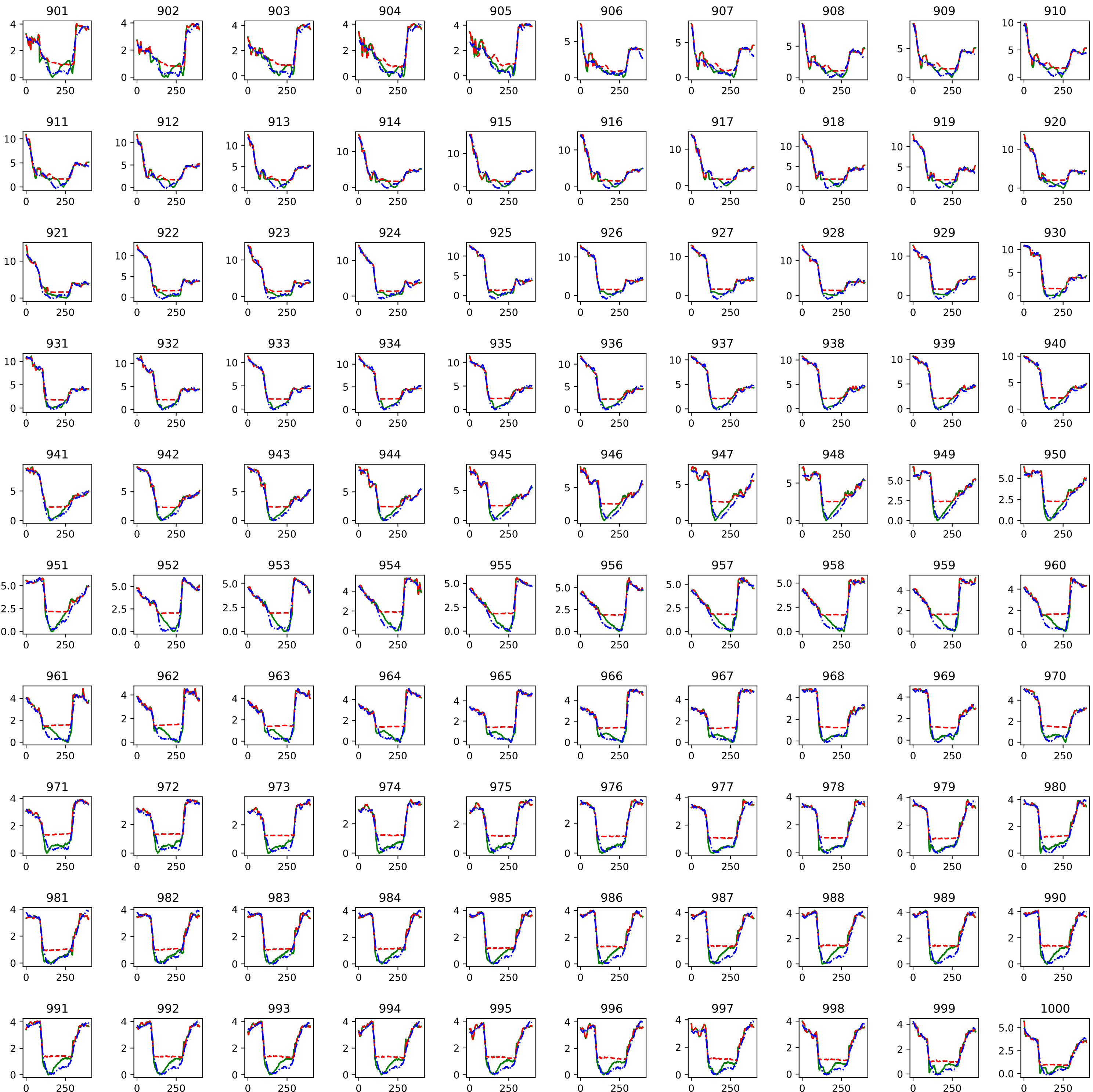


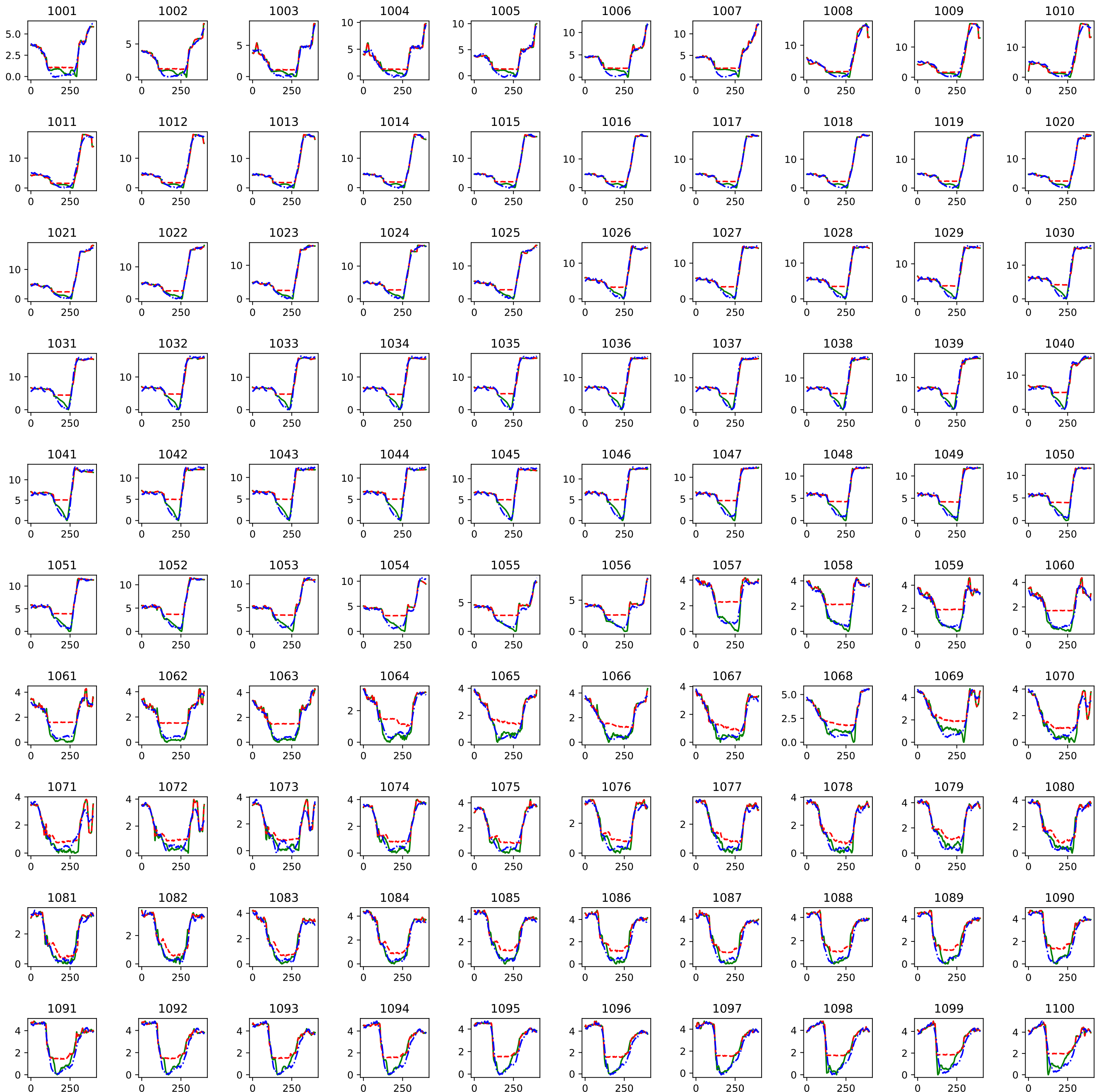


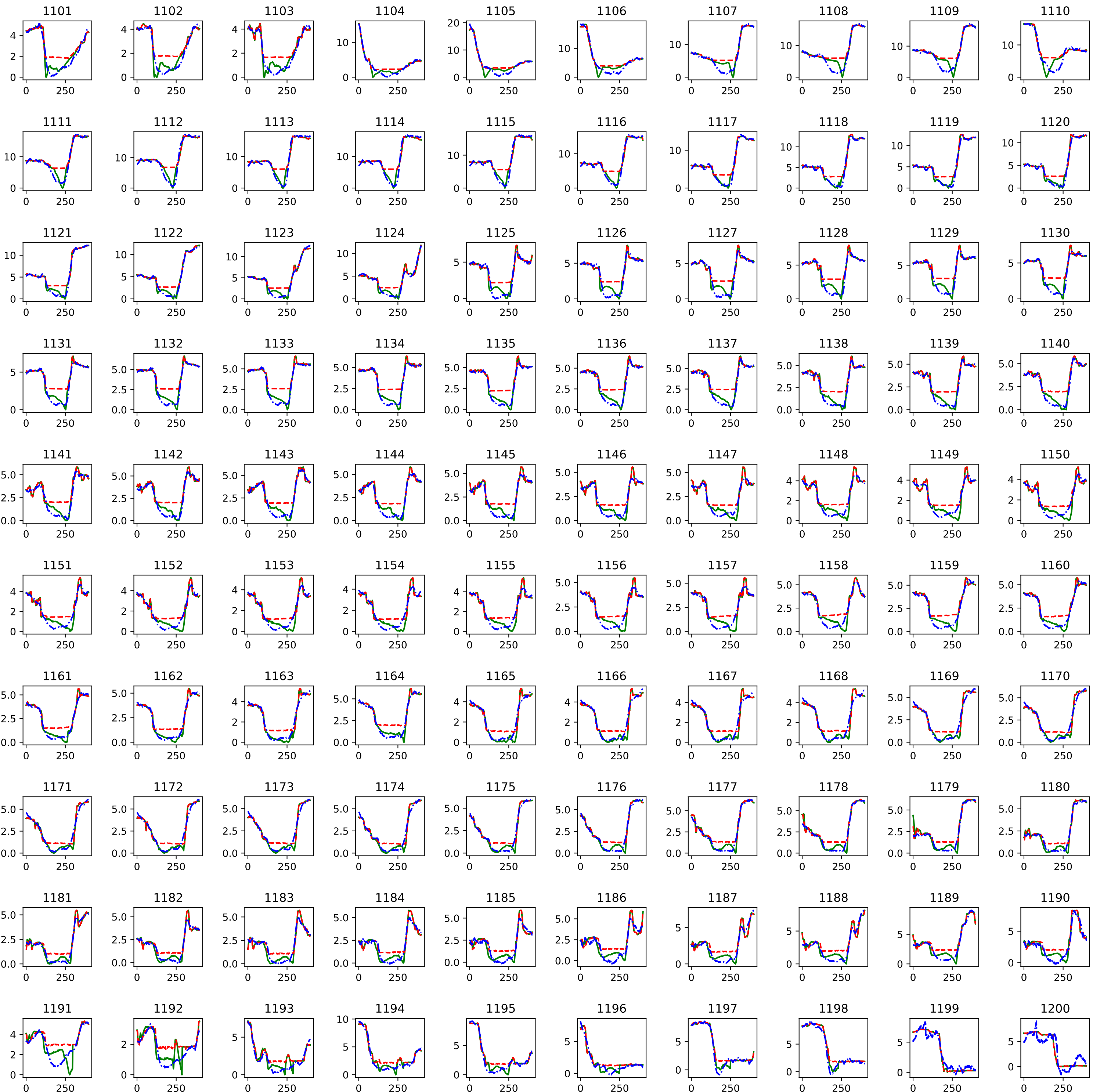












## Surna ReLU

In the next pages, all the cross sections predicted for Surna are shown using ReLU activation function.

The legend for all the graphs as follow:

 Green LiDAR

 Red LiDAR

 Prediction

